









Digitized by the Internet Archive  
in 2019 with funding from  
University of Alberta Libraries

<https://archive.org/details/Qureshi1965>











Thesis  
1965  
#65

THE UNIVERSITY OF ALBERTA

COORDINATION OF MODEL BRIDGE PIER SCOUR

by

ABDUL SALEEM QURESHI  
B.Sc. (Civil Eng.)(Pb)

A THESIS

SUBMITTED TO THE FACULTY OF GRADUATE STUDIES  
IN PARTIAL FULFILMENT OF THE REQUIREMENTS FOR THE DEGREE OF  
MASTER OF SCIENCE

DEPARTMENT OF CIVIL ENGINEERING

EDMONTON, ALBERTA

APRIL, 1965





UNIVERSITY OF ALBERTA  
FACULTY OF GRADUATE STUDIES

The undersigned certify that they have read, and recommend to the Faculty of Graduate Studies for acceptance, a thesis entitled "COORDINATION OF MODEL BRIDGE PIER SCOUR" submitted by Abdul Saleem Qureshi, in partial fulfilment of the requirements for the degree of Master of Science.

---





ABSTRACT

The possibility of phase difference between model and prototype was studied by experimenting in laboratory with light weight bed material (coal).

An attempt has been made to coordinate the scour results of Chatou laboratory (Reference 13) with the ones from experiments with light weight bed material, through dimensional analysis, introducing the densimetric Froude number, amended by an approximate drag coefficient.

It was found that fine gravel and gravel-sized coal, in the range of increasing scour and short distance past maximum scour, yield results which could be reduced to one line on a non-dimensional plot up to a diversion point.

The maximum scour depth for a given depth of flow and gravel sized bed material was found significantly less for the light weight bed material than for the heavy weight bed material.

It was found that sand, with its different settlement law from gravel, did not conform with gravel on non-dimensional plot.

An annotated selected bibliography was included in an effort to coordinate various essential facts and ideas about bridge pier scour.





ACKNOWLEDGEMENTS

The writer wishes to extend his sincere appreciation to Professor A. W. Peterson for his guidance, continuous help in the laboratory, and his indispensable work as editor. To Professor T. Blench, D.Sc., the writer is deeply indebted for his constant encouragement, inspiring interest in the present study, his invaluable advice and constructive criticism.

The writer also acknowledges his thanks to:

Dr. N. Rajaratnam, for giving freely of his valuable time for many extremely helpful discussions.

Mr. C. R. Neill of the Research Council of Alberta, for the generous lending of his library of bridge pier scour literature.

Mr. K. Subramanya, for many useful discussions.

Miss Evelyn R. Fenniak, for many useful suggestions.

The Civil Engineering Department and the National Research Council for the financial assistance, and

Mrs. P. Babet for typing the manuscript.



# TABLE OF CONTENTS

	<u>Page</u>
TITLE PAGE	i
APPROVAL SHEET	ii
ABSTRACT	iii
ACKNOWLEDGEMENTS	iv
TABLE OF CONTENTS	v
LIST OF FIGURES	vii
LIST OF TABLES	ix
LIST OF PLATES	x
 CHAPTER 1. LITERATURE REVIEW	
Introduction	1
Literature review	3
 CHAPTER 2. METHODS OF STUDYING BRIDGE PIER SCOUR	
General	24
Writer's Approach	26
Dimensional analysis	26
Actual problem	29
Graphical approach	36
Range of data used	36
 CHAPTER 3. SCOUR IN HEAVY WEIGHT BED MATERIAL	
Source of data	37
Experimental detail	37
Data collected	38
Analysis of data	38
Plots	38
Conclusions	46





	<u>Page</u>
CHAPTER 4.        SCOUR IN LIGHT WEIGHT BED MATERIAL	
Introduction	66
Experiments	67
Procedure	68
Sequence of test and data	70
Plottings	71
Other plots	72
Conclusions	72
CHAPTER 5.        STUDY OF EFFECT OF BED MATERIAL DENSITY ON BRIDGE PIER SCOUR	
Effect of bed material density	127
Log-log plot	128
Conclusions	129
Suggestions	130
BIBLIOGRAPHY	138
APPENDIX I.       PLATES	
APPENDIX II.      NOTATIONS	



LIST OF FIGURES

FIGURE

- 3.1-3.12      Considering the effect of variable  $\frac{W}{B}$  .
- 3.12-3.16      Finding suitable power of variable  $\frac{W}{B}$  .
- 3.17      Variation of  $\frac{d_s}{d} / (\frac{W}{B})^{7/8}$  with  

$$\frac{C_d V^2}{g d_m} \left( \frac{\rho_f}{\rho_s - \rho_f} \right) \quad (\text{gravel range}).$$
- 3.18      Variation of  $\frac{d_s}{d} (\frac{W}{B})^{7/8}$  with  

$$\frac{C_d V^2}{g d_m} \left( \frac{\rho_f}{\rho_s - \rho_f} \right) \quad (\text{sand range}).$$
- 3.19      Considering the effect of variable  $\frac{d}{B}$  .
- 3.20      Finding suitable power of variable  $\frac{d}{B}$  .
- 3.21      Variation of  $\frac{d_s}{d} / (\frac{W}{B})^{7/8} \times (\frac{B}{d})^{7/8}$  with  

$$\frac{C_d V^2}{g d_m} \left( \frac{\rho_f}{\rho_s - \rho_f} \right) .$$
- 4.1      Sieve Analysis.
- 4.2      Experimental Installation.
- 4.3      Enlarged Detail.
- 4.4-4.17      Considering the Effect of Variable  $\frac{W}{B}$  .
- 4.18-4.24      Finding suitable power of variable  $(\frac{W}{B})$  .





FIGURE

4.25 Variation of  $\frac{d_s}{d} / \left(\frac{W}{B}\right)^{7/8} \times \left(\frac{B}{d}\right)^{7/8}$  with

$$\frac{C_d V^2}{g d_m} \left( \frac{\rho_f}{\rho_s - \rho_f} \right) .$$

4.26 Considering the Effect of variable  $\frac{d}{B}$ .

4.27 Finding suitable power of variable  $\frac{d}{B}$ .

4.28-4.35 Variation of scour depth with velocity.

4.36-4.37 Variation of  $\frac{d_s}{d}$  with Froude number.

4.38 Variation of scour depth with time.

5.1 Considering the effect of variable

$$\frac{\rho_s - \rho_f}{\rho_f} .$$

5.2 Finding suitable power of variable  $\frac{\rho_s - \rho_f}{\rho_f}$  .

5.3 Variation of  $\frac{d_s}{d} / \left(\frac{W}{B}\right)^{7/8} \left(\frac{B}{d}\right)^{7/8}$  with

$$\frac{C_d V^2}{g d_m} \left( \frac{\rho_f}{\rho_s - \rho_f} \right) \left( \frac{\rho_s - \rho_f}{\rho_f} \right)^{7/8} .$$



LIST OF TABLES

TABLE

Chapter 3

- |   |   |
|---|---|
| 1 | Scour data (Chatou Laboratory) for S.G. = 2.65<br>$d_m = 3 \text{ mm}$    |
| 2 | Scour data (Chatou Laboratory) for S.G. = 2.65<br>$d_m = 1.5 \text{ mm}$  |
| 3 | Scour data (Chatou Laboratory) for S.G. = 2.65<br>$d_m = 0.52 \text{ mm}$ |
| 4 | Scour data (Chatou Laboratory) for S.G. = 2.65<br>$d_m = 0.26 \text{ mm}$ |

Chapter 4

- |   |  |
|---|--|
| 5 | Scour data (Writer) for S.G. = 1.25<br>$d_m = 1.56 \text{ mm}$ |
|---|--|

Chapter 5

- |   |   |
|---|---|
| 6 | Scour data (Writer) for S.G. = 2.65<br>$d_m = 1.56 \text{ mm}$      |
| 7 | Scour data (Inglis) for S.G. = 2.65<br>$d_m = 1.30 \text{ mm}$      |
| 8 | Scour data (Varzeliotis) for S.G. = 2.65<br>$d_m = 1.70 \text{ mm}$ |
| 9 | Scour data (Neill) for S.G. = 2.65<br>$d_m = 1.70 \text{ mm}$       |



LIST OF PLATESPLATE NO.

- 1 Overall view of flume (looking from the downstream side).
- 2 Slope adjustment devices.
- 3 Hopper for bed material feeding.
- 4 Water spray for washing down the coal in hopper.
- 5 Sliding gate device for adjusting hopper opening.
- 6 Main supply line with discharge regulating valve.
- 7 Flowmeter for discharge measurement.
- 8 Baffles for energy dissipation.
- 9 Ott currentmeter revolution counter.
- 10 Ott currentmeter propeller and point gauge.
- 11 Arrangement for initial water feeding from downstream side of flume.
- 12 Tail gate and sediment trap.
- 13 Pier graduation for reading scour depth below general bed level.
- 14 Typical scour hole in heavy weight bed material.
- 15 Typical scour hole in light weight bed material.





## CHAPTER 1

### LITERATURE REVIEW

#### Introduction

Ever since man learned to place piers and abutments in the streams in order to cross them, the problem of scour of stream bed about the piers and abutments has stood out prominently. Examples of bridge pier failure due to scour are not lacking in the field. Thus, the condition of the screw-pile type foundations was rendered very unsafe due to scour during high floods, warranting the reconstruction of the Mahatsara bridge on the river Ivandro in Madagascar, on new, this time, caisson-sunk foundations (Reference 13). Another example is the "sinking in winter" of the Arta bridge in Greece (Reference 7). The situation was remedied by building a one-span arched structure with no piers. Besides above cases, excessive scour around certain piers of the Hardinge bridge over the Ganges river in Poona, India, during high flood, necessitated the protection of piers by riprap (Reference 6).

Due to the overall complexity of field conditions and the large number of variables involved in bridge pier scour phenomenon, it is virtually impossible to account for the influence of each variable from the field data alone. Any



analytic approach can, again, not be attempted without a complete knowledge of flow pattern and the local transport capacity. Eventually, the best resort left for the solution of the scour problem is the laboratory experimental approach, tried in the past by numerous investigators. But the problem is still not fully resolved because the various approaches have been aimed at some one or other particular aspect of the problem.

Perhaps the earliest significant work in connection with bridge pier scour was done by H. Engels in Germany in 1894, whose experimental work showed that deepest scour occurred at the nose of the pier and that the scour could be arrested by the use of horse-shoe shaped riprap fill around the piers with open end downstream. The above work makes reference to a still earlier one in France by Durand-Claye. The above works were followed by a large number of experimental works by the various investigators over the last seventy years. These works, up to the present day, have sufficiently studied the effects of geometry of channel, geometry of pier, the characteristics of flow and bed material on scour.

Some work has also been done on the devices for protection of scour around pier. The writer recommends treating this as a topic for future research work, to have a more objective approach.





### Literature Review

Although the literature on bridge pier scour is not lacking, the design data are scarce. Amongst the voluminous literature available on bridge pier scour, the following is selected for presentation here because of its being relevant to the bridge pier scour.

The need for reviewing and summarizing the scour literature arises mainly from the fact that the work done on the problem so far is so detailed that its significance can only be fully realized when cast in an abridged form. A recent venture on these lines has been undertaken by Neill (References 4 and 5).

To keep the literature review of reasonable length, it has been felt necessary to be selective while summarizing any work. The following review has been presented in chronological order.

Engels, H. (1894). "Schutz der Strompfeilerfundamente gegen Unterspülung" (Germany). (Protection of the foundation of piers against underscouring). Zeitschrift fur Bauwesen, p. 407.

One of the earliest works pertaining to bridge pier scour, the work mainly embraced the experiments to find the

1. The first part of the document discusses the importance of maintaining accurate records of all transactions and activities. It emphasizes the need for transparency and accountability in financial reporting.

2. The second part of the document outlines the various methods and techniques used to collect and analyze data. It includes a detailed description of the experimental procedures and the statistical analysis performed.

3. The third part of the document presents the results of the study. It includes a series of tables and graphs that illustrate the findings of the research. The data shows a clear trend of increasing activity over time.

4. The fourth part of the document discusses the implications of the findings. It suggests that the results have significant implications for the field of study and may lead to further research in this area.

5. The fifth part of the document concludes the study. It summarizes the main findings and provides a final statement on the importance of the research.

best way to protect piers against scour. It recommended that the riprap or rock fill protection should be laid around pier before scour occurs. Different shapes of the riprap apron were studied. The study concluded that horse-shoe shaped rock fill around a pier, with the open end downstream, was the most simple and efficient. Engels found that the deepest scour occurred at the front of the nose. This has been observed by many subsequent authors, such as Laursen (Reference 11) and Chatou Laboratory (Reference 13), and has been found, by the writer, in Chapter 4.

Flammant, A. (1900) "Affouillements qui en sont la consequence" (French). "Protection around bridge pier as a consequence of the reduction of the section", Hydraulique, Chapter V, Paris.

In this text the author expressed his opinion on the experimental finding by Durand-Claye that a triangular nosed pier caused little scour at the nose although scour occurred at the sides. In the experiments by Durand-Claye three basic shapes of pier section were tried, viz., rectangular, semicircular nose and tail, and triangular nose and tail. It was found, as expected, that maximum scour occurred for the rectangular shaped pier while less depth of scour was noted for the other two shapes, relatively streamlined.



Commenting on Durand-Claye's opinion, Flammant concluded that the most effective shape for reducing scour around the pier was a triangular pier nose and a semi-circular tail portion.

Keuthner, C.H.R. (1932). "The flow around bridge piers of different shapes and its effect on river bed."

(Translated from the German by E.F. Wilsey (1937),  
U.S. Bureau of Reclamation Report HYD - 19,  
Translation No. 40).

Keuthner used 12.2 cm thick piers in a flume 0.6 m wide and with sand bed thickness and flow depth of 20.3 cm. The experiments showed the greatest scour depth occurring at the front of the pier as already concluded by H. Engels (1894). Water surface profiles were taken along the centre line of the pier and along the surface of the pier and transverse to the pier. Scour depth was measured as a function of the angle which the shape of the nose made with the centre line of the pier and it was found that scour was greatest for the semi-circular shape of pier nose. The most important conclusions by the author were that the transverse water surface slope from the pier caused formation of rollers about a horizontal axis, which caused scour, and that the transverse slopes depended upon the shape of the pier nose.





Ishihara, T., (1938). "Experimental study of scour at bridge piers" Trans. Japanese Society of Civil Engineers, Vol. 24, No. 1.

The author pointed out the lack of conformity between the model and the prototype of alluvial channels. Experiments showed that a pier with a sharp nose and tail gives minimum scour and backwater. Another important conclusion was that the scour depth at the pier front was a function of its shape and was independent of the length of the pier and the downstream shape. Later, this was confirmed by Varzeliotis (Reference 7).

Tison, L. J., (1940). "Erosion autour des piles de ponts en riviere" (French). "Erosion around bridge piers." Annales des travaux publics de Belgique, Vol. 41, No. 6.

One of the most extensive works on the bridge pier scour was done by L. J. Tison. The author showed that the velocity at the pier acquired a downward diving component. The strength of this component depended upon:

- 1) curvature of the stream line, which in turn depended upon the shape of the pier in horizontal section, and .
- 2) the vertical velocity gradient, which depended upon the roughness of the bed.



The above conclusions were arrived at by model experiments, with the following test conditions:

Discharge Intensity	0.46 ft <sup>2</sup> /sec
Mean velocity of flow	1.35 ft/sec
Depth of flow	0.34 ft.
Pier dimension in plan view	0.79 ft x 0.20 ft
Median diameter of bed material	0.50 mm

With the above laboratory set-up, various effects of the following different variables were studied, one at a time.

(i) Pier Shape: All other factors remaining constant, the scour depth (below general bed level) was a maximum for a square nosed pier and a minimum for the lenticular shape. For round nosed and bevel nosed piers the scour depth fell between the above two limits. Varzeliotis (Reference 7) later confirmed this.

(ii) Pier Width (Lenticular pier): The less broad the pier the less the scour depth. Indeed it would be so, for the broader the pier, the greater the curvature of flow at the pier, the greater the diving or downward component of velocity which was responsible for scour.



(iii) Pier Length (Rectangular pier): The length of the pier had almost no effect on the depth of the scour around the pier (as also found in Reference 7).

(iv) Angle of Attack (Lenticular pier): As expected, the scour depth increased with the angle of the attack. Thus for least scour, the pier should be aligned with the approach flow direction (as also found in Reference 7).

(v) Depth of Flow: It was found that doubling the flow depth (keeping other things constant) had no effect on scour depth.

(vi) Vertical Velocity Gradient: Different vertical velocity gradients were obtained by paving the bed of approaching channel with pebbles of different shapes. Tison predicted an increased scour depth with larger velocity gradient in an upward direction from the bed.

(vii) Protective devices: The protective devices consisted of piles in a triangular wedge arrangement, which resulted in reduced scour depth at the pier. Continuous paving between the piers was tried also. Whereas the latter eliminated nose scour, it caused deep scour downstream. So long as spacing was not too close, maximum depth of scour at the nose was hardly affected, for piers parallel to flow. Spacing did affect scour depths further downstream.





The author found that the velocity of stream was not necessarily the chief reason for scour at any point, as compared to other significant items listed above.

Inglis, C.C. (1949). "Behaviour and control of rivers and canals." Central Waterpower, Irrigation and Navigation Research Station, Poona, India.

The model experiments listed in this publication were made in connection with a bridge at which deep scour had been observed. The publication is one of the few works available with field data of scour.

Inglis' approach to the problem is based upon the Lacey's empirical formula derived from data of canals in the United Province in India, in which the regime depth of an alluvial channel is related to the dominant discharge and the bed material. Lacey also put forward factors to multiply this regime depth for estimating the maximum scoured depth at channel bends, the value of the factor depending upon the severity of the bend. Inglis went a step further and assumed that maximum total scoured depth at a structure could also be expressed as a multiple of what he termed the 'Lacey depth' (average regime depth calculated from Lacey's formula). The various multiplying factors to be applied to 'Lacey's depth' depended upon the type of the obstruction.



Thus from a table of total scour depths recorded in the field near piers of 17 bridges crossing various alluvial rivers in India, it was found that the multiplying factors fell between 1.7 to 2.4.

On the basis of the model experiments and subsequent plotting on double log paper, Inglis was able to conclude that scour depth could be calculated from the following formula:

$$\frac{d_s}{W} = 1.70 \left( \frac{q^{2/3}}{W} \right)^{0.78}$$

where  $d_s$  = scour depth (from water surface to bottom of scour hole).

Inglis' work needs special mention due to the following two main reasons:

1) The above formula is most widely quoted, in spite of the fact that it was published as early as 1949.

2) While running the experiments the discharge was increased for each test thus increasing simultaneously velocity and depth, as happens actually in a river at rising stage.



The various valuable conclusions drawn from field and laboratory experiments are listed briefly as follows:

(i) When no protection is laid, scour occurs around piers, so that a higher bed is left between the piers.

(ii) Normal practice is to lay stone around the piers of a bridge either as a flat apron or like an inverted boat, the stone usually being one man stone of 60 to 130 pounds weight. When deep scour occurs, it is resisted round piers, and takes place outside the pitching which is undermined and launches, so that maximum scour occurs now between adjoining piers.

(iii) The maximum attack on the loose stone protection occurs at the nose of the pier and sand and stone scoured from upstream are deposited at the tail.

(iv) The stones at the nose remain undisturbed until the attack reaches a critical stage, when the stones suddenly begin to be carried away and a deep scour pit is formed.

(v) The greater the depth at which stones are laid, the more stable they are. Stone should be placed at a level below the deepest general scour that would occur in the approach channel. Stone of adequate size will launch to form a cone around a pier but the resulting obstruction may cause





severe concentration of flow between piers and deep scour immediately downstream, with consequent loss of stone and danger to the pier. Even continuous bed-paving is liable to the same fate.

Hubbard, P.G., (1955). "Field measurement of bridge pier scour" and, Laursen, E.M., "Model-Prototype comparison of bridge-pier scour." Proceedings Highway Research Board, Volume 34, pp. 184 to 192.

The work done by P. G. Hubbard is especially worth mentioning because it is one of the few works available, in which field measurements of scour depths have been taken. The paper is, therefore, included here in somewhat detailed form, as follows:

The scour depth was measured on the Skunk River, Ames, Iowa, for more than a year by means of an electrical apparatus, based on the utilization of difference in conductivity of water and sand-water mixture (an apparatus working on the same principle was used in experiments in Reference 27 and discussed in Reference 26).

Because of the dependence of the scour upon flood duration and because of the scour hole partly filling during recession of water, the scour depth measurements were made



continuously during the course of a flood. The field data collected in the above manner were later compared by Laursen with data obtained from a 1/12th scale model of the Skunk River bridge. Due to the simple geometry of the field site, it was possible to simulate the river by the laboratory flume, so far as the stream and sediment characteristics were concerned. However the velocity of flow and the sediment size were not scaled. Sand size in the laboratory was 0.58 mm.

The equilibrium (maximum) scour depths obtained from the above model were multiplied by 12 and graphically superposed on the field measurements. There was a better agreement between the model and the prototype for small values of depth, whereas for larger depth the model scour depth was 15 percent low. The results indicated a simple scale relation between model and prototype scour. The authors recommended more field measurements to verify their conclusions.

Laursen, E.M., Toch, A. (1956). "Scour around bridge piers and abutments." Bulletin No. 4, Iowa Institute of Hydraulic Research.

The authors suggest that when an obstruction, such as a pier, is placed in a stream, the flow pattern



in the vicinity of that obstruction will be modified. Now since the transport capacity of sediment is a function of the flow, hence transport capacity in turn will also be modified. Thus in any area, where, as a result of modified pattern, the transport capacity out of the area is greater than the rate at which material is supplied to the area, scour will occur. The resultant changes, in the stream bed will further modify the flow pattern and in turn the capacity pattern, until equilibrium between capacity and supply is again reached at every point on the stream bed.

The authors chose the laboratory experimental approach for their further study.

In the experiment, the following standard test conditions were used:

$$W = 0.2 \text{ ft}$$

$$d = 0.3 \text{ ft}$$

$$V = 1.25 \text{ ft/sec}$$

$$d_m = 0.58 \text{ mm uniform sand}$$

A large variety of pier shapes, protective devices and different angles of attack were used. The results were recorded in the form of scour hole contour plans. The various findings by the authors could be abridged as follows:





(i) The upstream portion of the hole had the approximate form of an inverted cone, sometimes distorted from the circular, with side slopes equal to the angle of repose of the sand. The zone of greatest depth was observed at the nose of the pier.

(ii) For a double shaft pier, in the absence of a web, separate scour holes formed around each shaft. The scour hole around the downstream shaft enlarged when the angle of approach was more than  $10^{\circ}$ , the reason being the currents of higher velocity produced by the shaft upstream. At very large angles of approach interference had been seen to disappear. Again, when the columns were joined by a web to form a dumb-bell pier, the maximum scour depth increased greatly as the angle of attack increased.

(iii) As a result of added disturbance to the flow, the presence of debris resulted in more scour.

(iv) For small angles of approach, the nose shape of the pier had some effect on the scour depth.

(v) A separate test indicated that if a footing was set slightly above the bottom of the scour hole which otherwise would have been formed, the scour action was inhibited. A footing set too high was undermined.



(vi) A solid shaft pier starting at or above bed level with only an open piled foundation below, caused less scour than the standard type with a solid shaft below the bed level. The authors found, on the basis of balance between transport capacity of the roller and transport capacity of approach flow, that change in velocity had no effect on scour while change in depth had significant effect on scour. The authors also concluded that scour was not affected by sediment size.

Chabert, J. and Engeldinger, P. (1956) "Etude des affouillements autour des piles de ponts" (French). National Hydraulic Laboratory, France, Series 'A'.

A detailed experimental study was conducted in the laboratory and a large amount of data for maximum scour depth were collected. Most of these data have been used by the writer, for heavy weight bed material analysis in Chapter 2 of the present study. Various tests performed were:

(1) Tests on circular piers: In these tests effects on scour (below general bed level) of different pier diameter, depth of flow, velocity of flow and type of bed material, were studied.



(2) Tests on different pier shapes and the angle of approach.

(3) Test on scour protection measures.

The various important conclusions were:

(1) Under experimental conditions, a bed of silicious alluvium could not be fluidized by the mere action of the flow, even at appreciable slope.

(2) No scour depth took place below a certain threshold tractive force (boundary shear stress).

(3) The maximum scour depth varied linearly with tractive force when there was no movement of the approach bed.

(4) The maximum scour depth passed through a peak as the velocity of flow increased. The peak was reached at velocity close to that corresponding to the beginning of transport.

(5) The best protective device was found to be made of small diameter piles arranged in a triangle at a certain distance from the pier. The above conclusion had the restriction that the device suggested was useful only when the angle of attack did not change.





(6) The investigations did not yield any conditions of similitude probably because of the limited range of the experimental conditions.

Blench, T. (1957). "Regime behaviour of canals and rivers."  
Butterworth Scientific Publications, London and  
Toronto.

The book contained a plot by P. Andru (Reference 8) in which Inglis' field data were plotted on one diagram with experiments by Inglis, Laursen and Toch, Ahmad, Sanders and Smotrych and by Andru himself, using ordinate  $d_s F_b^{1/3}$  against  $q$ , the discharge intensity. Blench argued that this diagram showed a reconciliation between the field and model data. For design he defines a "zero bed-factor"  $F_{bo}$  as follows:

$$d_{fo} = q^{2/3} / F_{bo}^{1/3}$$

$d_{fo}$  is the regime depth of a canal having "zero bed factor" , and discharging through a breadth equal to that estimated for the flow channel diminished by the obstruction. The zero bed factor is the bed factor for a vanishingly small bed load.



The author laid down that the designed depth (measured from water surface) for scour at various obstructions where suitable designed aprons were provided, might be taken safely for adverse conditions of approach by multiplying the "zero flood depth" by the various factors given below:

- (a) Noses of spurs or guide banks: Factor = 2.0 to 2.75
- (b) Flow impinging at right angles on bank: Factor = 2.25
- (c) Between and around bridge piers: Factor = 2.0
- (d) Downstream of barrage with hydraulic jump on floor: Factor = 1.75 to 2.25

The above factors were based on his own practical experience and were also based on the assumption that the river could take any physically possible angle of attack, except for (b), in the course of meandering.

The author's rule for determining maximum scour depth found in a freely meandering channel, without obstacles that interfere in any way with normal meandering, was 1.70 times the regime depth of the approaching straight channel. The author also brought out that the bed material size was relevant to scour depth.



Further a procedure, common in India and Pakistan, was outlined for laying a flexible apron to prevent scour, which consisted of building a bank only above a convenient level, laying the protection on its side slope and then laying the protection that would be required for the rest of the bank (after scour has occurred) as an apron on the natural ground. Scour would undercut and the stones would slide down and settle in a non-cohesive ground, to a slope of 1 upon 2.

Sanden, E.J. (1960). "Scour at bridge piers and erosion of river banks." Proc. of the Western Canadian Association of Canadian Highway Officials.

Stressing the lack of any reliable formula for finding the pier scour, the author discussed the regime theory approach to scour measurement by Inglis and Blench. Methods were described for bank protection against erosion, by means of stone rip rap and by concrete slope-protection slabs with cement sand-bag rip rap.

Mention was also made by the author about the scanty literature available on actual scour measurement and on methods of measurement. According to the author, the depth through winter ice or in shallow depths by rod measurements of scour were impractical with high velocities.





At the end of the paper, the author described in detail a practical method for measuring the scour depth at bridges extensively. Sonic sounders were the chief equipment used in this method, which has the following advantages:

- (1) Portable equipment to avoid expensive duplication.
- (2) Measurements during even high flood possible.
- (3) Quick measurements.
- (4) Economy.
- (5) Sonic sounding instruments need only make contact with the water surface for a brief period because they give depth readings instantaneously.

The various types of sonic sounding instruments available in the market had been briefly mentioned with their electrical specifications. Various occasions and places were mentioned where the sonic sounder method measurement of scour had been tested and used.

Varzeliotis, A.N. (1960). "Model studies of scour around bridge piers." M.Sc. Thesis, University of Alberta, Edmonton, 1960.

The author studied the effect of the pier geometry on the scour depth and scour volume around bridge piers. The



experiments were conducted in a flume  $3\frac{2}{3}$  ft. wide with a bed material of median size equal to 1.7 mm. It was found by the author that:

(1) Shape of pier: Has no serious effect on the magnitude of scour.

(2) Pier length: Increase in pier length also has no serious effect upon the extent of the scour.

(3) Width of pier: Width of pier has a profound effect on the depth of scour. The author has suspected an upper limit up to which the scour depth goes, with increase of pier width.

(4) Angle of attack: Scour depth is seriously affected by the angle of attack which the general flow makes with pier. It has been observed that it is not possible to predict the scour due to this factor by using projected width in place of width of pier.

(5) Flow contraction has a negligible effect up to 10% value.

(6) Debris effect on scour is serious. The author has stressed the difficulty of assessing the amount of debris that a river can carry.



Tests with gravel rip rap laid around piers, showed:

(1) the apron should never, for best results, project above the general bed level around the pier.

(2) The best apron is composed of mixed sizes of stone with smaller stone sizes laid underneath the larger ones, thus preventing the bed material from being picked up.

(3) Further research on apron protection and scour depth are needed.



## CHAPTER 2

### METHODS OF STUDYING BRIDGE PIER SCOUR

#### General

Methods of attack on the bridge pier scour may be classified conveniently as follows:

1. Theoretical. In this method theory has aimed mainly at explaining the broader mechanism of the flow pattern associated with scour. Geometric (boundary conditions) difficulties have prevented useful quantitative formulas from predicting magnitude and extent of scour. Bernoulli's equation (References 21 and 29), jet impact theory (Reference 22) and the concept of secondary currents have been the main tools. Laursen (References 11 and 19) has made use of transport theory.

2. Laboratory experiment. This has been extensive but mainly in straight flumes (References 2, 6, 7, 11, 13, and 24) and with bed material either of quartzose sand or very fine gravel. Light weight bed material, so far as is known, has been used by Posey and Sybert (Reference 30). Flow has usually been directed along the axis of symmetry of a model pier; effect of flow inclined to the axis of symmetry of pier has, however, been studied (References 7 and 11).





Some experiments have been mainly qualitative, aimed at the study of the effects of flow characteristics, geometry of piers or the nature of bed material (References 2, 7, 11 and 13). Others have hoped to represent prototype cases to scale (References 6 and 24), but as prototype have hardly ever been observed, the effectiveness of such scaling is not proved. Dimensional analysis has been used considerably (References 10, 16, and 31) as a guide to extending laboratory results to prototype size; it indicates the number of factors that may be involved in the whole problem, so warns against incautious extrapolations without showing how to avoid them.

3. Field Observations. This approach is almost rare. An outstanding example of observation is by Inglis (Reference 6) and Hubbard (Reference 24). Sanden and Neill (Reference 27) have commented on the shortcomings of field observations and made constructive suggestions for remedy. In particular, Sanden has devised (Reference 26) a sonic sounding outfit for rapid scour traverses during floods. Sometimes the data from the field observations are superposed over laboratory data to test the validity of laboratory experiments (Reference 24).



### Writer's Approach

The writer's approach to the problem has been dimensional analysis combined with laboratory experiments and subsequent plottings. The advantages of such an approach are listed as follows:

1) Identifying, without the risk of missing any, by dimensional analysis the various important non-dimensional parameters, which may have any bearing on scour depth, and then plotting the data from laboratory experiments to study the effect of each parameter.

2) Final results and plots are in non-dimensional form and any other laboratory or field data can be plotted over them, to test their validity (provided the two data are in the same range of essential conditions).

3) Due to the complexity of pier scour problem, perhaps this is the best approach.

### Dimensional Analysis

#### Introduction

Before taking up the actual problem, it will perhaps be necessary to give a brief description, principles and technique of the dimensional analysis.



Dimensional analysis enables us to reduce the number of interconnected variables to a minimum. These variables can then be combined in many different ways, to allow an enormous range of alternative non-dimensional groups, made up of correct number of variables. Again the knowledge of quantitative experimental or field results, and knowledge of probably useful dimensional form relevant to the subject, may lead to selection of non-dimensional parameters that may give simple formulas. The dimensional analysis, by itself, cannot indicate the type of formula, though it gives various non-dimensional groups on which the phenomenon may depend. A prerequisite to the use of dimensional analysis is a dynamical specification of the problem.

Dimensionless parameters have given a great impetus to our understanding of the fluid flow phenomena, and have aided materially by permitting us to apply limited experimental results to cases dealing with different physical dimensions and different physical properties.

Sometimes there appears a dimensionless number in places where there, perhaps, is barely any justification of its occurrence. An example of such a situation occurs in the case of a flow meter, for which the non-dimensional form of phenomenon is:





$$\frac{Q}{A \sqrt{2 \frac{\Delta p}{\rho}}} = \text{fn} \left( \frac{\rho Q D}{\mu A} \right)$$

where

$Q$  = discharge  
 $\Delta p$  = measured pressure drop  
 $A$  = area of nozzle  
 $D$  = diameter of nozzle  
 $\rho$  = density of fluid  
 $\mu$  = dynamic viscosity of fluid.

The right hand side is a Reynold's number. The discharge term occurs in both sides of the equation and one has to resort to trial-and-error method. However, if we re-examine the situation more closely, we could get rid of  $Q$  on one side as follows:

$$\begin{aligned} \frac{Q}{A \sqrt{2 \frac{\Delta p}{\rho}}} &= \text{fn} \left[ \frac{\rho Q D}{\mu A} \times \frac{A \sqrt{2 \frac{\Delta p}{\rho}}}{Q} \right] \\ &= \text{fn} \left[ \frac{\rho D \sqrt{2 \frac{\Delta p}{\rho}}}{\mu} \right] \end{aligned}$$

which is a much better form, so that one can calculate discharge by measuring right hand side.



The above shows that it is possible to multiply or divide any independent or dependent non-dimensional parameter by any one or more other non-dimensional parameters, occurring in the dimensionless equation, and then re-write it.

### Actual Problem

In the most general form, the problem before us can be stated as follows: a bridge pier model is fixed vertically on the centre of the bed of a flume over which water is running with a certain velocity. The discharge in the flume is allowed to run long enough so that the scour depth around the pier reaches an equilibrium. It has been observed that the maximum depth of scour is almost invariably found at the upstream of pier nose and is readily measurable by means of graduation on the upstream nose of the pier. Let this time-maximum scour depth at the pier nose be called  $d_s$  (measured from the general bed level to the deepest point in the scour hole).

Calling  $d_s$  a dependent parameter, the primary problem is to identify various dimensional variables on which the maximum scour depth depends. All such dimensional parameters, can be classified in four categories:

...the ... of ...  
...the ... of ...  
...the ... of ...  
...the ... of ...

...the ... of ...  
...the ... of ...  
...the ... of ...  
...the ... of ...

...the ... of ...  
...the ... of ...  
...the ... of ...  
...the ... of ...

...the ... of ...  
...the ... of ...  
...the ... of ...  
...the ... of ...

...the ... of ...  
...the ... of ...  
...the ... of ...  
...the ... of ...

Hydraulic Variables: These are the parameters which describe the flow regime, such as

Velocity of flow upstream of pier =  $V$

Depth of flow =  $d$

Velocity Distribution above bed level

Pressure Distribution above bed level

Sediment Transport

Slope =  $s$

Geometric Variables: These parameters can also be called geometric parameters, as these describe mostly the geometrical features of experiment. These are:

Pier shape given by =  $A$

Pier Diameter =  $W$

Orientation of pier with respect to current

=  $\alpha$

Width of flume =  $B$

or Constriction Ratio =  $\frac{B-W}{B}$

Bed Variables: The third significant category of dimensional parameters is concerned with bed characteristics. These are mostly related to the composition of bed and bed material, such as:

THE UNIVERSITY OF CHICAGO

THE DIVISION OF THE PHYSICAL SCIENCES

DEPARTMENT OF CHEMISTRY

CHICAGO, ILLINOIS

RECEIVED

APRIL 10, 1954

1954

TO THE EDITOR

Enclosed for your information are two copies of a manuscript

entitled "The Structure of the Benzene Ring"

Yours very truly,

ROBERT M. MULLIKEN

Director, Division of Physical Sciences

Enclosure

cc - Mr. J. H. Van Vleet

10

Very truly yours,

ROBERT M. MULLIKEN

Director, Division of Physical Sciences

Enclosure

Median Grain Size (Diam.) =  $d_m$

Density of Bed Material =  $\rho_s$

Nature of Bed

Distribution of Bed particle sizes.

#### Fluid and Miscellaneous Variables:

Density of Water =  $\rho_f$

Dynamic viscosity =  $\mu$

Gravity acceleration =  $g$

#### Reduction of Variables

The numerous variables make it advisable to reduce their number as far as possible by simplifying the original problem. Thus, if we are able to attain the following conditions, the situation is rendered much simpler.

- (1) Circular Pier, placed along flume centre line vertically.
- (2) Bed is of non-cohesive coarse sand or coal.
- (3) Median size of coal and stone bed particle is same, and the size distribution is same (i.e., size distribution curves fall over one another).
- (4) Same velocity distribution, above bed level.





Due to the above conditions, the various variables will now become:

(1) Hydraulic variables

$$\text{Velocity} = V$$

$$\text{Depth} = d$$

(2) Geometric variables

$$\text{Diameter of pier} = W$$

$$\text{Width of flume} = B$$

(3) Bed Variables

$$\text{Median diameter of bed particle} = d_m$$

$$\begin{aligned} \text{Difference in specific gravity} &= \left( \frac{\rho_s - \rho_f}{\rho_f} \right) = S-1 \\ \text{of bed material and water} & \end{aligned}$$

(4) Fluid and Miscellaneous variables

$$\text{Dynamic viscosity} = \mu$$

$$\text{Density of water} = \rho_f$$

$$\text{Gravity acceleration} = g$$

Let  $d_s$  be chosen as a dependent variable, then, we can write that:

$$d_s = \text{fn} \left[ d, V, W, \frac{\rho_s - \rho_f}{\rho_f}, g, \nu, d_m, B \right] \quad (A)$$

Making the parameters non-dimensional:

$$\frac{d_s}{d} = \text{fn} \left[ \frac{V^2}{gd_m} \cdot \left( \frac{\rho_f}{\rho_s - \rho_f} \right), \frac{W}{B}, \frac{d}{d_m}, \frac{d}{B}, \frac{Vd_m}{\nu} \right]$$



The Reynolds number can be found by using average velocity, neglecting the effect of velocity gradient, which is not yet fully known. From the logarithmic velocity distribution law by Prandtl, the velocity at particle level can be taken as a function of the average velocity. It would appear as the average velocity in calculating the Reynolds number.

Considering drag coefficient ' $C_d$ ' as a function of Reynolds number, field of turbulence, proximity of boundaries and surrounding particles, except for the Reynolds number, the effects of the other factors listed in the above equation are not yet fully known. The scour phenomenon itself makes the effects of the above factors still more complicated. Because of the uncertainties involved in the above factors, the writer has taken, as a first approximation, the drag coefficient as a function of Reynolds number.

Replacing  $\frac{Vd_m}{\nu}$  in the above equation by the drag coefficient  $C_d$ :

$$\frac{d_s}{d} = \text{fn} \left[ \frac{V^2}{gd_m} \cdot \frac{\rho_f}{(\rho_s - \rho_f)} , \frac{W}{B}, \frac{d}{d_m}, \frac{d}{B}, C_d \right]$$



On closely examining the expression  $\frac{v^2}{gd_m} \left( \frac{\rho_f}{\rho_s - \rho_f} \right)$ , it can be seen that it is similar to the densimetric Froude number except that the densities, here, refer to the solid and liquid. As a first attempt to improve the above simple expression, it can be multiplied by the drag coefficient  $C_d$ , knowing that it is not strictly applicable, but in the expectation that it is better than not making a correction at all. Using  $C_d$  with the above expression, we can write the new expression as follows:

$$C_d \frac{1}{2} \rho_f v^2 \left( \frac{\pi}{4} d_m^2 \right) \div (\rho_s - \rho_f) g \frac{\pi}{6} d_m^3$$

To be more appropriate, the above expression should be called a measure of the ratio of drag and buoyant weight of the particle.

Thus:

$$\frac{d_s}{d} = \text{fn} \left[ \frac{C_d v^2 \rho_f}{gd_m (\rho_s - \rho_f)} , \frac{W}{B} , \frac{d_m}{d} , \frac{d}{B} , C_d \right] \quad (B)$$

### Meaning and Importance of First Parameter

Multiplying the numerator and denominator of the first expression by  $d_m^2$ , we get

$$\frac{C_d \rho_f v^2 d_m^2}{gd_m^3 (\rho_s - \rho_f)} = \text{Measure of the } \frac{\text{drag force on particle}}{\text{buoyant weight of particle}}$$





The above parameter stands out as it gives a measure of the ratio of the two important factors or forces, that play a dominant role in the scour phenomenon.

The drag force on a particle always tries to wash it away, hence it can be considered as a scouring force, whereas the only resistive force is provided by the buoyant weight of the particle. Taking the case of a single particle at bed level, as the velocity of flow increases from zero, the drag force on the bed particles increases whereas the submerged weight of the particle remains constant. Very soon the velocity reaches a value where the drag force on the particle becomes sufficient to dislodge it from its position. At this stage the submerged weight of the particle will become effective and will tend to prevent its being washed away. Thus the dislodging of the particle from its position, i.e., scouring of particle, is only a matter of 'tussle' between the drag force and the gravity force on submerged particle.

Since the primary object of the present study is to identify and account for the effects of variable bed material density, the above parameter has the additional advantage of its having included in it the bed density factor.



### Graphical Approach

The following is the line of graphical approach used in Chapter 3, 4, and 5.

The plots between  $[\frac{d_s}{d}]$  as ordinate and  $[\frac{C_d V^2}{g d_m} \cdot \frac{\rho_f}{\rho_s - \rho_f}]$  for different pier diameters 'W', can be combined into a single plot, by multiplying the ordinate term by a suitable power of the only variable term  $\frac{W}{B}$ . Next the plots for different grain size can be combined into a single one by including in the ordinate term, proper power of the pertaining variable  $\frac{d_m}{d}$ . Similarly the plots for various depths and different densities of bed material can also be brought together into one single plot by considering suitable powers of concerned variables 'd/B' and  $(\rho_s - \rho_f)/\rho_f$  respectively.

### Range of Data Used

In order to test the range of stone data (taken from References 13 and 14), some data with stone as bed material instead of coal were obtained by the writer and plotted on final Figure 5.1 in Chapter 5.



### CHAPTER 3

#### SCOUR IN HEAVY WEIGHT BED MATERIAL

##### Source of Data.

The data for the heavy weight bed material analysis are taken from a report entitled "Etude Des Affouillements Autour Des Piles Des Ponts", Series 'A', October, 1956, of the Laboratoire National D'Hydraulique, 6 Quai Watier, Chatou, France. The original paper uses the metric system of measurements. The data listed in Tables 1 to 4 have been taken from the English translation of the above paper by C. R. Neill (July 1961) (Reference 14).

##### Experimental Detail

###### Set up:

The set up of Chatou Laboratory experiments was as follows:

Straight Glass flume:

width = 2.6'

total length = 69.0'

length of mobile bed = 49.0'

Entry section for stilling = 10.0' long

total height = 2.3'

slope variation = 0 to 10%



Discharges were measured by two venturimeters in parallel. The excess energy of water entering the flume was destroyed by use of transverse baffles and a floating plank.

#### Data Collected

Maximum scour depth (measured below general bed level) data were collected over a considerable range of discharge, with:

1) Four different sizes of circular-sectioned piers, i.e., with diameters = 0.164', 0.246', 0.328' and 0.491'. The data listed in Tables 1 to 4 were pertaining to pier sizes 0.164', 0.246' and 0.491', as the fourth size, i.e., 0.328' was not aligned on the centre line of the flume.

2) Four different grain sizes, represented by mean diameters of particles of 3, 1.5, 0.52, and 0.26 mm.

The velocity was varied between 0.41 to 0.82 ft/sec.

#### Analysis of Data

##### Compilation of Tables:

The data have been listed in Tables 1 to 4, each respectively for the particle sizes 3, 1.5, 0.52 and 0.26 mm.





The values of  $\frac{d_s}{d}$  and  $\frac{C_d V^2}{g d_m} \cdot \frac{\rho_f}{(\rho_s - \rho_f)}$  were calculated. The specific gravity for stone was used equal to 2.65.

Before calculating  $\frac{C_d V^2}{g d_m} \cdot \frac{\rho_f}{\rho_s - \rho_f}$ , the value of drag coefficient  $C_d^*$  was found out for each case. For that the Reynolds number was calculated as  $V d_m / \nu$  in which a kinematic viscosity of  $1.2 \times 10^{-5} \text{ ft}^2/\text{sec}$  was used.

### Plots

To start with  $\frac{d_s}{d}$ , as ordinate, was plotted against  $\frac{C_d V^2}{g d_m} \cdot \frac{\rho_f}{\rho_s - \rho_f}$  as abscissa for each of the depths 0.656', 0.328' and 1.15', in Figures 3.1, 3.2, and 3.3, for  $d_m = 3\text{mm}$ . Similar plots were made for the other particles sizes of 1.5 mm, 0.52 mm and 0.26 mm in figures 3.4 to 3.12. In each case the plotted points fell in such a way that a smooth curve could be passed through these.

#### 1) Considering the Effect of Variable W/B

In each of Figures 3.1 to 3.12, there were three curves for the three different-sized piers. The only variable different for these three curves, in each figure, was the ratio W/B. For three pier diameters of 0.491', 0.328' and 0.164', the values of W/B were 0.189, 0.126, and 0.063 respectively. The aim, then, was to find

---

\* Value of  $C_d$  in Tables 1 to 9, were taken from Figure 10' of Reference 9.



a suitable power of  $W/B$  so that when this was multiplied by the ordinate  $d_s/d$  of each curve, we could end up with one single plot.

Before finding the suitable power of  $W/B$  it was ascertained that in each of Figures 3.1 to 3.12 the curves between  $\frac{d_s}{d}$  and  $\frac{C_d V^2}{g d_m} \left( \frac{\rho_f}{\rho_s - \rho_f} \right)$  for different pier sizes had the same shape and their peaks lie, more or less, above each other's. The required power was given by the slope of parallel lines in Figures 3.13 to 3.16 obtained by plotting values of  $W/B$  as abscissae against values of the  $\frac{d_s}{d}$  for three reasonably apart values of  $\frac{C_d V^2}{g d_m} \left( \frac{\rho_f}{\rho_s - \rho_f} \right)$  represented by vertical lines in figures 3.1 to 3.12. Numbers on the vertical lines in Figures 3.1 to 3.12 correspond to the same numbers on lines in Figure 3.13 to 3.16. All the lines in Figure 3.13 and 3.14 gave a slope of  $7/8$ , whereas the slope of the lines in Figure 3.15 and 3.16 was  $1/2$ . Figures 3.13 and 3.14 were concerned with the bed particle sizes of 3 mm and 1.5 mm whereas the figures 3.15 and 3.16 corresponded to the bed particle sizes of 0.52 mm and 0.26 mm. Hence the exponent of  $W/B$  for gravel sized bed material was  $7/8$  while its value for sand sized bed material was  $1/2$ .



Check for the suitability of the exponent found for  $W/B$  was applied by multiplying the ordinates of curves in Figures 3.1 to 3.12, by the corresponding value of  $(W/B)^{7/8}$ , and replotting them. If the value of the exponent was correct, it could be possible to pass one single plot through them. This single plot was labelled "resultant curve" in Figures 3.1 to 3.12. These resultant curves were, thus, a plot between  $\frac{d_s}{d} / (W/B)^{7/8}$  and  $\frac{C_d V^2}{g d_m} \left( \frac{\rho_f}{\rho_s - \rho_f} \right)$  and considered the effect of variable  $W/B$ , characteristic of the pier diameter "W".

## 2) Considering the effect of variable $\frac{d_m}{d}$

On studying the resultant curves in Figures 3.1 to 3.12, it was observed that there was a greater possibility of considering the effect of the variable  $\frac{d_m}{d}$  with reference to the resultant curves in Fig. 3.1 to 3.6, due to the reason that the resultant curves of Figures 3.7 to 3.12 belonged to a different type of the curves.

a) Gravel range: The resultant curves in Figure 3.1 to 3.6 were transferred to one sheet in Figure 3.17. It was observed from Figure 3.17 that the resultant curves between  $\frac{d_s}{d} / (W/B)^{7/8}$  and  $\frac{C_d V^2}{g d_m} \cdot \left( \frac{\rho_f}{\rho_s - \rho_f} \right)$  have coincided, for the portions up to some distance beyond the peaks. This showed that the parameter  $\frac{d_m}{d}$  was not





effective up to approximately a value of 6 of  $\frac{C_d V^2}{g d_m} \left( \frac{\rho_f}{\rho_s - \rho_f} \right)$ . Beyond this value of  $\frac{C_d V^2}{g d_m} \left( \frac{\rho_f}{\rho_s - \rho_f} \right)$ , the two curves (for one the same depth) did not coincide. For non-coincident portions of curves, the curve for smaller bed particle size, for each depth lay above the one for the large particle size, showing, as expected, that there would be larger scour depth for smaller particle size than for the one for larger particle size.

The no-effect of the  $\frac{d_m}{d}$  for values less than approximately six of the  $\frac{\text{drag force}}{\text{buoyant weight}}$  ratio, as observed above, could also be justified from the consideration of fall velocity. For  $d_m$  greater than approximately one mm, the fall velocity is proportional to the square root of the particle diameter. Hence the fall velocity does not change much for the change of particle size (or  $\frac{d_m}{d}$  ratio for a constant depth). Now since scour is dependent upon the fall velocity of particle, there is, therefore, no significant change in the nature of scour, for the variation of particle diameter, when the size is the approximately above one mm.

The non-coincidence of portions of plots in Figure 3.17 could be also due to the complicated effect of the bed transport which enters the picture for the range of



$$\frac{C_d V^2}{g d_m} \left( \frac{\rho_f}{\rho_s - \rho_f} \right), \text{ under consideration.}$$

Since, from the practical point of view, we are more concerned with the worst conditions of scour, i.e., the peaks in Figure 3.17, so we should be satisfied from the point of view of further analysis with the coincidence of the peaks.

b) Sand Range: The resulting six curves in Figures 3.7 to 3.12 were traced on one sheet in Figure 3.18 'A', which showed that the various plots lay so divergently from each other that their combination into one curve seemed difficult. This indicates the divergent effect of the  $\frac{d_m}{d}$  in the sand range.

### 3) Considering the Effect of Variable $d/B$

The coincident portions of plots in Figure 3.17 were transferred to Figure 3.19. It was observed that the three different curves in Figure 3.19 had almost the same shape and their peaks were almost above each other. The only different variable for the three curves in Figure 3.19 was  $d/B$ , which also occurred in equation (B) of the dimensional analysis in Chapter 2. Exactly by the same technique, as employed for finding the power of variable  $W/B$ , the power for the variable  $d/B$  was found to be  $7/8$  from



the log-log plot in Figure 3.20. The resulting single curve appeared in Figure 3.19. This new curve was between

$$\frac{d_s}{d} / \left(\frac{W}{B}\right)^{7/8} \times \left(\frac{B}{d}\right)^{7/8} \quad \text{and} \quad \frac{C_d V^2}{g d_m} \left(\frac{\rho_f}{\rho_s - \rho_f}\right).$$

### Log-log Plot:

The resultant curve in Figure 3.19 was plotted on a log-log paper in Figure 3.21. The equation of the straight line obtained was:

$$\frac{d_s}{d} / \left(\frac{W}{B}\right)^{7/8} \times \left(\frac{B}{d}\right)^{7/8} = 0.27 \left[ \frac{C_d V^2}{g d_m} \left(\frac{\rho_f}{\rho_s - \rho_f}\right) \right]^{1.33} \quad \text{-----}(3.1)$$

### Conclusions

1) The non-dimensional scour depth is zero, until the  $\frac{\text{drag force}}{\text{buoyant weight}}$  reaches a certain value.

2) From the consideration of the equation 3.1 when all the other factors remain unchanged, the non-dimensional scour depth varies

- i) Directly with the  $7/8$  power of the parameter  $W/B$
- ii) Inversely with the  $7/8$  power of the parameter  $d/B$
- iii) Directly with  $1.33 \simeq 1\frac{1}{3}$  power of the  $\frac{\text{drag force}}{\text{buoyant weight}}$
- iv) The maximum scour depth from practical point of view is (from Figure 3.19) equal to  $1.5 \left(\frac{W}{d}\right)^{7/8}$



The above shows the important effect of the parameters  $W/B$  and  $d/B$  on the scour depth; the effect of  $\frac{\text{drag force}}{\text{buoyant weight}}$  is relatively more important since the last parameter has a power of  $1\frac{1}{3}$ .

3) For flow on a gravel bed for a given depth the grain size has almost negligible effect on the non-dimensional scour depth (Figure 3.17), up to slight distance after the peak. Beyond that, the scour is more for fine gravel than for coarse.





HEAVY WT. BED MATERIAL

CONSIDERING THE EFFECT OF VARIABLE  $W/B$

FOR

$$d_m = 3 \text{ mm}$$

$$d = 0.656$$

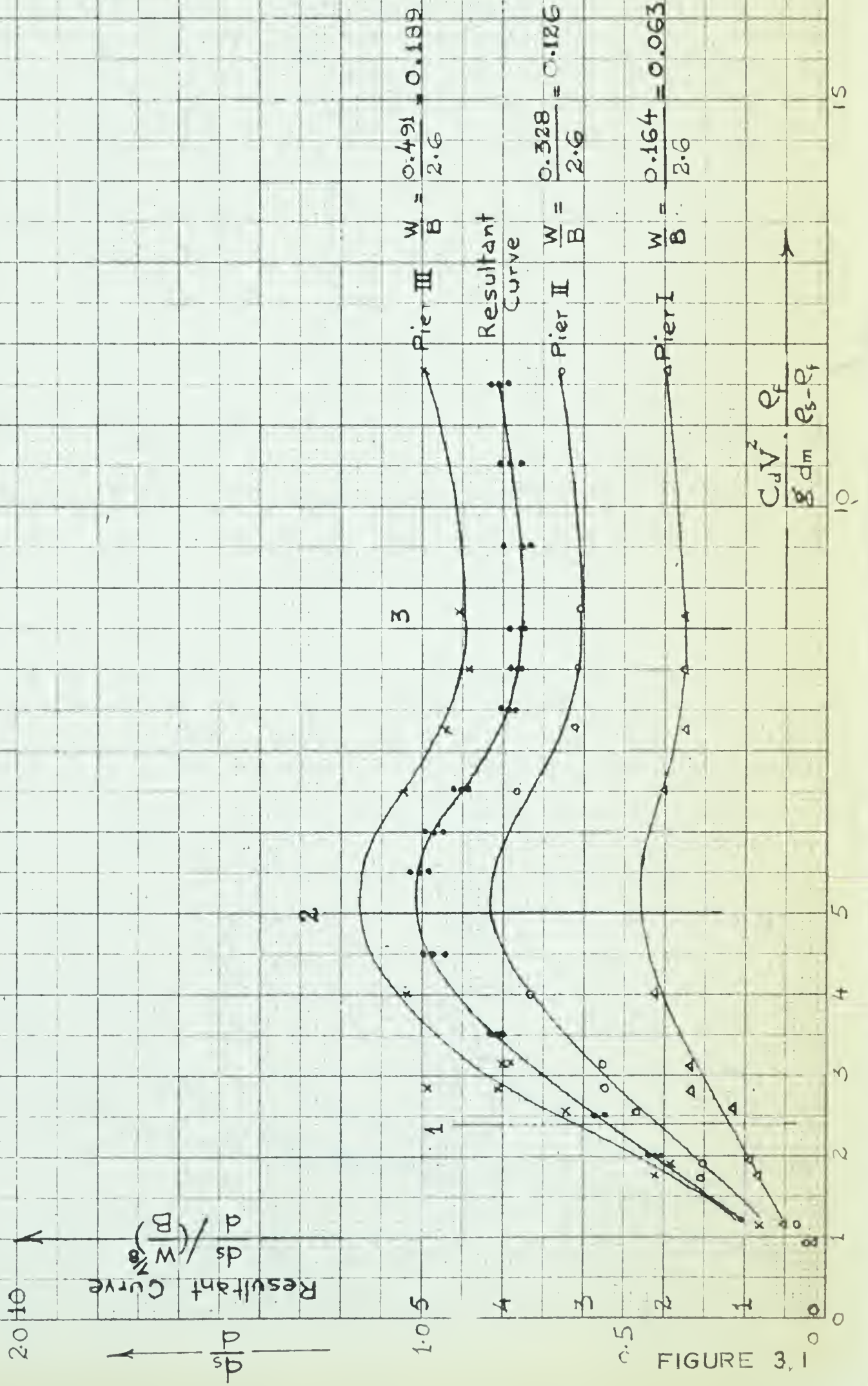


FIGURE 3.1





HEAVY WT. BED MATERIAL

# CONSIDERING THE EFFECT OF VARIABLE $W/B$

FOR

$d_m = 3 \text{ mm}$

$d = 0.328'$

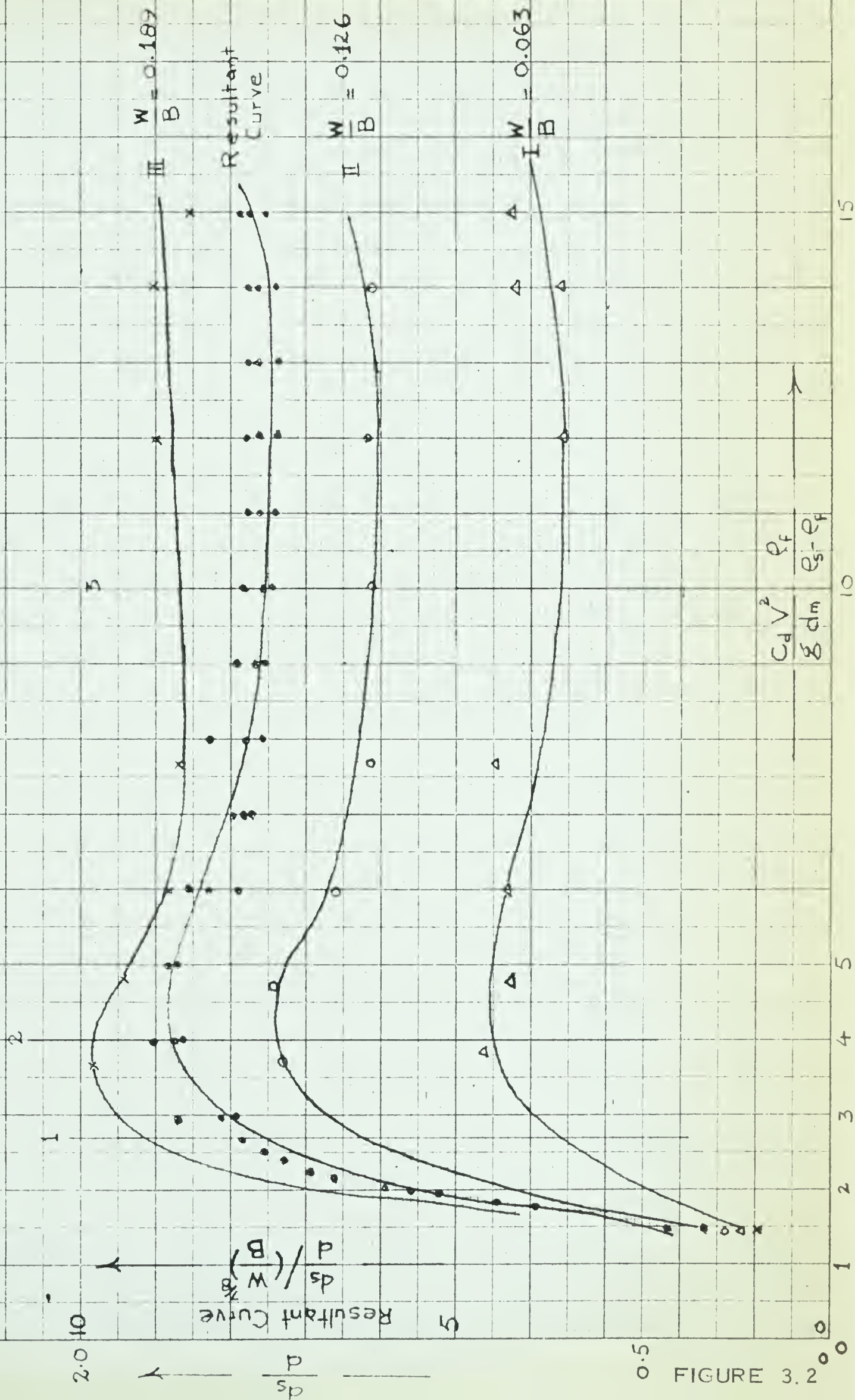


FIGURE 3.2





HEAVY WY. DED MATERIAL

CONSIDERING THE EFFECT OF VARIABLE W/B

FOR  
 $d_m = 3 \text{ mm}$   
 $d = 1.15'$

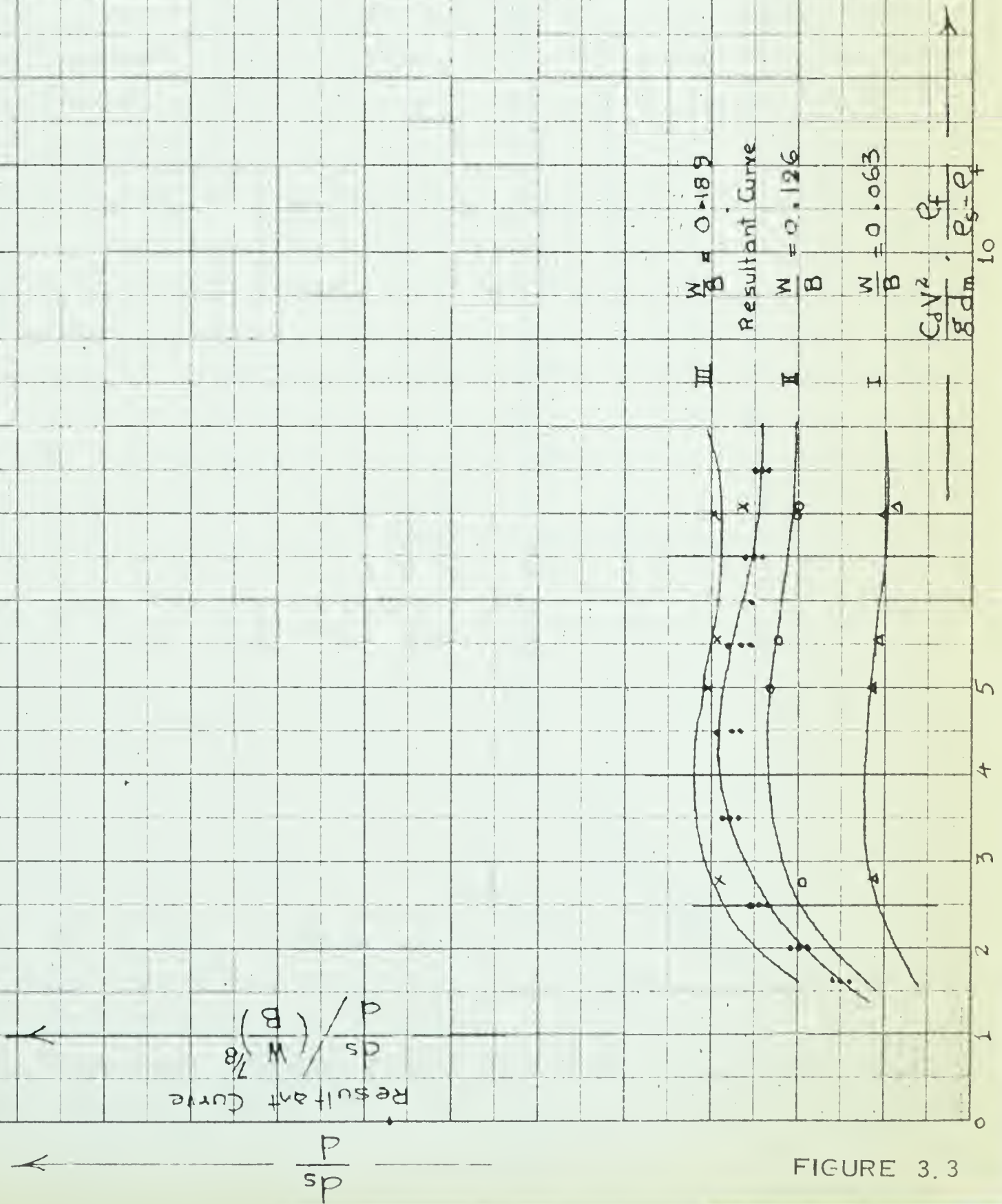


FIGURE 3.3





HEAVY WT. BED MATERIAL

CONSIDERING THE EFFECT OF VARIABLE  $W/B$

FOR

$d_m = 1.5 \text{ mm}$

$d = 0.656$

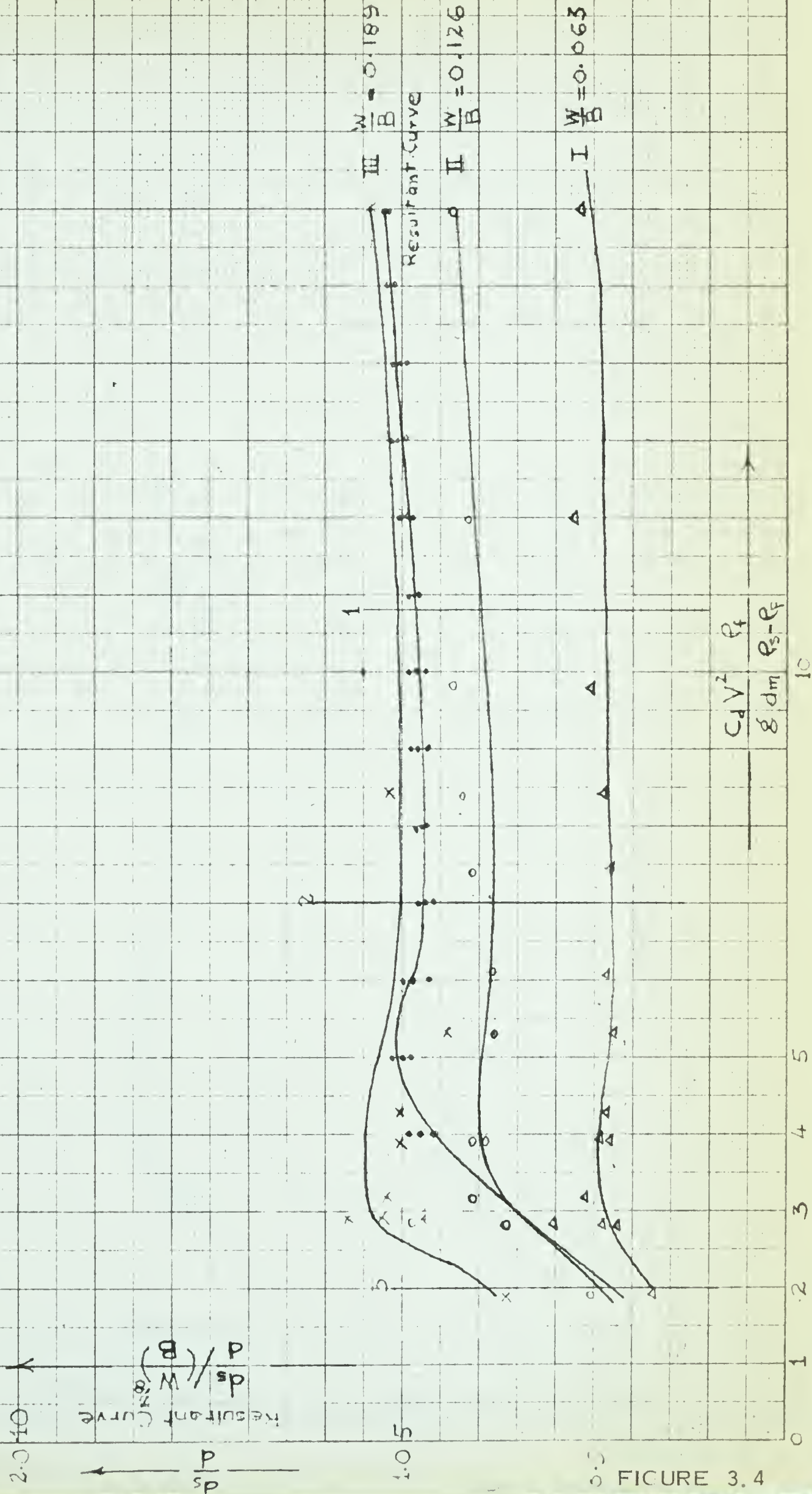


FIGURE 3.4





HEAVY WT. BED MATERIAL

CONSIDERING THE EFFECT OF VARIABLE  $W/B$

FOR

$$d_m = 1.5 \text{ mm}$$

$$d = 0.328'$$

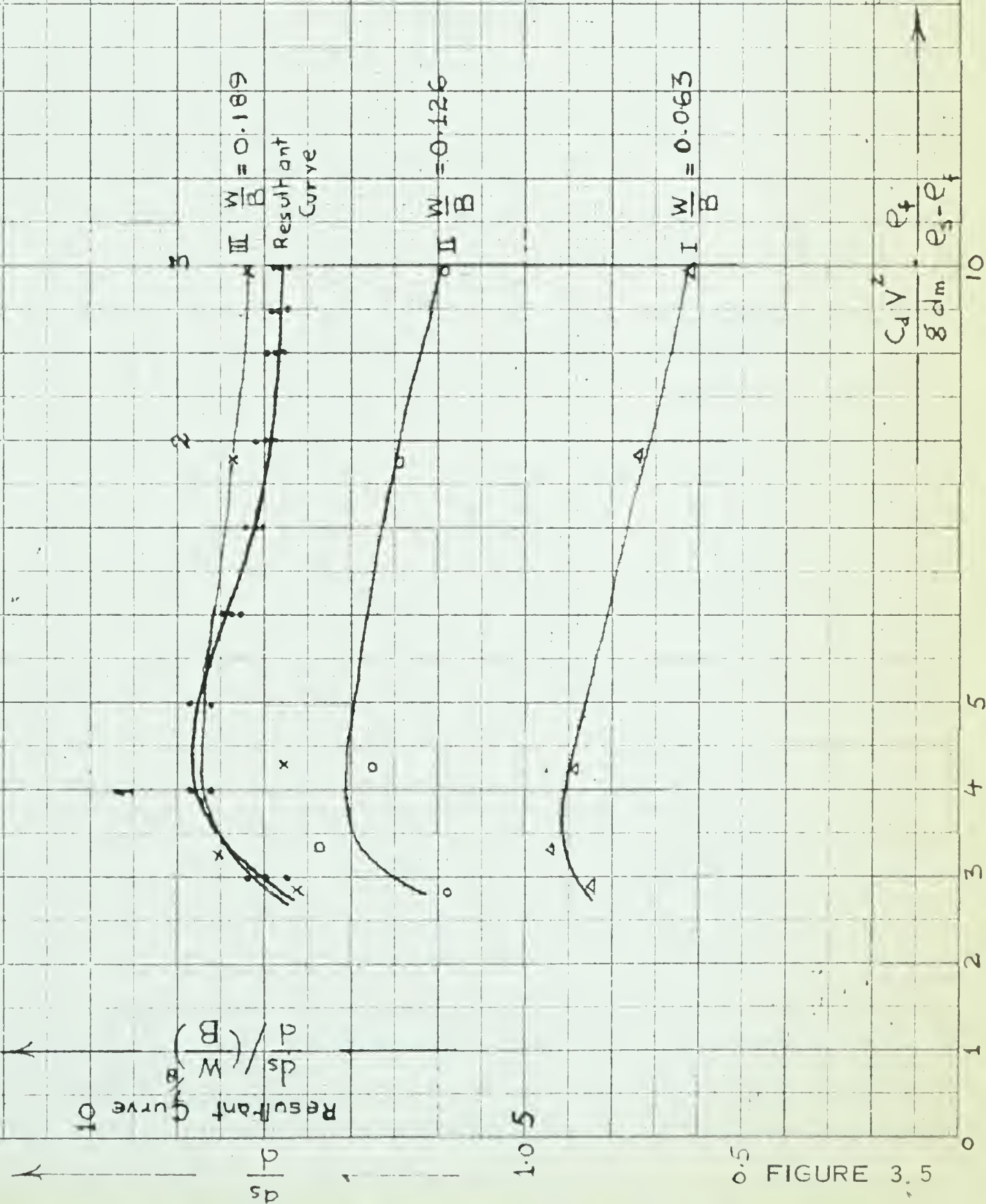


FIGURE 3.5



HEAVY WT. BEU MATERIAL

# CONSIDERING THE EFFECT OF VARIABLE W/B

FOR

$$d_m = 1.5 \text{ mm}$$

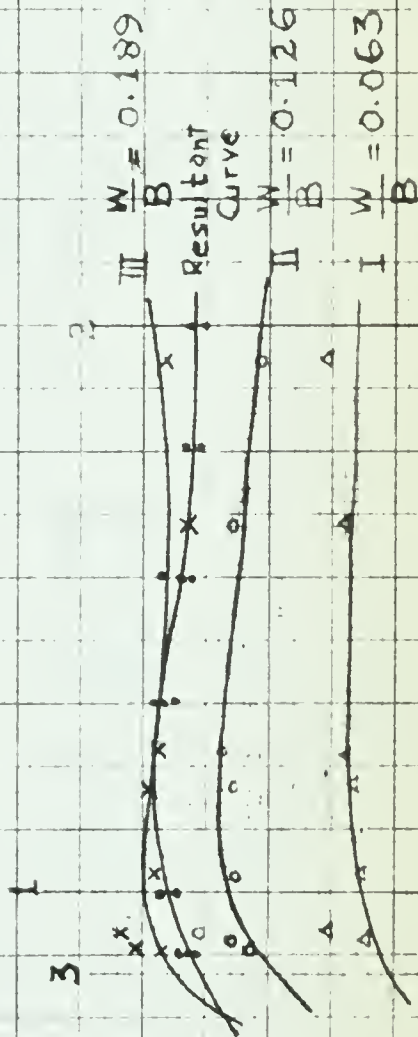
$$d = 1.15'$$

Resultant Curve  
 $\frac{d_s}{d} / \left( \frac{B}{W} \right)^{1/2}$

1.0 5

0.5

FIGURE 3.6



$$\frac{C_d V^2}{g d_m} \cdot \frac{e_f}{e_s - e_f}$$

10





# CONSIDERING THE EFFECT OF VARIABLE W/B

FOR

$$d_m = 0.52 \text{ mm}$$

950-01

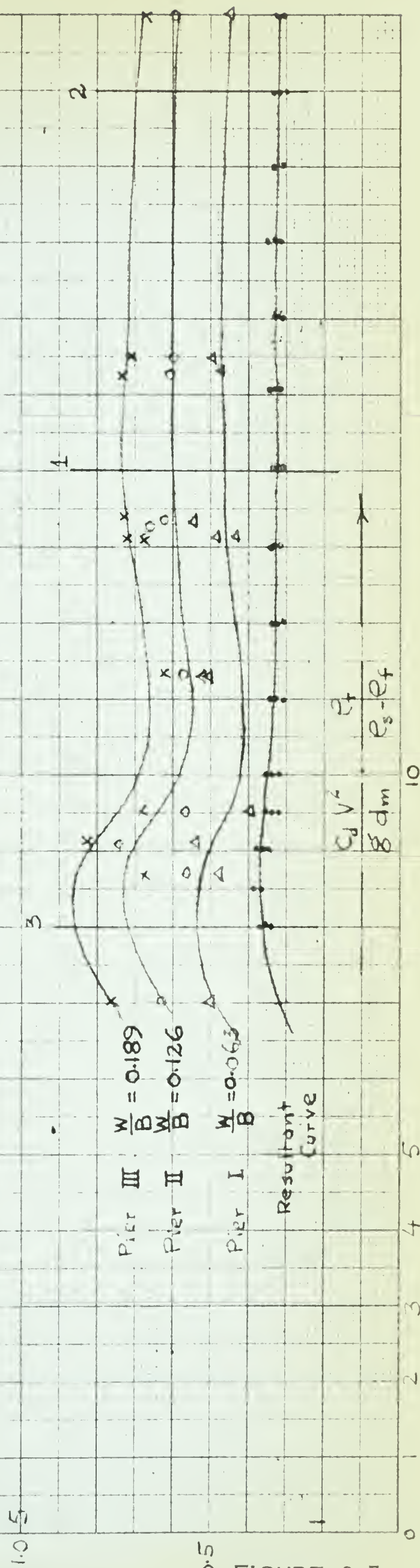
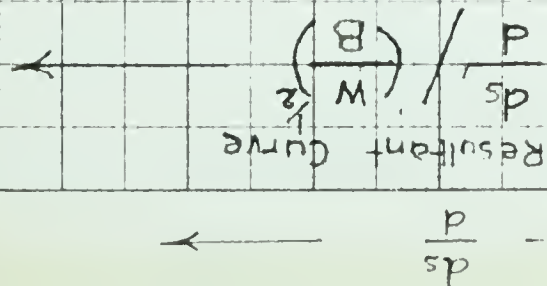


FIGURE 3.7





HEAVY WT. TIED MATERIAL

CONSIDERING THE EFFECT OF VARIABLE W/B

FOR

$$d_m = 0.52 \text{ mm}$$

$$d = 1.15'$$

Resultant Curve  
 $\frac{ds}{dw} \left( \frac{B}{d} \right)^{1/2}$

Resultant Curve  
 $\frac{W}{B} = 0.189$  III  
 $\frac{W}{B} = 0.126$  II  
 $\frac{W}{B} = 0.063$  I

$C_d V^2$   
 $g d_m$   
 $\rho_f$

FIGURE 3.8





HEAVY WT. BEN MATERIAL

CONSIDERING THE EFFECT OF VARIABLE W/B

FOR

$$d_m = 0.52 \text{ mm}$$

$$d = 0.528'$$

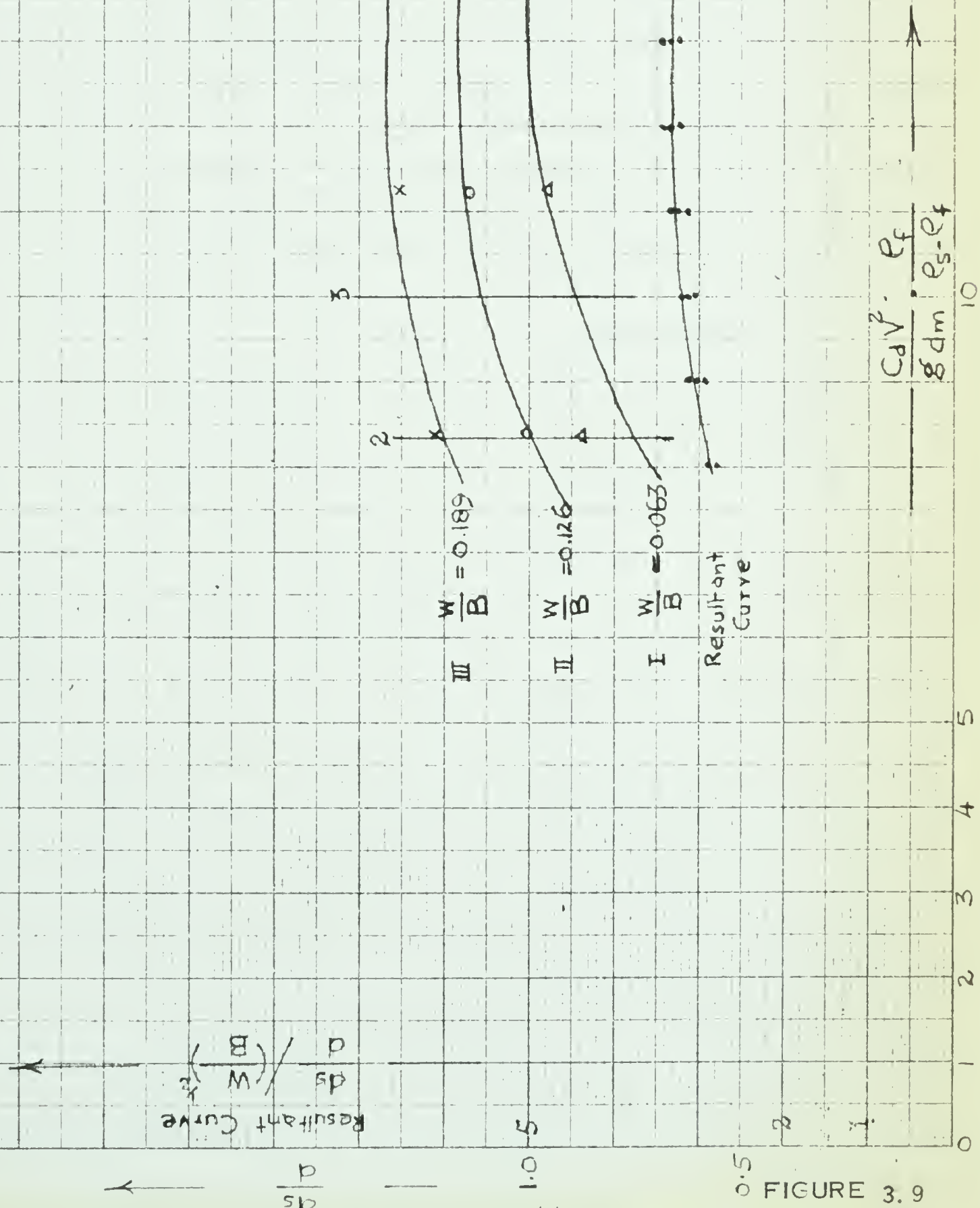


FIGURE 3.9





HEAVY WT. BED MATERIAL

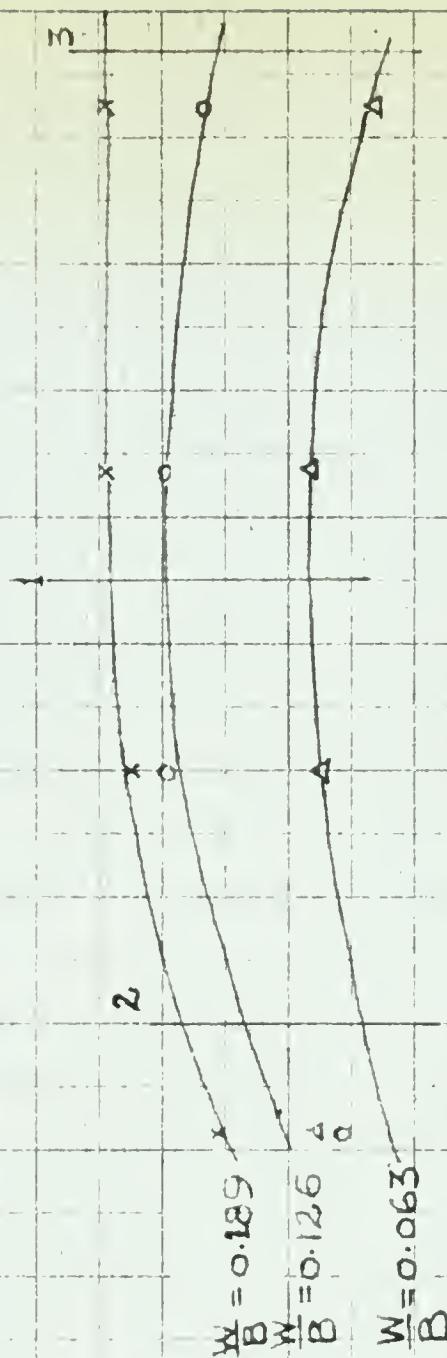
CONSIDERING THE EFFECT OF VARIABLE  $W/B$

FOR

$$d_m = 0.26 \text{ mm}$$

$$d = 0.656'$$

Resultant Curve  
 $\frac{ds}{dW} \left( \frac{B}{W} \right)^{1/2}$



Resultant Curve:

$$\frac{C_d V^2}{g d_m} \cdot \frac{e_t}{e_s - e_t}$$

20 21 22 23 24 25 26 27 28 29 30 31 32 33 34 35 36 37 38 39 40

FIGURE 3.10



LIGHT WT. RED MATERIAL

CONSIDERING THE EFFECT OF VARIABLE  $W/B$

FOR

$d_m = 0.26 \text{ mm}$

$d = 1.15'$

$\frac{ds}{d}$   
Resultant Curve  
 $\frac{ds}{d} \left( \frac{W}{B} \right)$

III  $\frac{W}{B} = 0.189$   
II  $\frac{W}{B} = 0.126$   
I  $\frac{W}{B} = 0.063$

Resultant Curve

20 21 22 23 24 25 40 40  
 $C_d V^2$   $\rho_f$   $8'd_m$   $e_s - e_f$

FIGURE 3.11





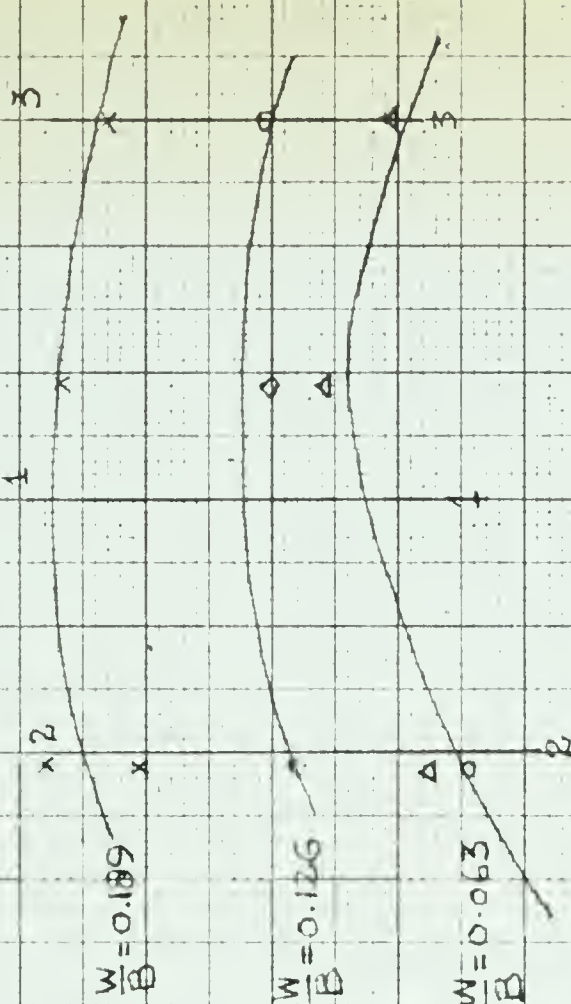
HEAVY WT. BED MATERIAL

CONSIDERING THE EFFECT OF VARIABLE  $W/B$

$P_t/R$

$$d_m = 0.26 \text{ mm}$$

$$d = 0.328'$$



Resultant Curve

$$\frac{C_d V^2}{g' d_m} \cdot \frac{P_t}{e_s - e_f}$$

(Resultant Curve)

0 20 21 22 23 24 25 40 40

FIGURE 3.12





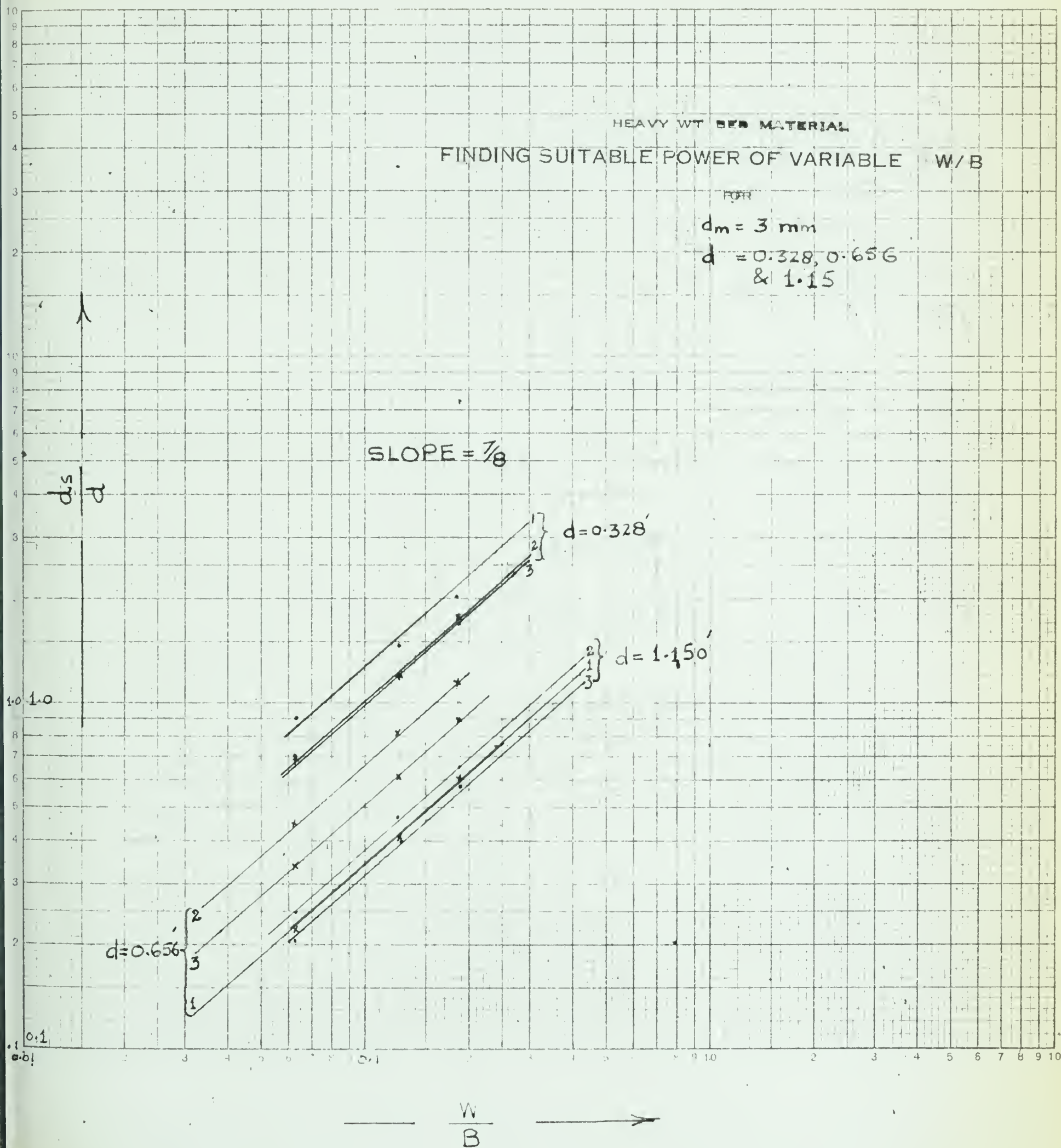


FIGURE 3.13



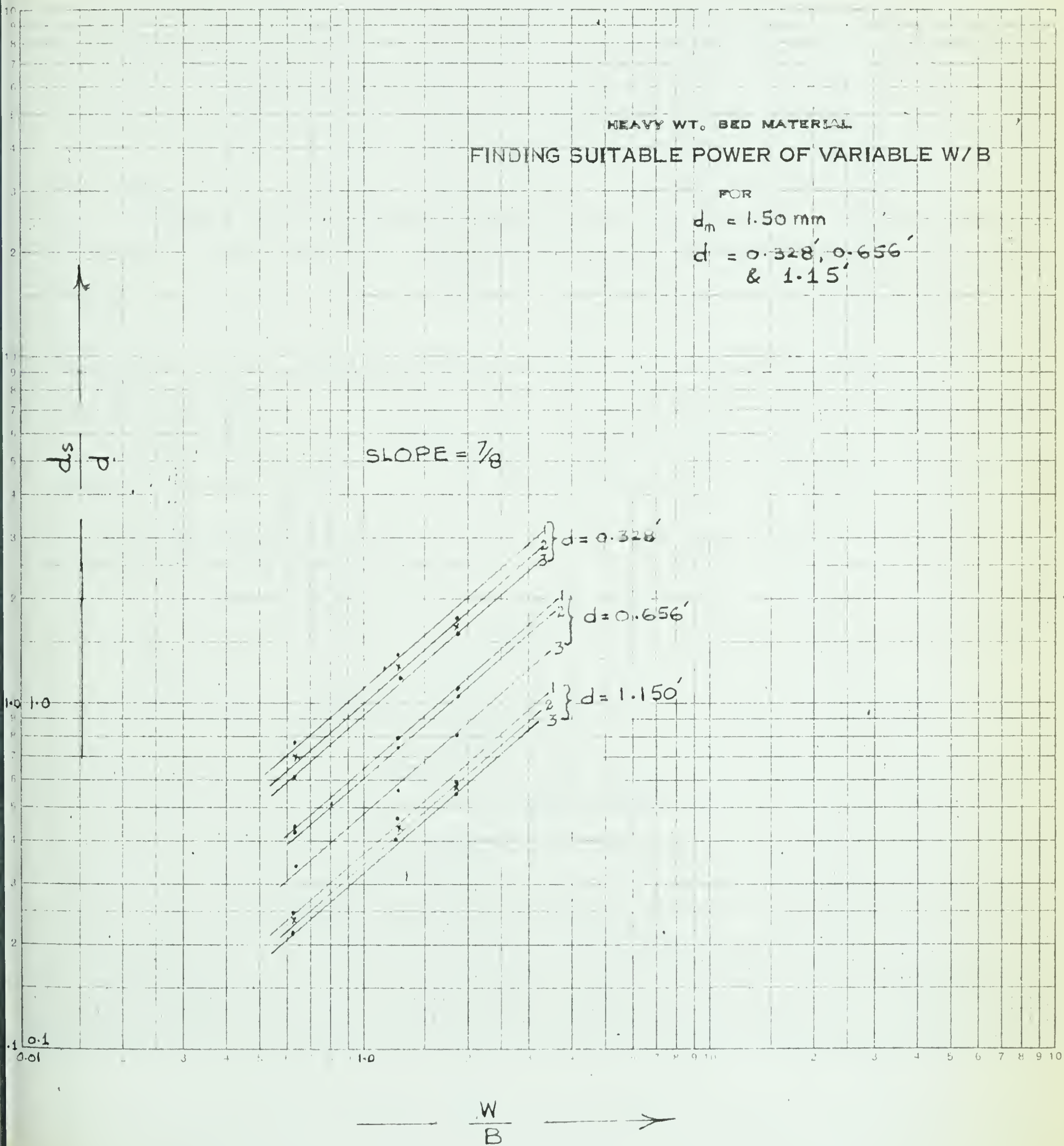


FIGURE 3.14





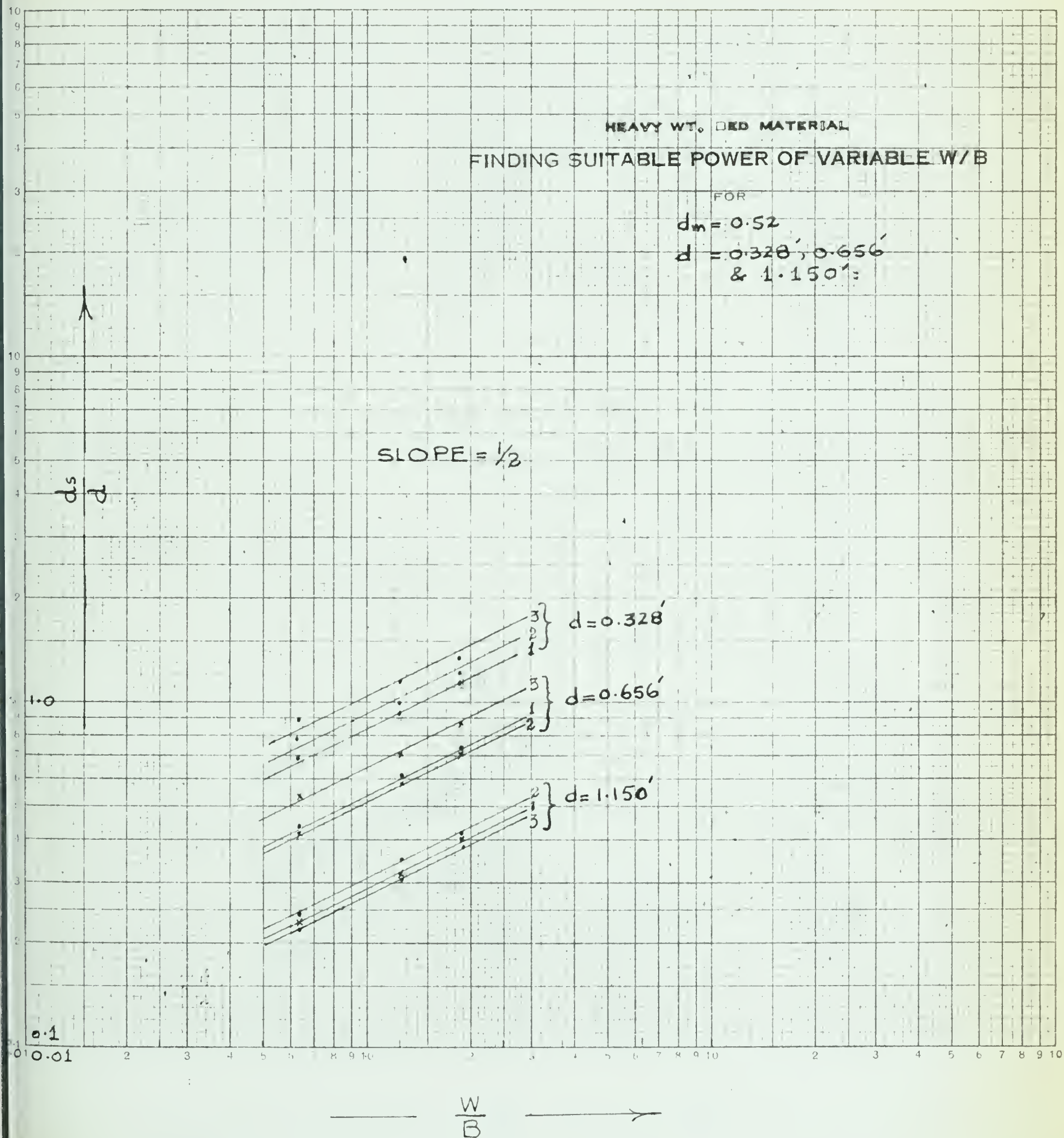


FIGURE 3.15





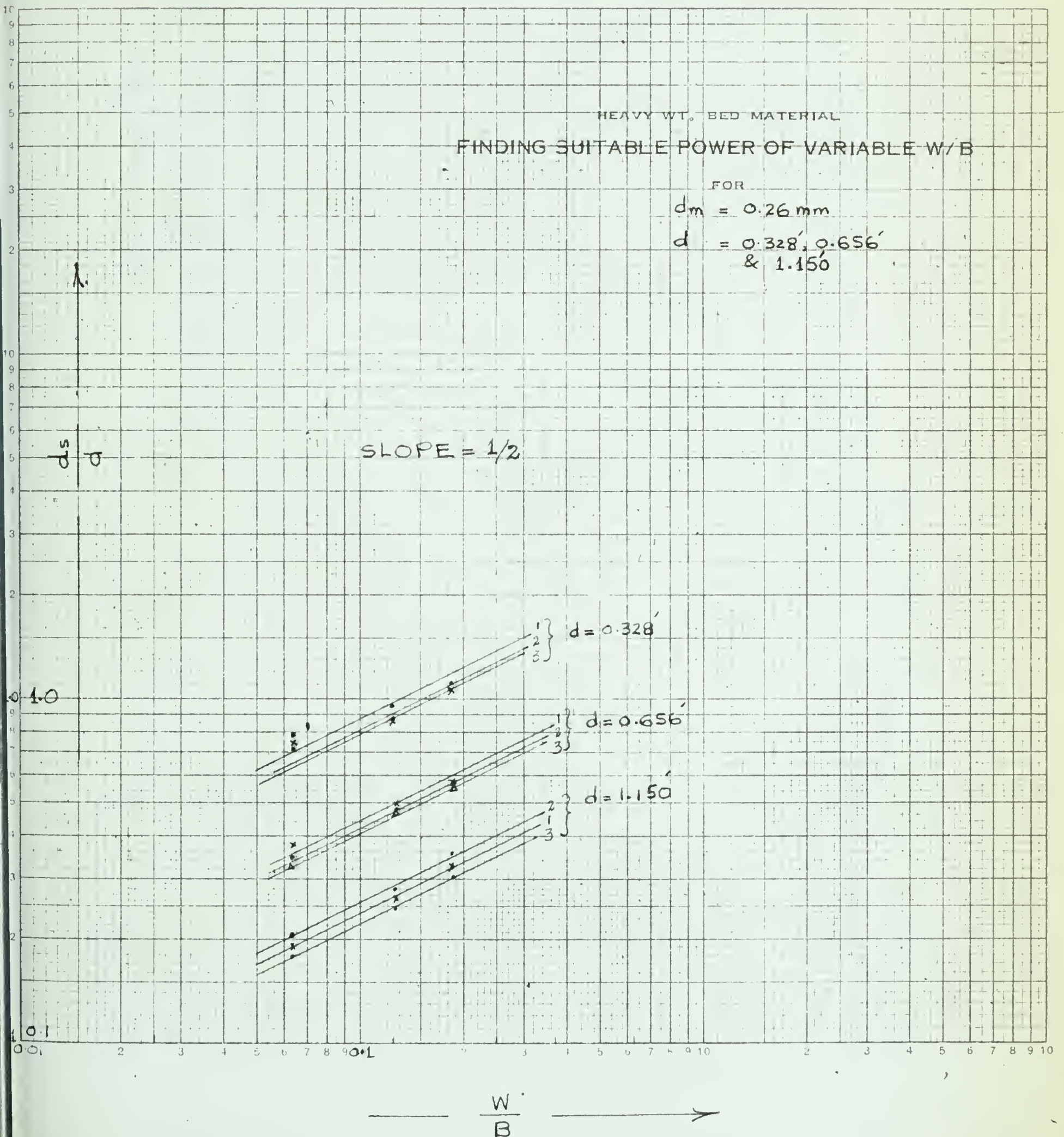


FIGURE 3.16



HEAVY WT. LIQ. MATERIAL

variation of  $\left[ \frac{d_s}{d} / \left( \frac{W}{B} \right)^{1/8} \right]$  WITH  $\left[ \frac{C_d V^2}{g d_m e_s - e_f} \right]$

[GRAVEL RANGE]

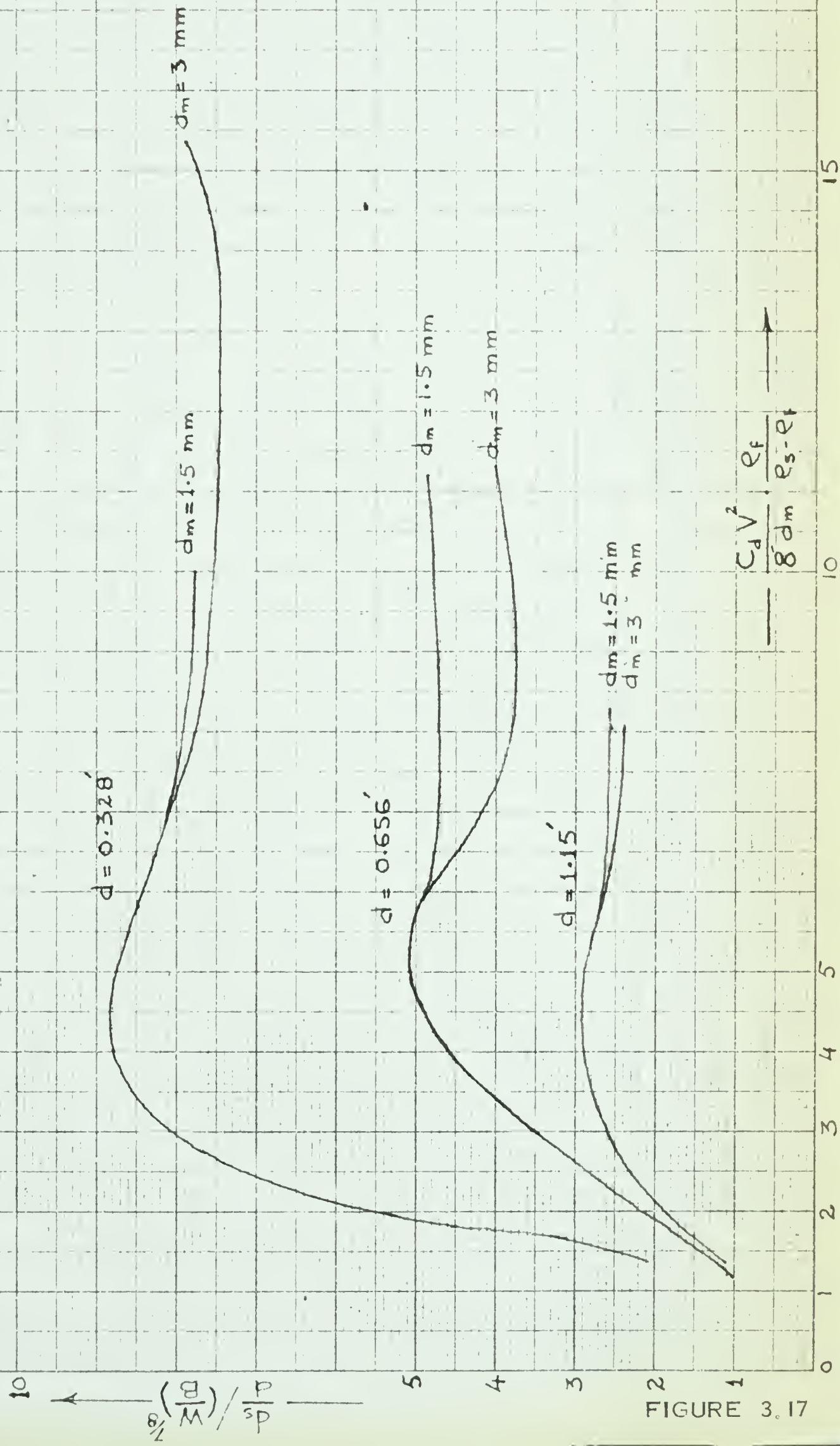


FIGURE 3.17





HEAVY WT. BED MATERIAL

VARIATION OF  $\left[ \frac{d_s}{d} \left( \frac{W}{B} \right)^{1/2} \right]$  WITH  $\left[ \frac{C_d V^2}{g d_m} \cdot \frac{e_f}{e_s - e_f} \right]$

[SAND RANGE]

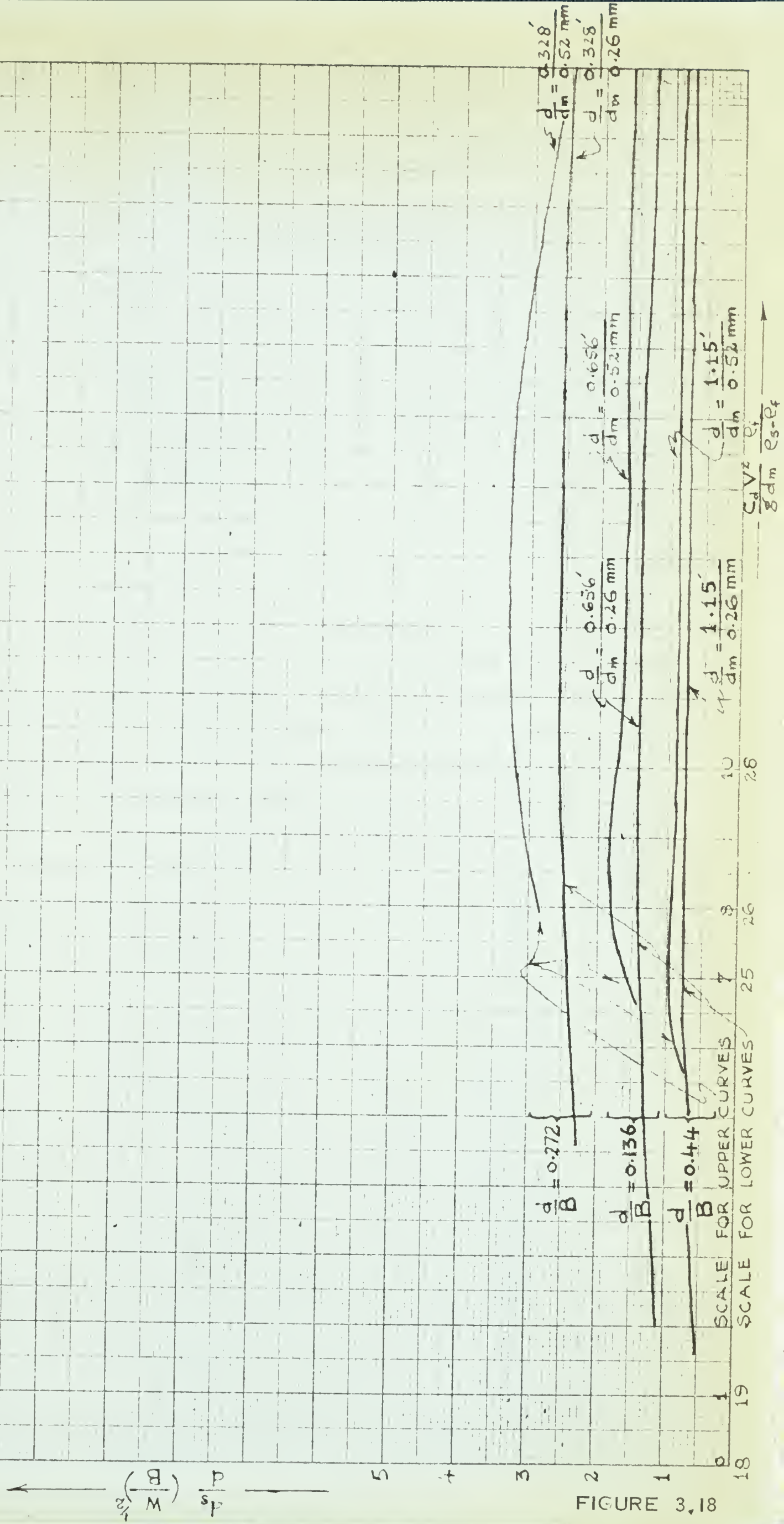
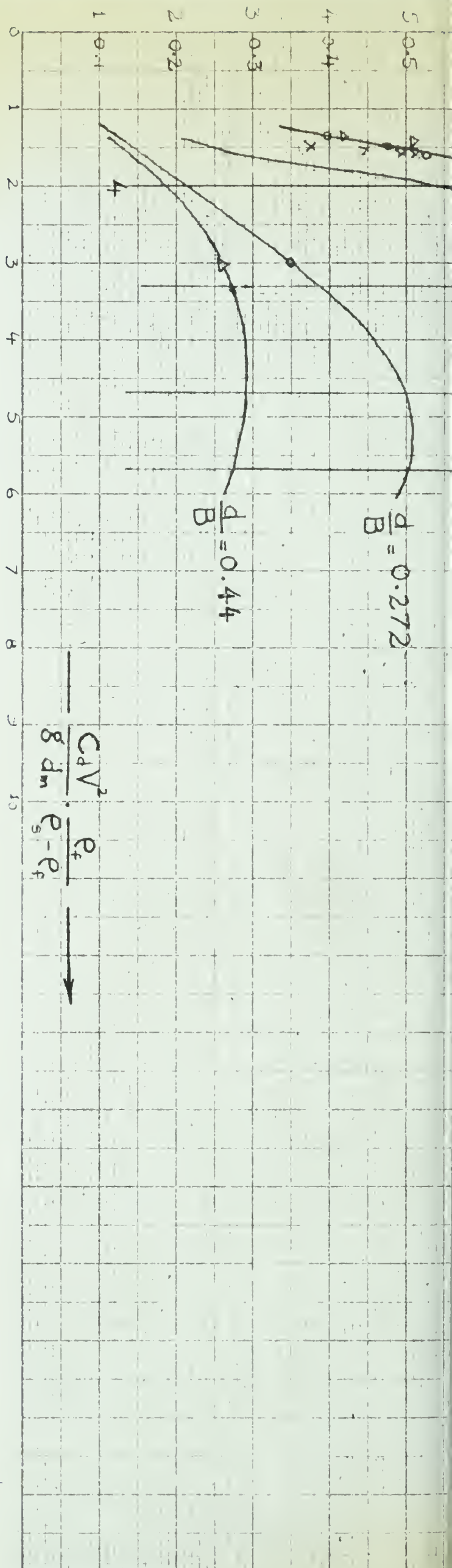


FIGURE 3.18

FIGURE 3.19

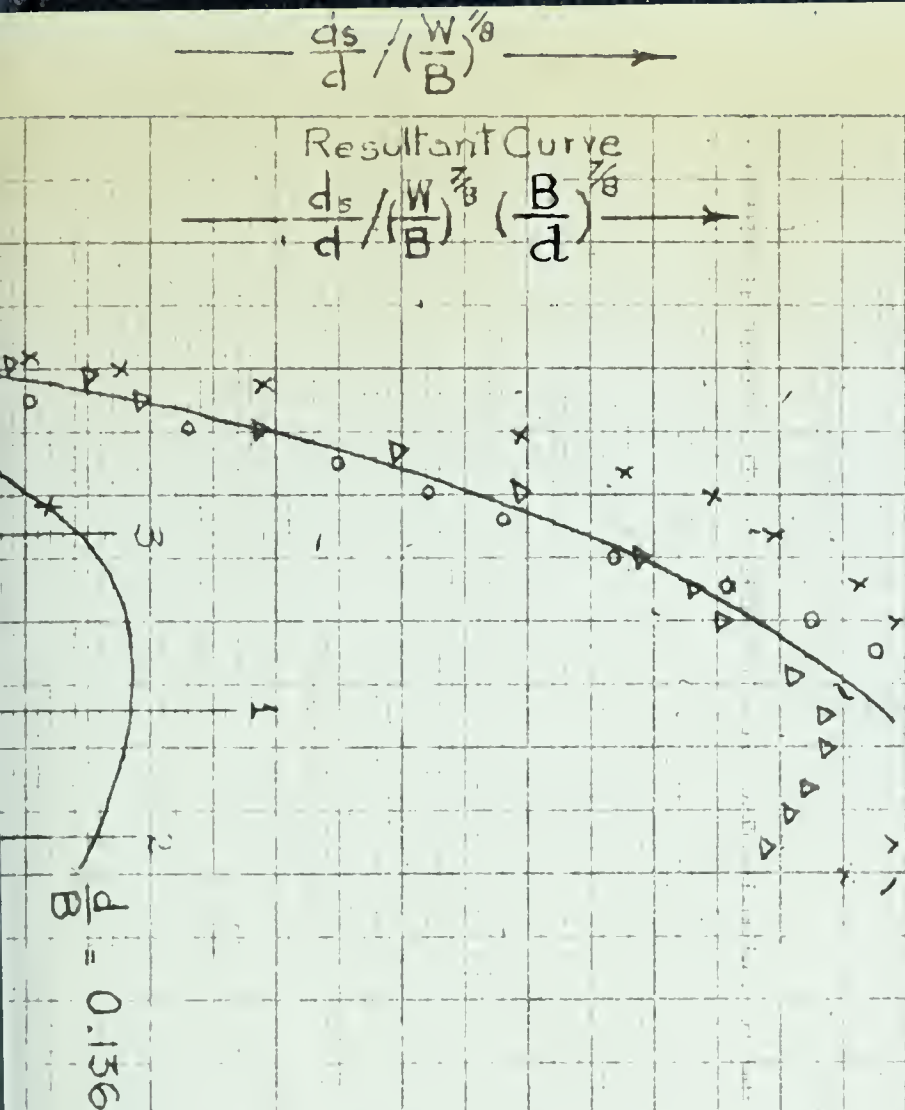




HEAVY WEED MATERIAL

CONSIDERING THE EFFECT OF VARIABLE  $d/B$

GRAVEL RANGE





HEAVY WT. BED MATERIAL  
FINDING SUITABLE POWER OF VARIABLE  $d/B$   
[GRAVEL RANGE]

SLOPE =  $7/8$

$\frac{d_s}{d} \left( \frac{W}{B} \right)^{7/8}$

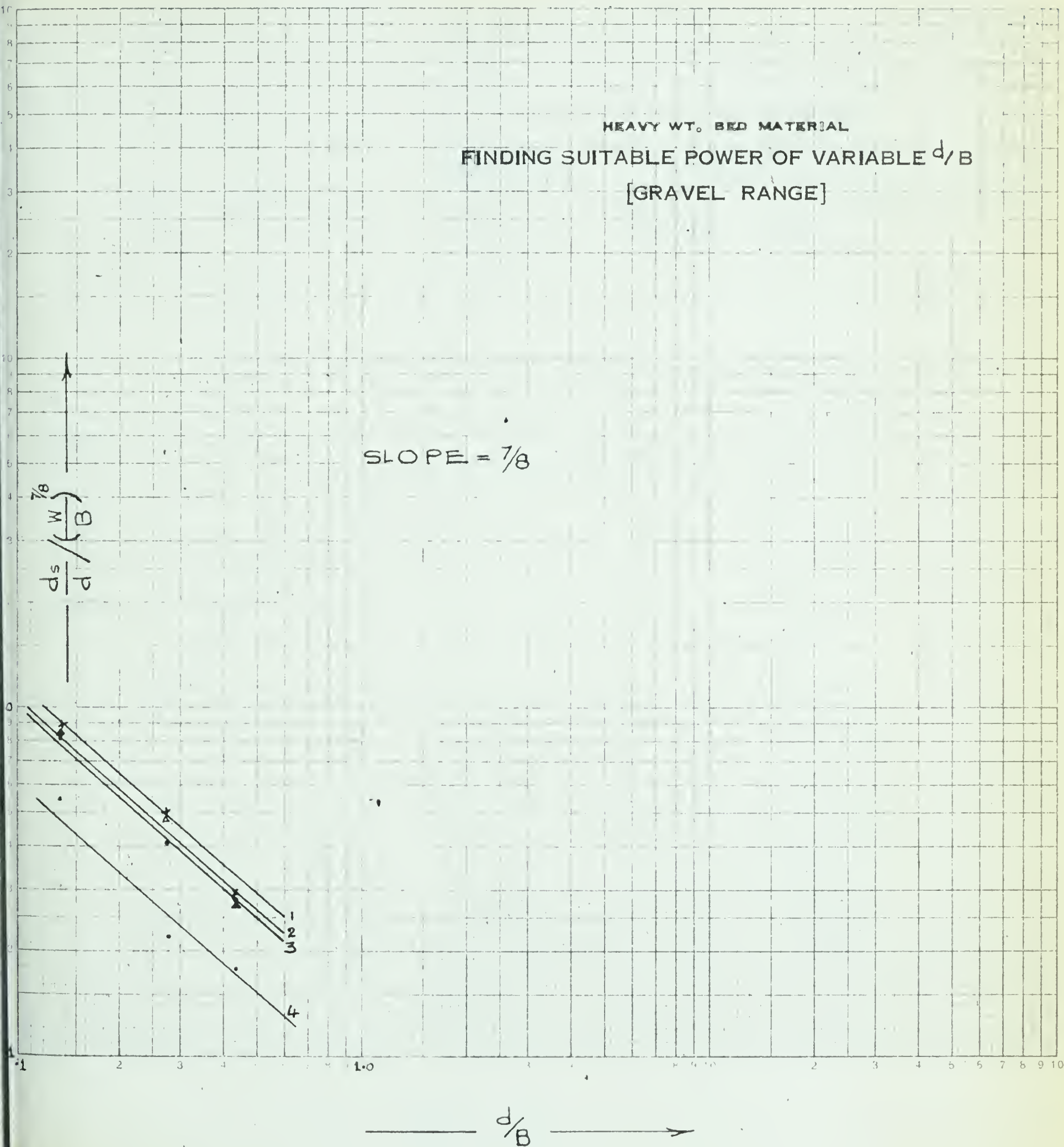


FIGURE 3.20





HEAVY WT. BED MATERIAL

VARIATION OF  $\left[ \frac{d_s}{d} / \left( \frac{W}{B} \right)^{\frac{1}{8}} \left( \frac{B}{d} \right)^{\frac{1}{8}} \right]$  WITH  $\left[ \frac{C_d V^2}{g d_m} \cdot \frac{e_f}{e_s - e_f} \right]$   
[GRAVEL RANGE]

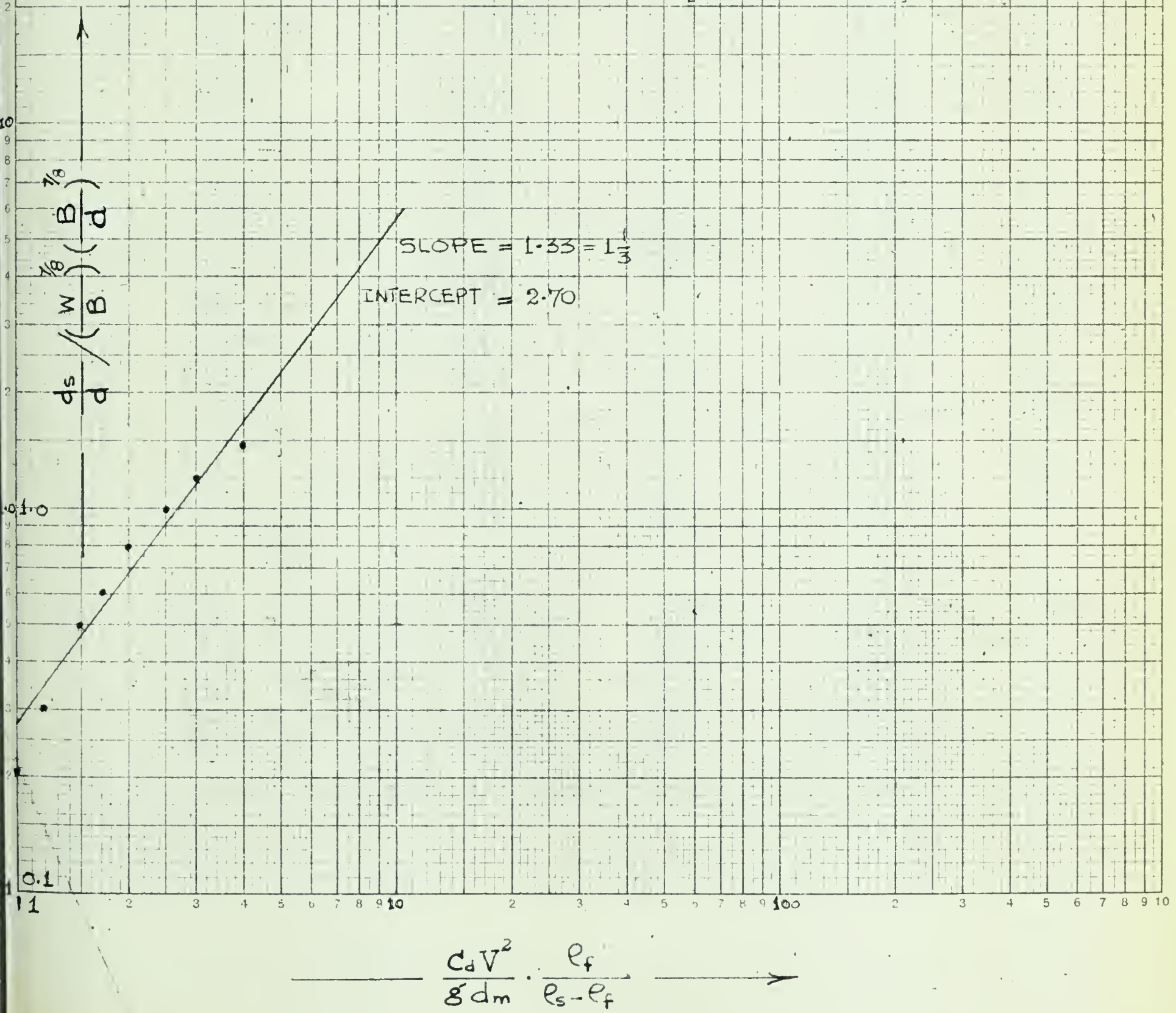


FIGURE 3.21





Table 1  
SCOUR DATA (CHATOU, LABORATORY)

S.G. = 2.65  
 $d_m = 3.00$  mm

d (ft)	S (%)	Q (cusecs)	V (ft/sec)	q (cusecs/ft)	$d_s$ (ft)			Pier III dia=0.492'	C (Parts/100,000)	$d_s/d$			$\frac{v^2}{gd} = \frac{F_b}{g}$	$\frac{v^2}{gd_m} \frac{\rho_f}{(\rho_s - \rho_f)}$	$R = \frac{Vd_m}{v}$	$C_d$	$\frac{C_d v^2}{gd_m} \left( \frac{\rho_f}{\rho_s - \rho_f} \right)$
					Pier I dia=0.164'	Pier II dia=0.328'				Pier I	Pier II	Pier III					
1	2	3	4	5	6	7		8	9	10	11	12	13	14	15	16	17
0.656	0.3	1.73	1.01	0.661	-	0.26		0.033	Not Recorded	-	0.04	0.051	0.048	1.95	840	0.5	0.995
0.656	0.6	2.54	1.36	0.981	0.108	0.204		0.269		0.165	0.31	0.41	0.087	3.5	>1000	0.5	1.75
0.656	0.36	1.87	1.09	0.715	0.066	0.049		0.105		0.101	0.075	0.16	0.056	2.3	910	0.5	1.15
0.656	0.84	2.74	1.59	1.045	0.154	0.318		0.414		0.232	0.484	0.63	0.119	5.15	>1000	0.5	2.58
0.656	0.68	2.44	1.42	0.932	0.122	0.197		0.240		0.186	0.300	0.365	0.093	3.9	>1000	0.5	1.95
0.656	1.22	3.29	1.91	1.26	-	-		0.526		-	-	0.80	0.171	6.3	>1000	0.5	3.15
0.656	1.18	3.22	1.87	1.23	0.220	0.364		0.516		0.336	0.555	0.79	0.164	6.5	>1000	0.5	3.25
0.656	2.00	4.21	2.44	1.61	-	0.359		0.510		-	0.54	0.78	0.280	11.4	>1000	0.5	5.7
0.656	3.40	5.2	3.02	1.98	0.230	0.394		0.592		0.350	0.60	0.90	0.430	17.5	>1000	0.5	8.75
0.656	2.6	4.78	2.78	1.83	0.230	0.410		0.608		0.350	0.625	0.93	0.364	14.5	>1000	0.5	7.25
0.656	2.8	4.95	2.87	1.89	0.230	0.410		0.575		0.350	0.625	0.88	0.387	16.0	>1000	0.5	8.0
0.656	1.44	3.5	2.04	1.34	0.286	0.483		0.657		0.436	0.735	1.03	0.196	8.0	>1000	0.5	4.0
0.656	2.24	4.46	2.59	1.70	0.263	0.510		0.690		0.400	0.77	1.05	0.315	13.0	>1000	0.5	6.5
0.656	1.0	2.96	1.71	1.13	0.230	0.371		0.528		0.350	0.57	0.81	0.138	5.6	>1000	0.5	2.8
0.656	1.0	2.95	1.71	1.13	-	-		0.646		-	-	0.99	0.138	5.6	>1000	0.5	2.8
0.656	4.4	6.01	3.49	2.3	0.262	0.423		0.656		0.400	0.645	1.00	0.575	23.3	>1000	0.5	11.65
1.15	0.64	5.16	1.71	1.97	0.253	0.436		0.633	0	0.220	0.38	0.578	0.079	5.6	>1000	0.5	2.8
1.15	1.2	7.3	2.42	2.79	0.246	0.515		0.689	13.02	0.214	0.45	0.595	0.158	11.1	>1000	0.5	5.55
1.15	1.5	8.18	2.71	3.12	0.230	0.469		0.705	39.4	0.200	0.41	0.615	0.198	14.0	>1000	0.5	7.0
1.15	1.1	6.83	2.27	2.61	0.263	0.591		0.689	17.0	0.230	0.47	0.60	0.138	10.0	>1000	0.5	5.0
1.15	1.5	8.12	2.72	3.11	0.197	0.469		0.606	Nil	0.171	0.404	0.527	0.20	14.2	>1000	0.5	7.1
0.328	1.0	1.06	1.23	0.406	0.076	0.095		0.665	-	0.232	0.29	0.198	0.144	2.9	>1000	0.5	1.45
0.328	2.0	1.67	1.94	0.64	0.306	0.479		0.646	-	0.93	1.46	1.97	0.356	7.4	>1000	0.5	3.7
0.328	3.0	1.91	2.22	0.731	0.279	0.489		0.620	-	0.85	1.49	1.89	0.466	9.5	>1000	0.5	4.75
0.328	4.0	2.16	2.51	0.821	0.286	0.429		0.574	43.6	0.87	1.31	1.75	0.60	12.0	>1000	0.5	6.00
0.328	5.0	2.44	2.83	0.934	0.296	0.400		0.567	89.4	6.9	1.22	1.73	0.76	15.3	>1000	0.5	7.65
0.328	8.0	3.29	3.83	1.26	0.236	0.403		0.590	286.0	0.72	1.23	1.80	1.46	28.0	>1000	0.5	14.0
0.328	10.0	3.44	3.98	1.32	0.28	0.420		0.557	358.0	0.85	1.28	1.70	1.50	30.0	>1000	0.5	15.0



Table 2  
SCOUR DATA (CHATOU LABORATORY)

S.G. = 2.65  
d<sub>m</sub> = 1.5 mm

d (ft)	S (%)	Q (cusecs)	V (ft/sec)	q (cusecs/ft)	d <sub>s</sub> (ft)	
					Pier I dia=0.164'	Pier II dia=0.328'
1	2	3	4	5	6	7
0.656	0.28	1.91	1.11	0.73	0.288	0.482
0.656	0.44	2.4	1.39	0.918	0.318	0.518
0.656	0.7	3.0	1.74	1.14	0.312	0.508
0.656	1.0	3.61	2.15	1.38	0.321	0.557
0.656	0.2	1.66	0.964	0.634	0.226	0.334
0.656	1.36	4.31	2.5	1.65	0.314	0.541
0.656	1.8	4.94	2.87	1.89	0.354	0.571
0.656	0.44	2.4	1.39	0.918	0.312	0.564
0.656	2.7	6.0	3.48	2.29	0.351	0.592
0.656	0.44	2.4	1.39	0.918	0.308	0.537
0.656	0.6	2.82	1.64	1.08	0.292	0.495
0.656	0.28	1.91	1.11	0.73	0.321	0.551
0.656	0.4	2.27	1.31	0.868	-	-
0.656	0.4	2.13	1.23	0.815	0.351	0.544
0.656	0.3	1.98	1.15	0.757	0.406	0.632
1.15	0.3	3.71	1.23	1.42	0.351	0.594
1.15	0.35	4.59	1.52	1.75	0.305	0.528
1.15	0.48	5.44	1.8	2.08	0.321	0.522
1.15	0.35	4.59	1.52	1.75	0.328	0.555
1.15	0.2	3.22	1.07	1.23	0.295	0.492
1.15	0.6	6.01	1.99	2.3	0.354	0.469
1.15	0.2	3.22	1.07	1.23	0.374	0.626
1.15	0.3	3.72	1.23	1.42	0.378	0.642
0.328	0.6	0.99	1.15	0.378	0.278	0.387
0.328	1.0	1.27	1.47	0.486	0.292	0.443
0.328	0.8	1.13	1.31	0.432	0.308	0.487
0.328	1.5	1.7	1.97	0.65	0.249	0.432
0.328	3.0	2.27	2.62	0.82	0.229	0.400
0.328	0.7	1.06	1.23	0.405	0.380	0.509

Pier III dia=0.492'	C (Parts/100,000)	d <sub>s</sub> /d			$\frac{v^2}{gd} = \frac{F_b}{g}$	$\frac{v^2}{gd_m} \frac{\rho_f}{(\rho_s - \rho_f)}$	$R = \frac{Vd_m}{v} = 400V$	C <sub>d</sub>	$\frac{C_d V^2}{gd_m} \left( \frac{\rho_f}{\rho_s - \rho_f} \right)$
		Pier I	Pier II	Pier III					
8	9	10	11	12	13	14	15	16	17
0.623		0.44	0.735	0.95	0.58	4.7	442	0.6	2.82
0.597		0.484	0.79	0.90	0.073	7.4	555	0.535	3.96
0.640		0.475	0.775	0.975	0.143	11.5	695	0.525	6.05
0.666		0.49	0.85	1.015	0.217	16.6	860	0.51	8.4
0.482		0.344	0.51	0.735	0.044	3.02	390	0.6	1.812
0.650		0.478	0.825	0.99	0.294	24.0	1000	0.5	12.00
0.712		0.54	0.87	1.09	0.386	31.0	>1000	0.5	15.50
0.656		0.474	0.86	1.00	0.096	7.9	550	0.54	4.26
0.705		0.535	0.90	1.075	0.57	47.0	>1000	0.5	28.50
0.650	0	0.47	0.82	0.99	0.091	7.4	550	0.53	3.9
0.574		0.45	0.755	0.875	0.126	10.3	660	0.52	5.35
0.696		0.49	0.84	1.06	0.058	4.7	440	0.57	2.84
-		-	-	-	-	6.3	525	0.53	3.34
0.682		0.535	0.83	1.04	0.071	5.7	490	0.55	3.14
0.737		0.62	0.965	1.13	0.062	15.3	460	0.575	2.88
0.731		0.306	0.516	0.636	0.041	5.8	490	0.55	3.2
0.685		0.265	0.46	0.596	0.062	8.3	610	0.525	4.35
0.600		0.28	0.456	0.522	0.088	12.3	720	0.52	6.4
0.650		0.286	0.484	0.566	0.062	8.8	610	0.52	4.6
0.650		0.256	0.428	0.566	0.031	5.1	430	0.60	3.06
0.650		0.308	0.408	0.566	0.103	15.0	800	0.51	7.7
0.764		0.325	0.545	0.665	0.031	6.0	430	0.59	3.54
0.443		0.328	0.561	0.685	0.041	5.7	490	0.55	3.14
0.497		0.846	1.18	1.52	0.126	5.8	460	0.57	2.85
0.509		0.89	1.35	1.55	0.203	8.2	590	0.525	4.30
0.584		0.94	1.48	1.78	0.117	6.3	525	0.53	3.34
0.557		0.744	1.29	1.67	0.365	15.3	790	0.51	7.8
0.547		0.685	1.19	1.64	0.650	26.0	>1000	0.5	13.0
0.685		1.13	1.52	2.04	0.143	5.7	49	0.55	3.14





Table 3

## SCOUR DATA (CHATOU LABORATORY)

S.G. = 2.65

 $d_m = 0.52$  mm

d (ft)	S (%)	Q (cusecs)	V (ft/sec)	q (cusecs/ft)	$d_s$ (ft)		Pier III dia=0.492'	C (Parts/100,000)	$d_s/d$			$\frac{V^2}{gd} = \frac{F_b}{g}$	$\frac{V^2}{gd_m} \left( \frac{\rho_f}{\rho_s - \rho_f} \right)$	$R = \frac{Vd_m}{v} = 143V$	$C_d$	$\frac{C_d V^2}{gd_m} \left( \frac{\rho_f}{\rho_s - \rho_f} \right)$
					Pier I dia=0.164'	Pier II dia=0.328'			Pier I	Pier II	Pier III					
1	2	3	4	5	6	7	8	9	10	11	12	13	14	15	16	17
0.656	0.1	1.38	0.803	0.528	0.262	0.374	0.449		0.40	0.57	0.685	0.0305	7.1	76	1.3	9.5
0.656	0.2	1.84	0.94	0.704	0.364	0.459	0.541		0.555	0.755	0.825	0.0416	9.7	134	0.94	9.1
0.656	0.3	2.26	1.31	0.864	0.334	0.397	0.468		0.51	0.606	0.715	0.081	18.9	187	0.82	15.5
0.656	0.4	2.62	1.51	1.0	0.298	0.390	0.442		0.454	0.595	0.675	0.108	25.0	218	0.8	20.0
0.656	0.25	2.05	1.19	0.784	0.39	0.419	0.489		0.545	0.64	0.745	0.067	15.6	167	0.86	13.4
0.656	0.55	3.29	1.91	1.26	0.328	0.406	0.505		0.5	0.62	0.77	0.172	10.0	274	0.7	7.0
0.656	0.25	2.05	1.19	0.784	0.321	0.451	0.462		0.49	0.69	0.705	0.067	15.6	170	0.86	13.3
0.656	0.15	1.59	0.92	0.608	0.318	0.361	0.430		0.485	0.55	0.656	0.040	9.3	132	0.94	8.7
0.656	0.2	1.84	1.07	0.703	0.348	0.380	0.451		0.53	0.58	0.69	0.054	12.6	153	0.90	11.3
0.656	0.2	1.84	1.07	0.703	0.355	0.386	0.471		0.54	0.59	0.72	0.054	12.6	153	0.90	11.3
0.656	0.3	1.91	1.31	0.73	0.311	0.400	0.487		0.475	0.61	0.745	0.082	18.7	186	0.82	15.3
1.15	0.1	2.68	0.89	1.03	0.311	0.367	0.416		0.27	0.32	0.364	0.0214	8.8	127	0.94	8.3
1.15	0.135	1.01	1.29	0.344	0.387	0.432	0.432		0.29	0.337	0.376	0.0275	11.2	144	0.92	10.3
1.15	0.2	0.682	1.26	0.36	0.292	0.403	0.481	Not given	0.254	0.35	0.42	0.043	17.5	179	0.84	14.7
1.15	0.16	3.46	1.15	1.32	0.292	0.403	0.458		0.254	0.35	0.399	0.036	14.5	163	0.87	12.7
1.15	0.23	4.17	1.38	1.59	0.295	0.393	0.448		0.256	0.343	0.39	0.05	20.8	195	0.81	16.8
1.15	0.3	4.73	1.57	1.81	0.278	0.387	0.448		0.242	0.337	0.39	0.0665	27.0	224	0.95	20.2
1.15	0.08	2.47	0.82	0.944	0.256	0.363	0.448		0.224	0.316	0.39	0.0181	7.4	117	0.80	5.92
0.328	0.372	0.92	1.07	0.352	0.312	0.377	0.430		0.96	1.15	1.31	0.108	12.6	153	0.90	11.3
0.328	0.3	0.81	0.90	0.31	0.288	0.364	0.400		0.88	1.11	1.22	0.077	9.0	128	0.94	8.46
0.328	0.5	1.06	1.23	0.405	0.358	0.377	0.435		1.09	1.15	1.35	0.143	16.5	175	0.85	14.0
0.328	0.6	1.2	1.39	0.459	0.285	0.361	0.422		0.87	1.1	1.29	0.183	21.2	197	0.80	16.9
0.328	0.75	1.34	1.56	0.512	0.338	0.351	0.409		1.03	1.07	1.25	0.230	26.2	222	0.75	20.0
0.328	0.25	0.707	0.82	0.27	0.252	0.294	0.370		0.77	0.9	1.13	0.067	7.4	117	0.80	5.92



Table 4  
SCOUR DATA (CHATOU, LABORATORY)

S.G. = 2.65  
 $d_m = 0.26$  mm

d (ft)	S (%)	Q (cusecs)	V (ft/sec)	q (cusecs/ft)	d <sub>s</sub> (ft)		C (Parts/100,000)	d <sub>s</sub> /d			$\frac{V^2}{gd} = \frac{F_b}{g}$	$\frac{V^2}{gd_m} \left( \frac{\rho_f}{\rho_s - \rho_f} \right)$	$R = \frac{Vd_m}{v}$ = 71.5V	C <sub>d</sub>	$\frac{C_d V^2}{gd_m} \left( \frac{\rho_f}{\rho_s - \rho_f} \right)$	
					Pier I dia=0.164'	Pier II dia=0.328'		Pier III dia=0.492'	Pier I	Pier II						Pier III
1	2	3	4	5	6	7	8	9	10	11	12	13	14	15	16	17
0.656	0.05	0.972	0.565	0.372	0.249	0.239	0.302		0.38	0.364	0.46	0.0151	7.15	40	3.1	22.2
0.656	0.07	1.185	0.690	0.453	0.246	0.325	0.344		0.375	0.495	0.525	0.0225	10.0	50	2.8	28
0.656	0.08	1.27	0.738	0.485	0.252	0.328	0.358		0.384	0.50	0.545	0.0257	12.2	53	2.7	32.8
0.656	0.10	1.43	0.833	0.546	0.220	0.308	0.358		0.335	0.47	0.545	0.0328	15.4	60	2.5	38.5
1.15	0.045	1.98	0.656	0.756	0.233	0.318	0.370	Not Recorded	0.203	0.276	0.322	0.0204	9.5	47	2.9	27.5
1.15	0.056	2.17	0.722	0.830	0.229	0.298	0.370		0.199	0.259	0.322	0.0245	11.5	52	2.8	32.2
1.15	0.036	1.78	0.591	0.680	0.223	0.236	0.322		0.194	0.272	0.28	0.0166	7.7	43	3.0	23.1
0.328	0.11	0.566	0.656	0.213	0.256	0.246	0.354		0.78	0.75	1.08	0.0204	9.6	47	2.9	27.8
0.328	0.15	0.655	0.755	0.250	0.282	0.295	0.351		0.86	0.9	1.07	0.027	12.5	54	2.7	33.8
0.328	0.175	0.708	0.820	0.271	0.266	0.298	0.338		0.81	0.91	1.03	0.0317	15.2	59	2.5	38.0



CHAPTER 4  
SCOUR IN LIGHT WEIGHT BED MATERIAL

Introduction.

Various materials which could be used as light weight bed material, are listed below:

<u>Material</u>		<u>Specific Gravity</u>
Gilsonite	=	1.04
Amber	=	1.06
Blacksmith-Coal	=	1.25
Lignite	=	1.27

Blacksmith coal was selected for use as light weight bed material due to the following main advantages:

- 1) Can be procured in large quantities at low cost.
- 2) Specific gravity is not as low as that of amber and gilsonite materials, which present the difficulty of reaching active bed transport for relatively low velocities, thus making it impossible to go up to higher velocity ranges without an elaborate bed feeding system.





The result of sieve analysis test on coal sample was shown in Figure 4.1. The 50% passing or median size of particle was 1.56 mm. In Figure 4.1 was also shown the size distribution plot for the stone sample used for data in Table 6.

### Experiments

Installation: The experiments were performed in the Graduate Hydraulics Laboratory with a glass-walled 18" x 18" flume (Plate 1) the plan and elevation views of which are shown in Figure 4.2. The flume had arrangement to control the slope of water surface (Plate 2).

The flume was equipped with a wooden hopper, shown in Figure 4.3 and Plate 3, for feeding the coal. In the same Figure has been shown in detail the arrangement employed to wash the coal down the hopper, into the flume (Plates 4 and 5).

The flume was supplied with water through an 8" supply line, fitted with a discharge control valve, (Plate 6). The maximum capacity of the main supply pump was 3 cfs.

The discharge was measured by an orifice type flow meter (Plate 7), which recorded the discharge on a circular chart. The clock-work arrangement in the flowmeter



enabled to run a discharge for any required amount of time.

Due to its lightness, some of the coal was washed away from the surface of layer of the bed material, thus resulting in initial drop of general bed level. The situation was remedied by an arrangement shown in Plate 11, for initial water feeding from downstream side.

The velocity of flow was measured by means of Ott currentmeter (Plates 9 and 10). The velocity from currentmeter was checked by finding the velocity from the flowmeter reading.

### Procedure

The flume was filled with coal or stone bed material for the first 0.5 ft. depth. Piers as required were fixed on steel stands (Figure 4.3) vertically, on the centre line of the flume.

Prior to any experiment the coal was soaked for at least 24 hours. This not only washed down the fines but also made the coal slightly heavier. The water was fed from the upstream side through the baffles (Plate 8) provided in the first  $1\frac{1}{2}$  ' length of flume, so as to destroy excess energy of water. The discharge was gradually increased from





zero to the required amount. The depth of the water above the general bed level, could be controlled by the adjustment of the tail gate (Plate 12).

From the time a discharge and a required depth was attained in the flume, readings were taken of the deepest scour depth below general bed level, occurring at the upstream nose of the pier, on the graduations marked on the upstream face of the pier (Plate 13). The first and second readings were taken after two and five minutes after the start of the experiment and then repeated every five minutes until there was no significant increase in the scour depth. The maximum scour depth was recorded in Table 5.

Velocity distributions for each experiment were taken for each pier along two symmetrically located vertical sections, at  $1\frac{1}{2}$ ' upstream of the pier centre.

Sufficient supply of soaked coal was kept in the hopper in advance, for use when necessary. For higher range of velocities, when the general bed would go down by an average of 0.005 to 0.01 feet, coal was fed from the hopper by washing it down by gradually opening the sliding gate (Plate 5) of the hopper, and kept on being fed till the general bed was replenished to the original level. The washed-away coal got accumulated in a sediment trap provided in the last four feet of flume length (Plate 12), which was



transferred to the hopper at the end of an experiment, for re-use.

The bed activity was noted for each experiment and recorded in Table 5. Before starting a new experiment, the scour holes from the previous experiments were filled and the bed levelled.

### Sequence of Tests and Data

Experiments were performed with light weight bed material of median size 1.56 mm. Two piers of diameters 0.18' and 0.11' were placed four feet apart along the centre line of the flume. For depths of 0.3', 0.35', 0.4', 0.45', 0.5', 0.55', 0.6', 0.65', 0.7', 0.75', 0.80', 0.85', 0.9' and 0.95', the velocity was raised from a value when maximum scour depth was almost zero to the **extent** where dunes formation occurred and maximum scour depth below bed level noted in Table 5. The discharge was varied between 0.12 to 1.8 cfs.

### Test Results Analysis

#### Compilation of Tables:

The values of  $\frac{d_s}{d}$  and  $\frac{C_d V^2}{g d_m} \left( \frac{\rho_f}{\rho_s - \rho_f} \right)$  were calculated in Table 5. The values of the drag coefficient are based on the Reynolds number  $\frac{V d_m}{\nu}$ .



## Plottings

The plotting procedure and sequence was exactly similar to the one employed in Chapter 3. In brief,  $\frac{d_s}{d}$  values were plotted against  $\frac{C_d V^2}{g d_m} \left( \frac{\rho_f}{\rho_s - \rho_f} \right)$  values, for each depth separately, as shown in Figure 4.4 to 4.17.

### 1) Considering the Effect of Variable $\frac{W}{B}$ :

An exponent of  $7/8$  was found in Figures 4.18 to 4.24 for variable  $W/B$ . The resultant curves were plotted in Figures 4.4 to 4.17.

### 2) Considering the Effect of Variable $\frac{d_m}{d}$ :

Since the size of  $d_m$  was not varied, no question of considering the effect of  $\frac{d_m}{d}$  for a constant depth. However, the bed material is gravel sized.

### 3) Considering the Effect of Variable $\frac{d}{B}$ :

The resultant curves between  $\frac{d_s}{d} / \left( \frac{W}{B} \right)^{7/8}$  and  $\frac{C_d V^2}{g d_m} \left( \frac{\rho_f}{\rho_s - \rho_f} \right)$  in Figure 4.4 to 4.17 were transferred to Figure 4.25. Due to the small flume and close depths, the plots in Figure 4.25 were found to be lying very close to each other. However, Figure 4.25 shows that there is a general lowering of peaks as the depth increases. Curves for five representative depths, i.e., 0.3', 0.40', 0.65', 0.75' and 0.90' were transferred to Figure 4.26.





An exponent of  $7/8$  was found for variable  $d/B$  from Figure 4.27. The resultant curve shown in Figure 4.26 took into account the effect of the variable  $d/B$ .

### Other Plots

- I) Variation of scour depth with velocity: was plotted in Figures 4.28 to 4.35.
- II) Variation of  $\frac{d_s}{d}$  with Froude number:  $\frac{d_s}{d}$  was plotted against Froude number in Figures 4.36 and 4.37.
- III) Variation of scour depth with time: was plotted in Figures 4.38 to 4.52

### Conclusions

1) Below an approximate threshold value of 4.7 of  $\frac{\text{drag force on particle}}{\text{buoyant weight of particle}}$ , no scour takes place (as appears in Figure 4.26.)

2) The resultant curve in Figure 4.26 can be regarded as more or less a straight line for its length before the peak point, which shows that the parameter  $\frac{d_s}{d} / \left(\frac{W}{B}\right)^{7/8} \times \left(\frac{B}{d}\right)^{7/8}$  varies linearly with the ratio of drag force on and buoyant weight of a particle.



3) The equation of the straight line portion of the resultant curve in Figure 4.26 can be written as follows:

$$6.0 \left\{ \frac{d_s}{d} / \left(\frac{W}{B}\right)^{7/8} \times \left(\frac{B}{d}\right)^{7/8} \right\} + 4.7 = \frac{C_d V^2}{g d_m} \left( \frac{\rho_f}{\rho_s - \rho_f} \right)$$

4) From the above equation, it may be concluded that, when all other factors remain constant, the non-dimensional scour depth varies

- i) directly with  $7/8$  power of  $W/B$
  - ii) inversely with  $7/8$  power of  $d/B$
- and iii) directly with  $\left[ \frac{\text{drag}-4.7}{\text{buoyant weight of particle}} \right]$ .

5) It may also be seen from the resultant plot in Figure 4.26 that the non-dimensional scour depth for given  $W$ ,  $B$ , and  $d$ , reaches a maximum, when the drag force reaches about 12 times the submerged weight of the particle or when the general bed transport reaches active stage. From a practical point of view the maximum non-dimensional scour depth is given as

$$\frac{d_s}{d} = \left(\frac{W}{B}\right)^{7/8} \left(\frac{B}{d}\right)^{7/8} = \left(\frac{W}{d}\right)^{7/8} .$$





Conclusion from Plots I to III.

1) There is no scour below a certain threshold represented by a velocity, as observed from Figures 4.28 to 4.35.

2) The maximum scour depth measured below general bed level in Figures 4.28 to 4.35, passes through a maximum with respect to velocity of flow. The maxima in Figures 4.28 to 4.35 reached, on the average, for a velocity of about 0.8 ft/sec, which is the stage preceding the dune formation or when the bed material is moving above the bed level in the form of a thin layer containing most particles of all sizes (slight to medium type of sheet flow).

3) The occurrence of peaks in Figures 4.28 to 4.35 with respect to velocity, can be due to the compensatory effect of transport. The peaks occur at a stage when the bed is significantly moving. It can be possible that for velocities beyond peak a thin layer of bed material in motion may be covering the bottom of the scour hole, thus making us read less scour depth over pier graduation. As the velocity increases further the moving bed material layer grows thicker, thus making maximum scour depth reading less and less. For further increase of velocity, dunes are observed moving along the bed, but the maximum scour depth is still less than peak value.



4) It can also be observed from Figures 4.28 to 4.35 that there is a tendency for maximum scour depth decrease as the depth increases.

5) The non-dimensional scour depth, as seen from Figures 4.36 to 4.37, increases with Froude number, till it reaches a peak.

6) There is no scour until the Froude number reaches a certain threshold value.

7) The scour depth, as seen from scour depth versus time plots in Figures 4.38 to 4.52 increases with time. When there is no transport the scour depth increases progressively, the rate being faster in the first few minutes and slowing down as the time passed, till, like heavy weight bed material (References 2 and 13) the scour depth, reaches a maximum with respect to time, i.e., when the increase in scour depth with time is negligibly small. When there is transport the scour depth underwent fluctuations of a periodic nature as dunes from upstream, passed by the scour hole and scour depth reached a peak much earlier than the case of no transport.



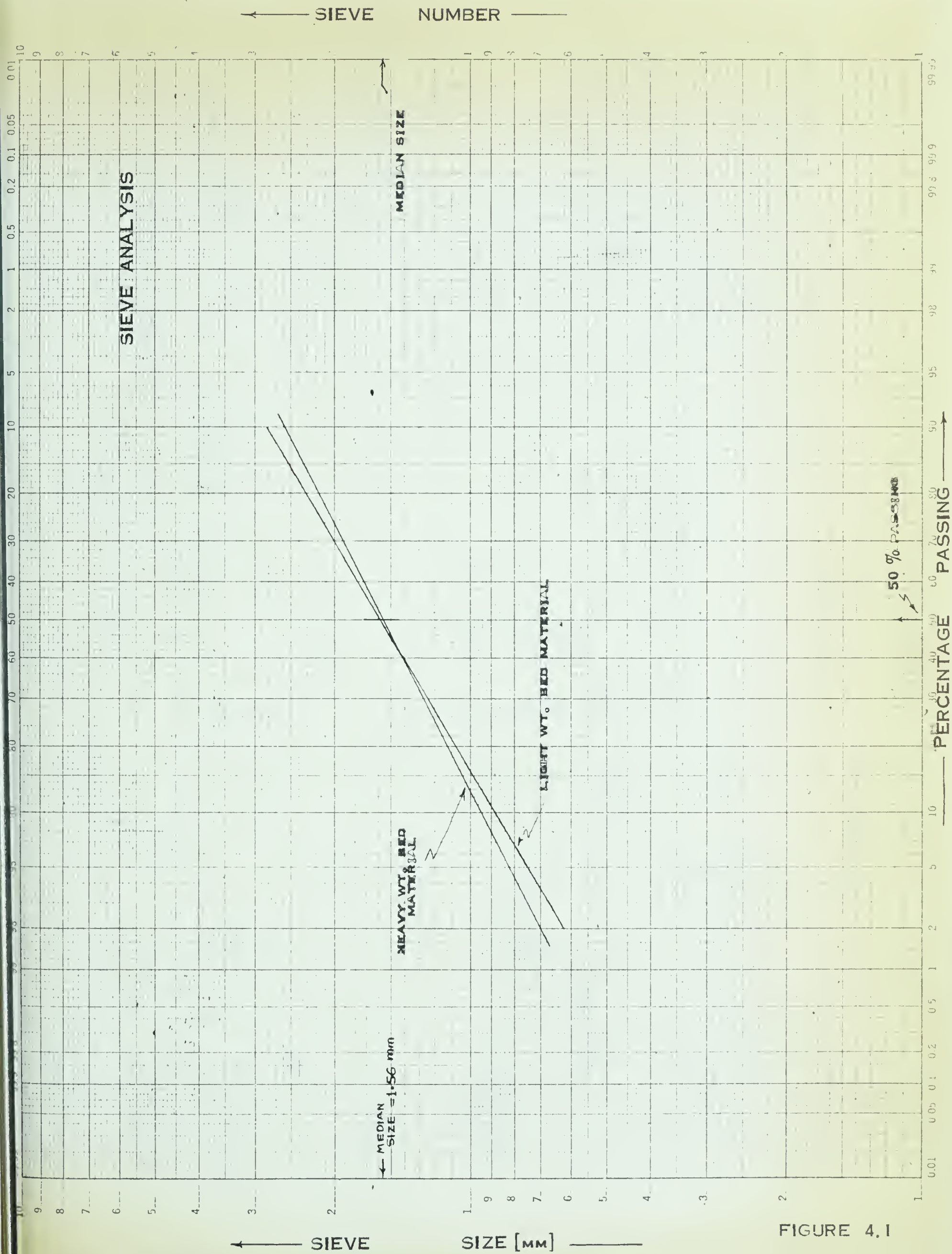


FIGURE 4.1





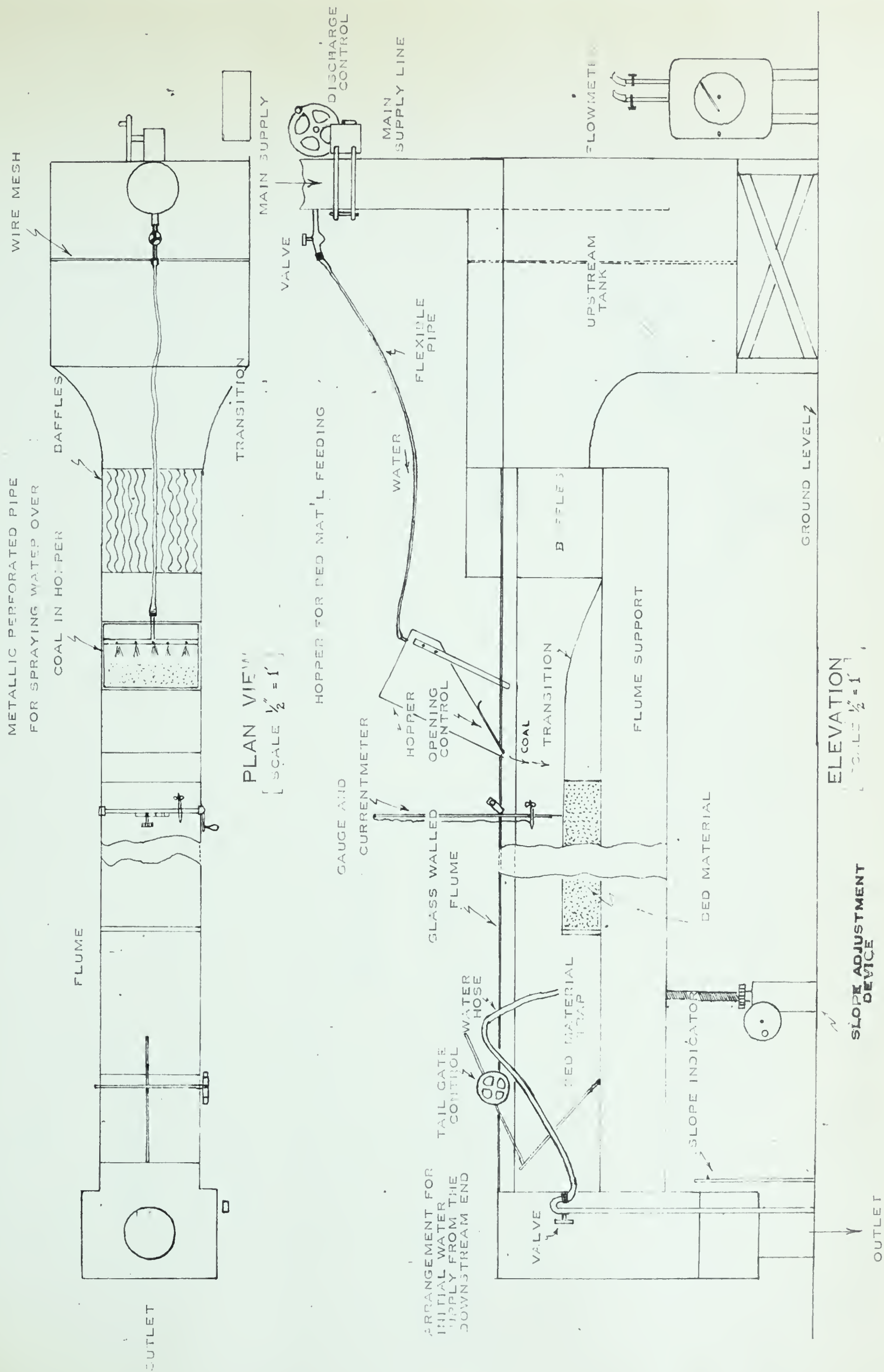
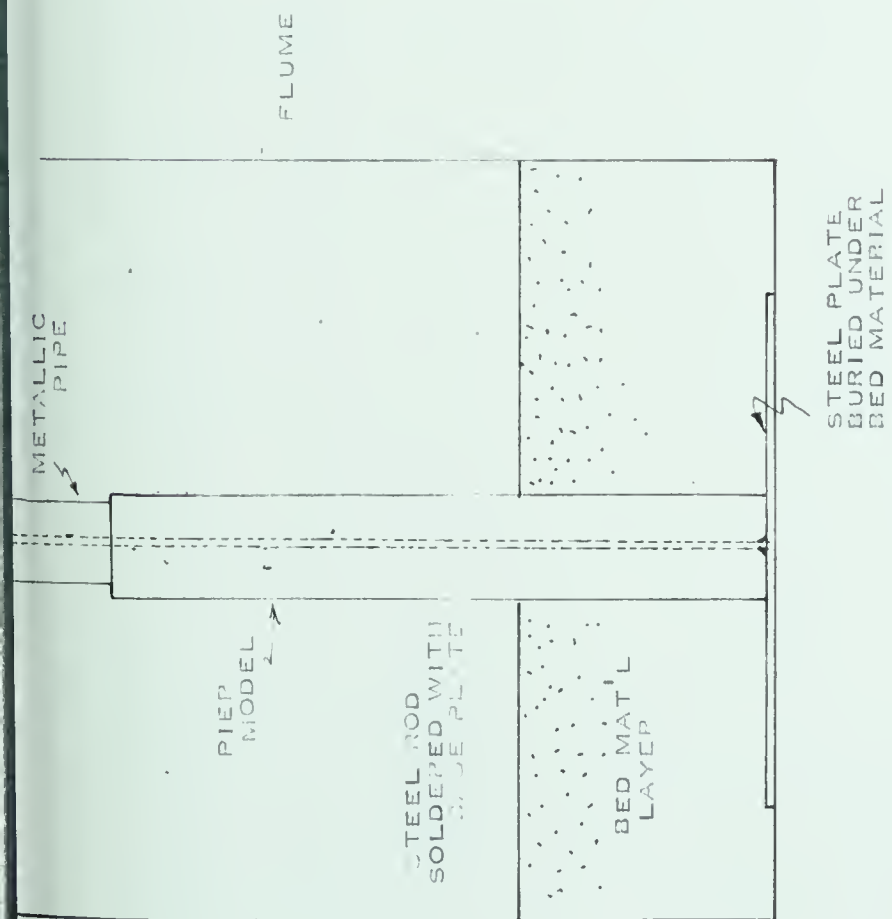
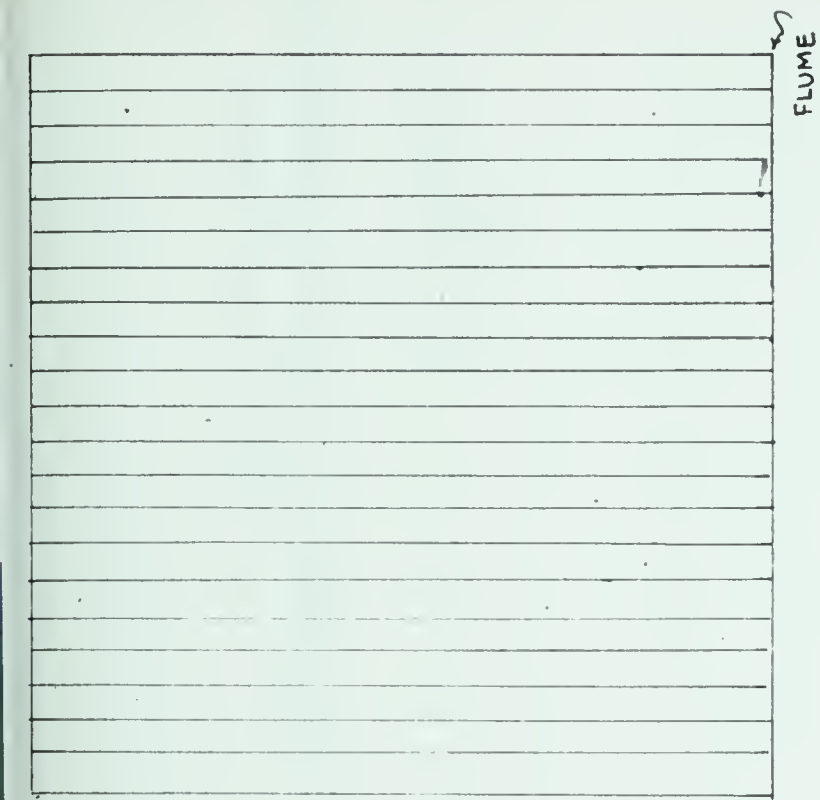


FIGURE 4.2

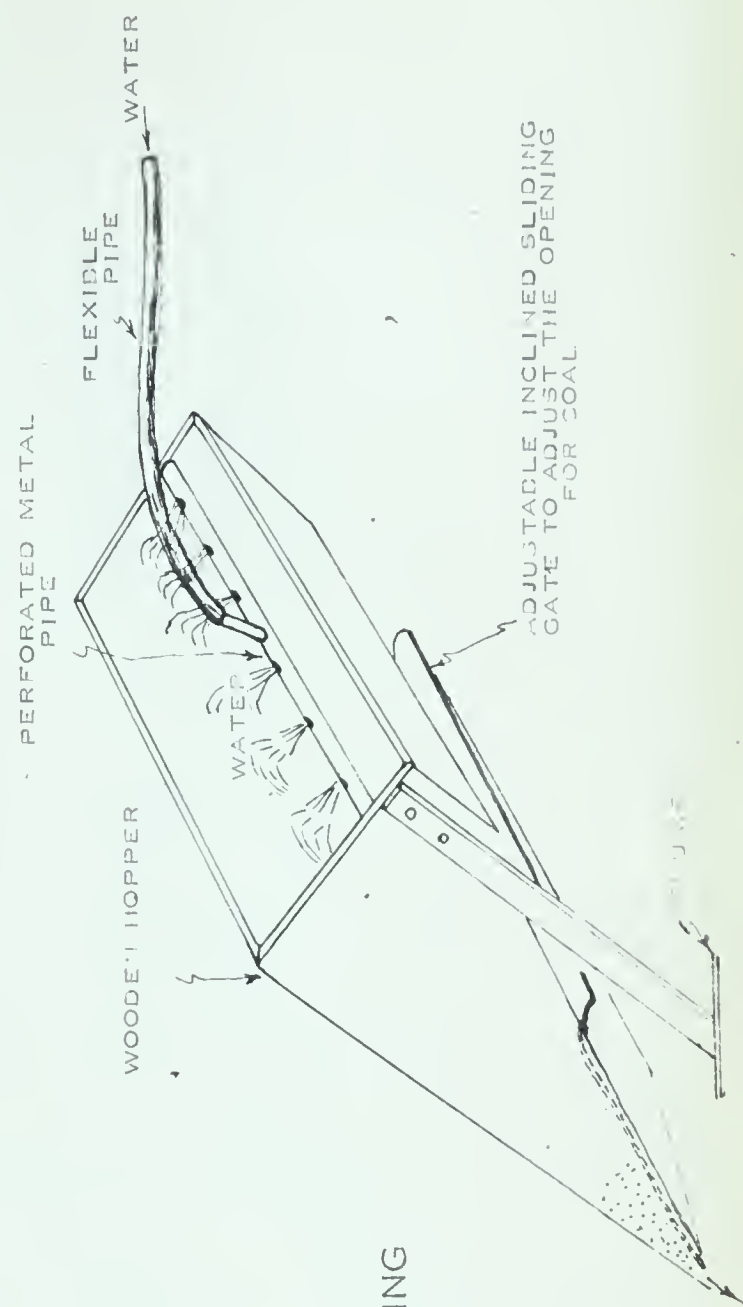




PIER MODEL INSTALLATION



BAFFLES FOR ENERGY DISSIPATION



HOPPER FOR BED MATERIAL FEEDING

FIG. 4 3 ENLARGED DETAIL





LIGHT WT. SED MATERIAL

CONSIDERING THE EFFECT OF VARIABLE W/B

FOR

$$d_m = 1.56 \text{ mm}$$

$$d = 0.30'$$

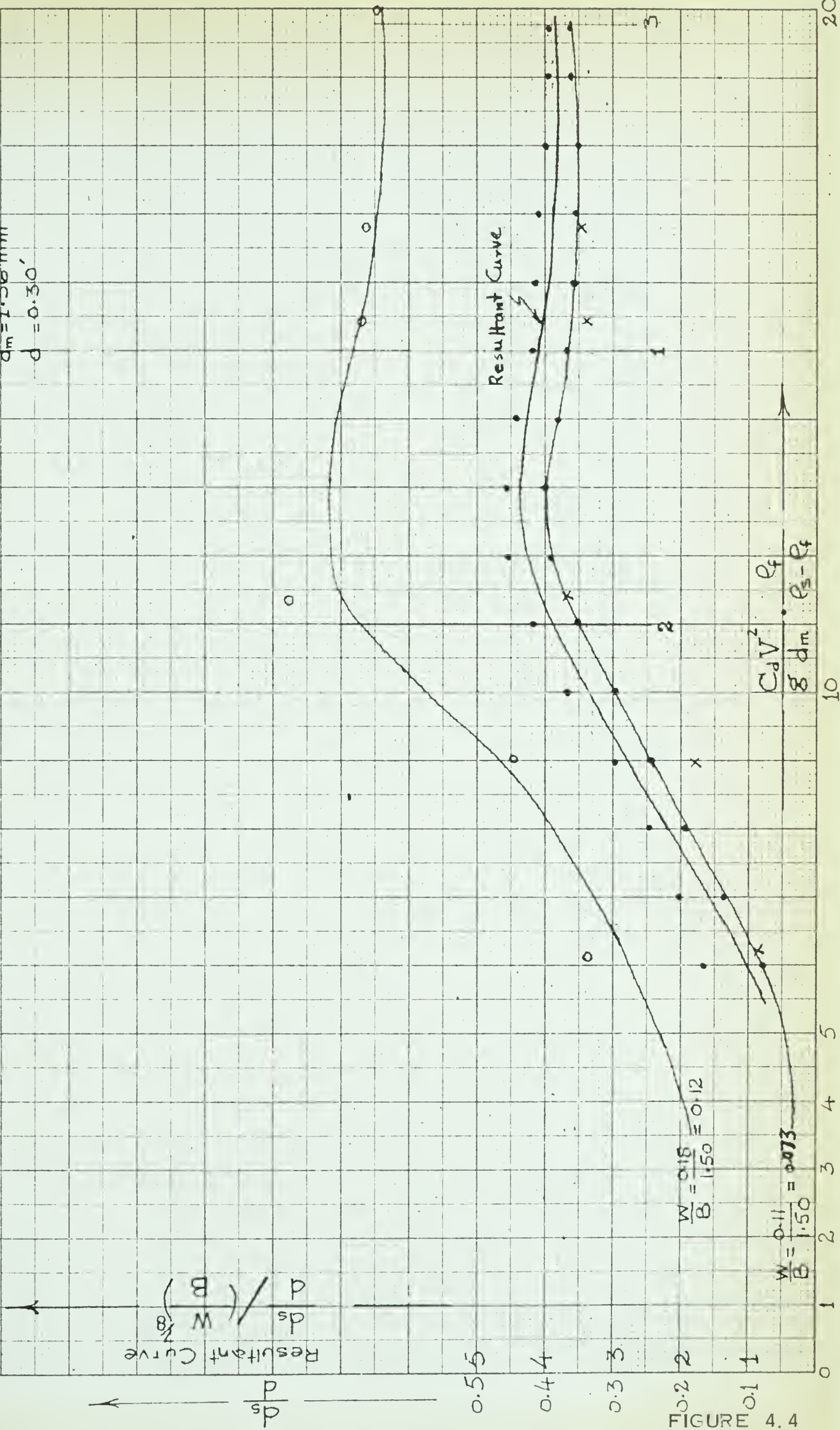


FIGURE 4.4





LIGHT WT. DED MATERIAL

CONSIDERING THE EFFECT OF VARIABLE  $W/B$

FOR

$d_m = 1.56 \text{ mm}$

$d = 0.35'$

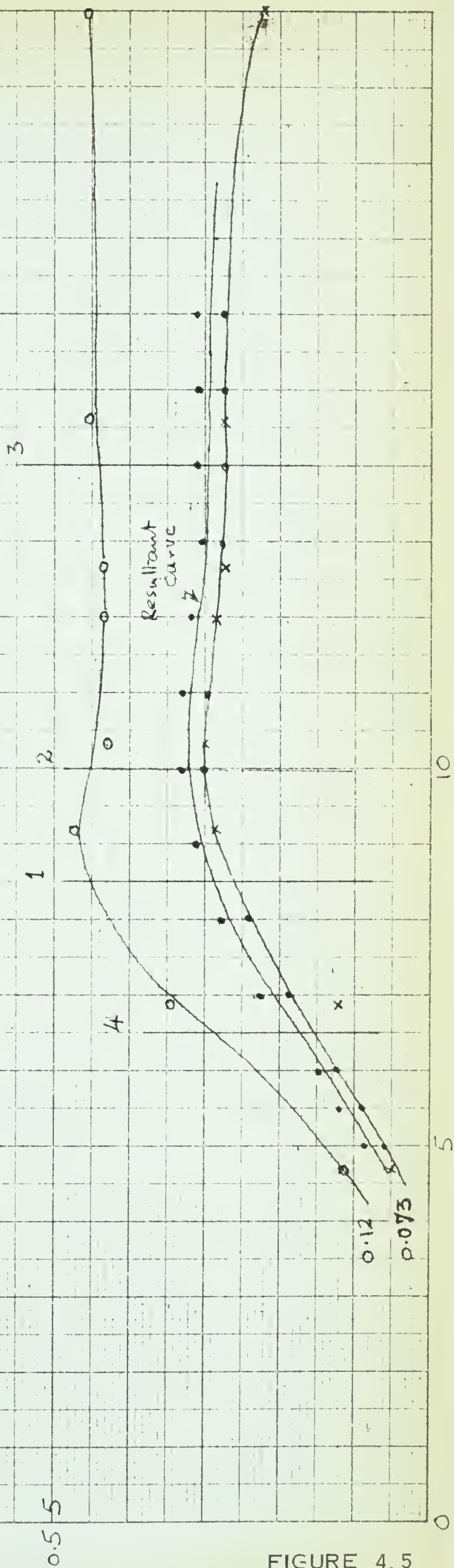


FIGURE 4.5



LIGHT WT BED MATERIAL

CONSIDERING THE EFFECT OF VARIABLE W/B

FOR

$d_m = 1.56 \text{ mm}$

$d = 0.40'$

$\frac{ds}{sp} \left( \frac{B}{M} \right) / \frac{p}{sp}$

$\frac{1}{sp} \frac{p}{sp}$

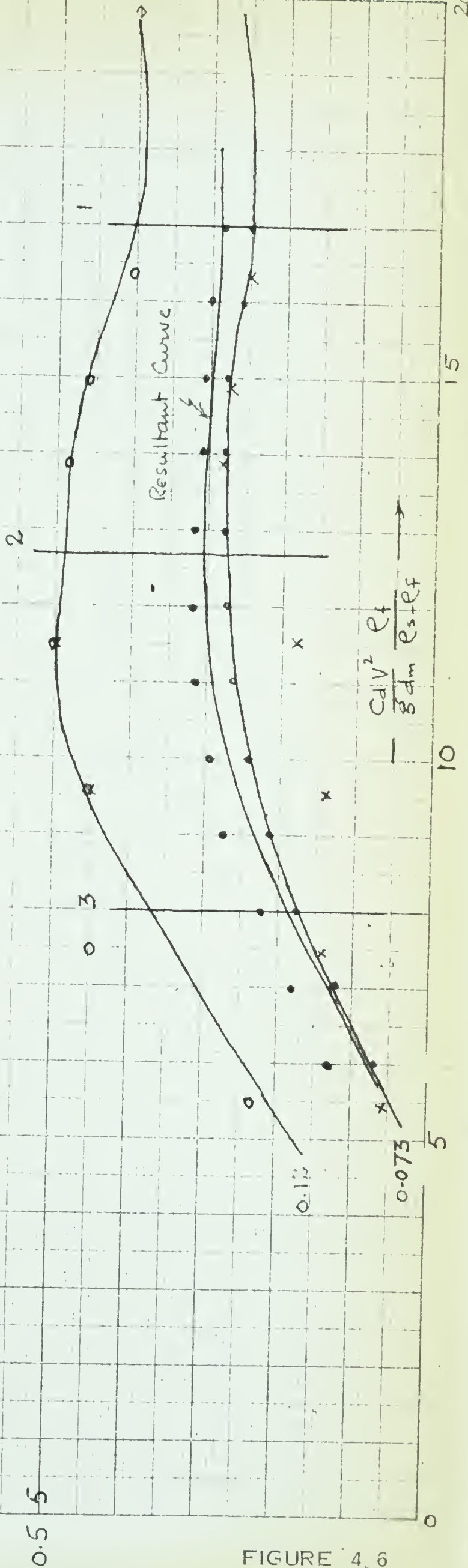


FIGURE 4.6





LIGHT WT. BED MATERIAL

CONSIDERING THE EFFECT OF VARIABLE W/B

FOR

$$d_m = 1.56 \text{ mm}$$

$$d = 0.45'$$

$$\frac{(\frac{B}{M})}{\frac{P}{sp}}$$

$$\frac{P}{sp}$$

0.5 5

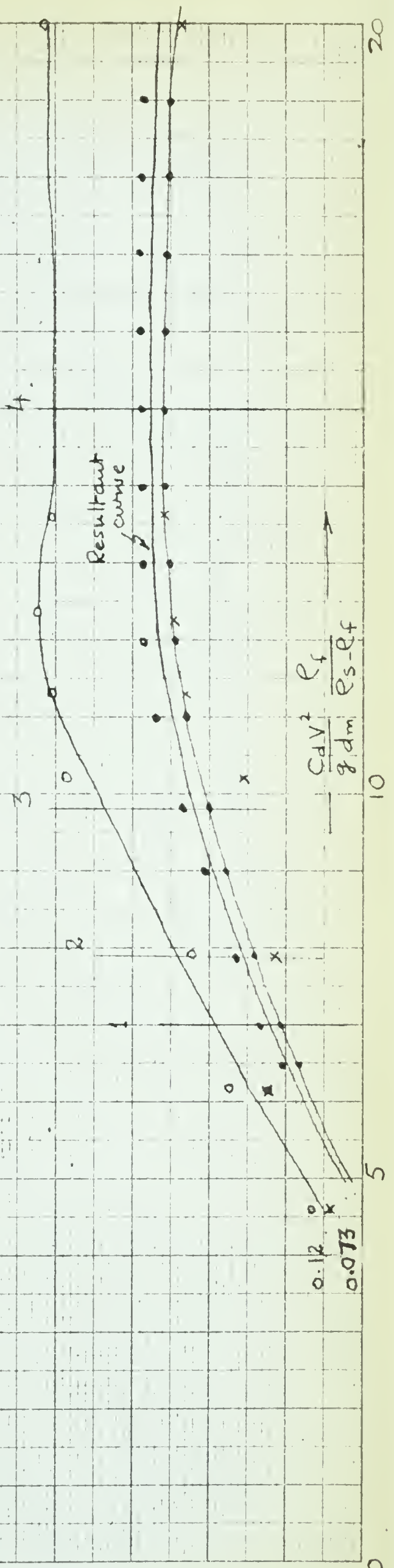


FIGURE 4.7



LIGHT WT. FED MATERIAL

CONSIDERING THE EFFECT OF VARIABLE W/B

FOR

$$d_m = 1.56 \text{ mm}$$

$$d = 0.50$$

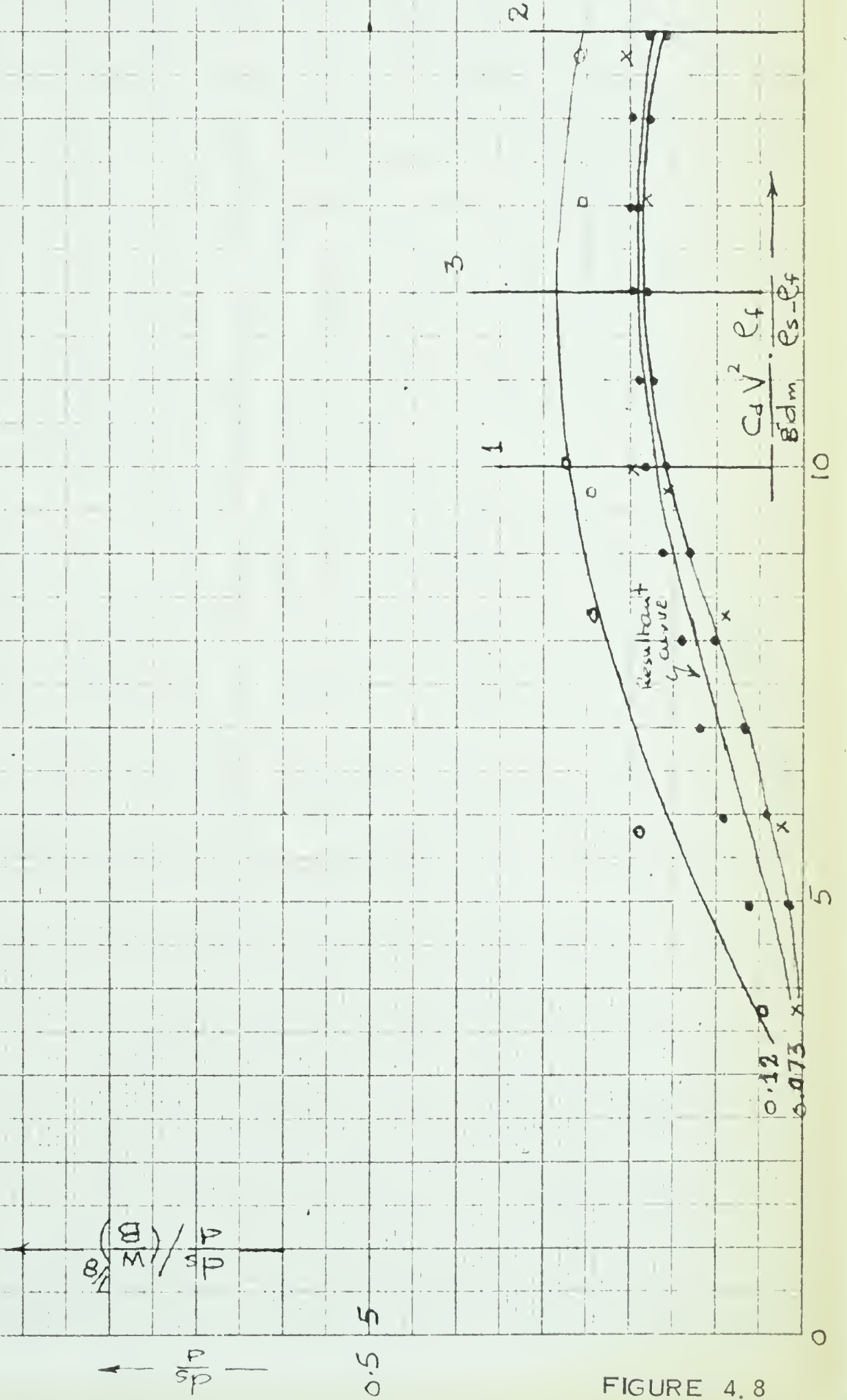


FIGURE 4.8





LIGHT WT. OEO MATERIAL

CONSIDERING THE EFFECT OF VARIABLE W/B

FOR

$d_m = 1.56 \text{ mm}$

$d = 0.55$

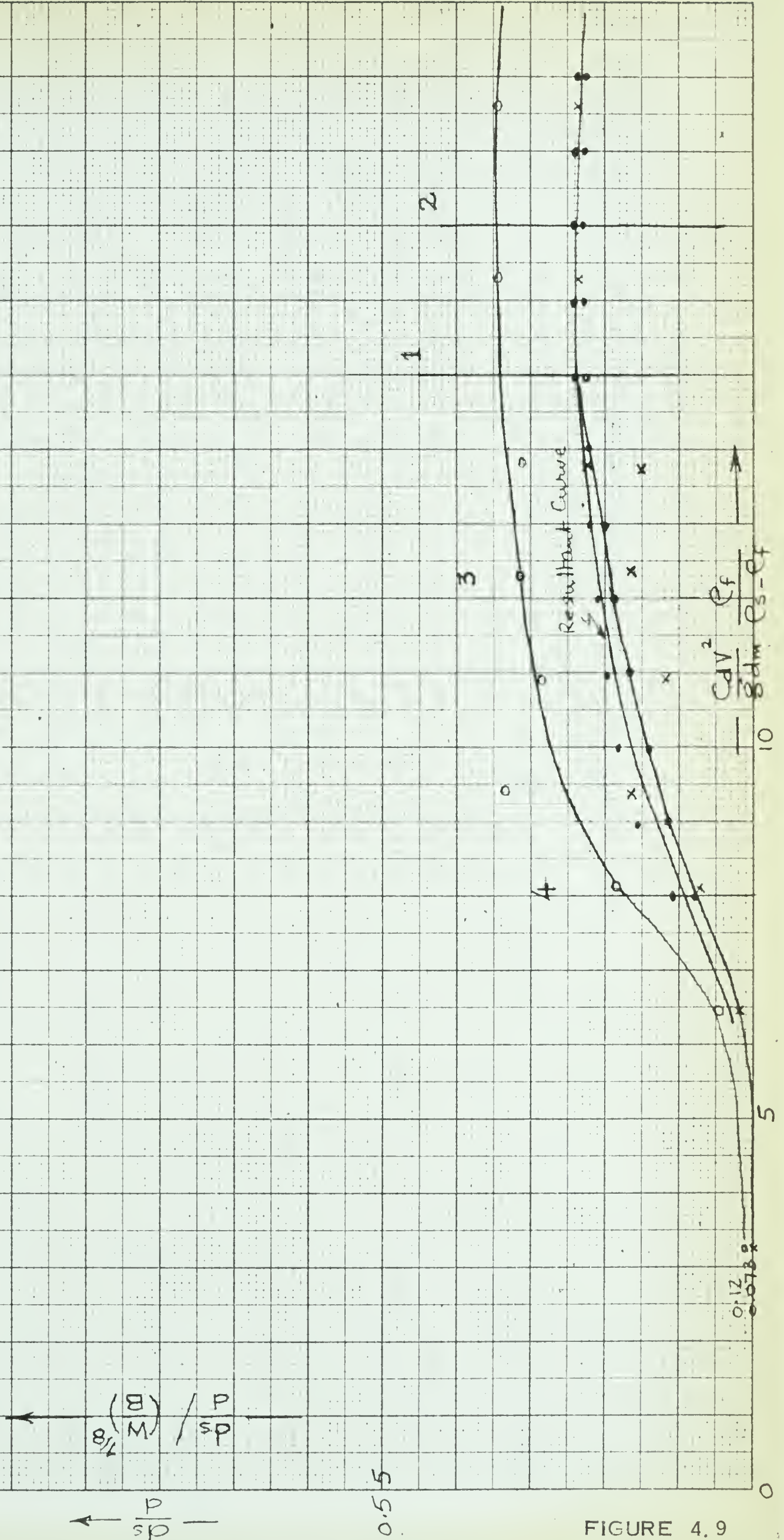


FIGURE 4.9





LIGHT WYLD MATERIAL

CONSIDERING THE EFFECT OF VARIABLE W/B

FOR

$$d_m = 1.56 \text{ mm}$$

$$d = 0.60'$$

$$\frac{ds}{s} = \frac{1}{8} \left( \frac{B}{M} \right) \frac{1}{11}$$

←  $\frac{1}{s}$

0.5 — 5

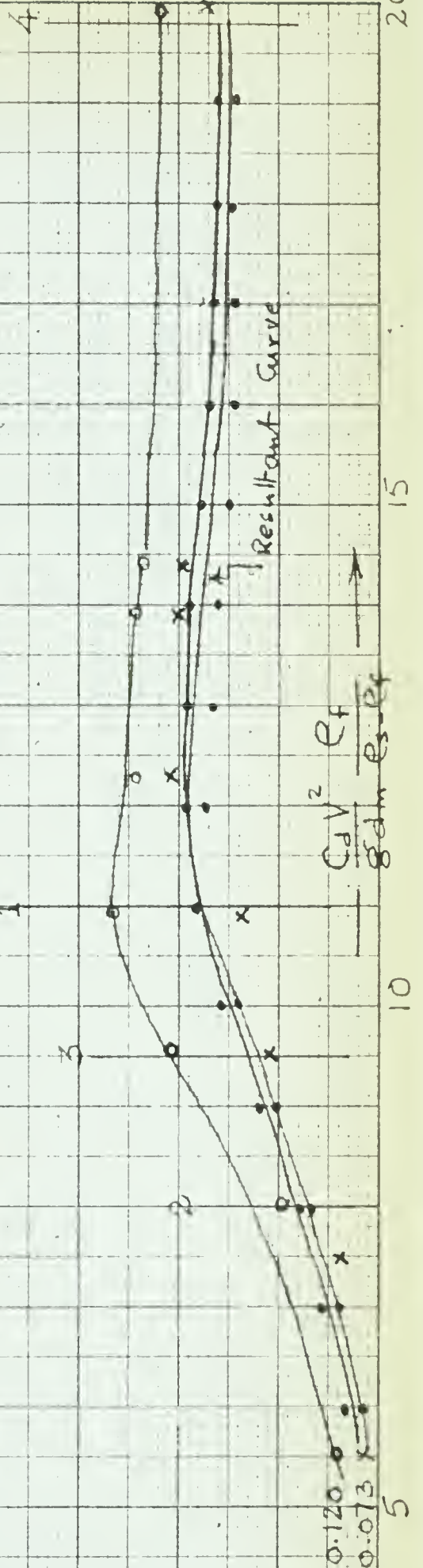


FIGURE 4.10





LIGHT WT. RED MATERIAL

CONSIDERING THE EFFECT OF VARIABLE W/B

FOR

$$d_m = 1.56 \text{ mm}$$

$$d = 0.65'$$

$$\frac{d_s}{d_p} \left( \frac{B}{M} \right) \frac{P}{I_B}$$

$$\frac{P}{d_p}$$

0.5 5

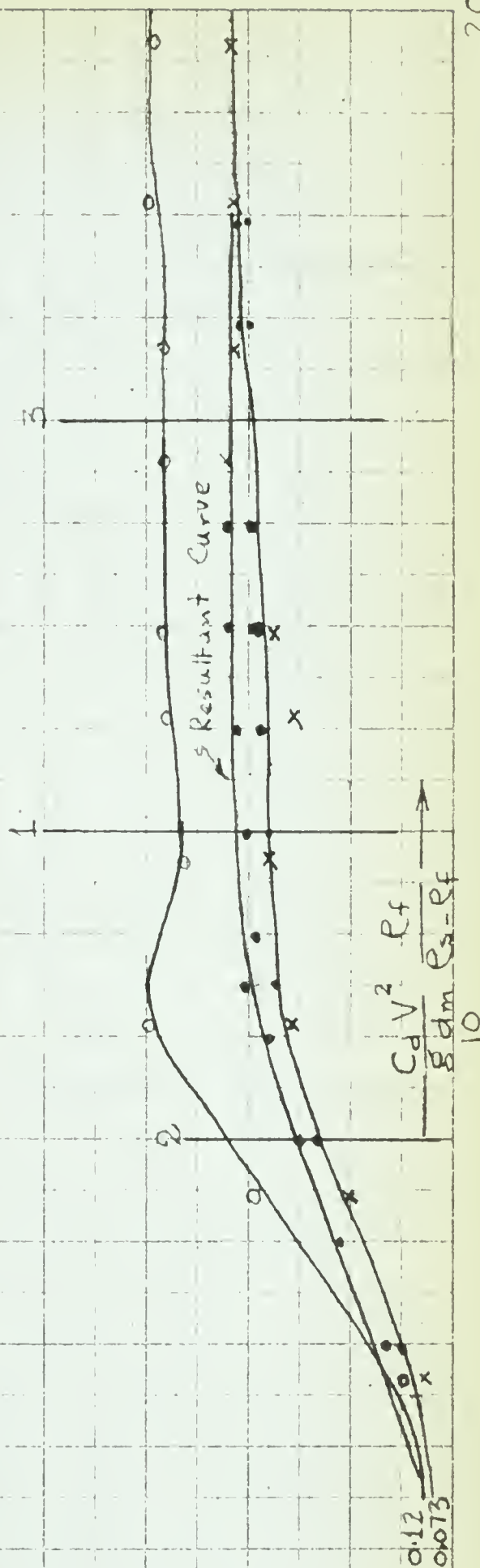


FIGURE 4. II





LIGHT WT BED MATERIAL

CONSIDERING THE EFFECT OF VARIABLE  $W/B$

FOR

$$d_m = 1.56 \text{ mm}$$

$$d = 0.70'$$

$$\frac{ds}{ds} / (W/B)^{1/8}$$

$$\frac{P}{sp}$$

0.5 5

2

3

4

0

10

0.12  
0.073

$$\frac{CdV^2 \cdot Cf}{g d_m \cdot Ps - Cf}$$

Resultant Curve

FIGURE 4.12

20



LIGHT WT. BED MATERIAL

CONSIDERING THE EFFECT OF VARIABLE  $W/B$

FOR

$$d_m = 1.56 \text{ mm}$$

$$d = 0.75'$$

$$\frac{d_s}{d} \left( \frac{B}{M} \right)^{1/8}$$

0.5 5

3

2

1

Resultant Curve

$$\frac{C_d V^2}{g d_m} \cdot \frac{R_f}{C_s - R_f}$$

10

0.12  
0.073

FIGURE 4.13

0

20





LIGHT WT. RED MATERIAL

CONSIDERING THE EFFECT OF VARIABLE W/B

FOR

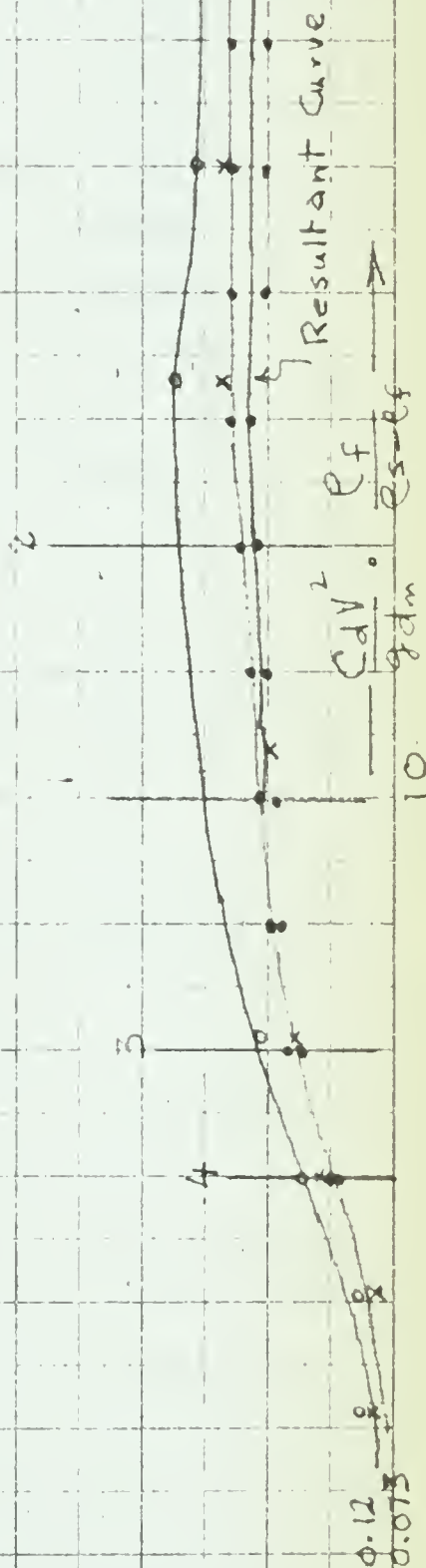
$$d_m = 1.56 \text{ mm}$$

$$d = 0.80'$$

$$\frac{ds}{sp} \rightarrow \frac{ds}{sp} \left( \frac{B}{M} \right)^{1/8}$$

0.5

FIGURE 4.14





LIGHT WT. DRED MATERIAL

CONSIDERING THE EFFECT OF VARIABLE W/B

FOR

$$d_m = 1.56 \text{ mm}$$

$$d = 0.85'$$

$\frac{ds}{dp}$  —  $\frac{ds}{d(W/B)}$   $\frac{1}{16}$

0.5 5

2

3

4

Resultant Curve

$$\frac{C_d V^2}{g d_m} \cdot \frac{e_f}{e_s - e_f}$$

10

0.12  
0.073

FIGURE 4.15

0

20





LIGHT WT. BED MATERIAL

CONSIDERING THE EFFECT OF VARIABLE  $W/B$

FOR

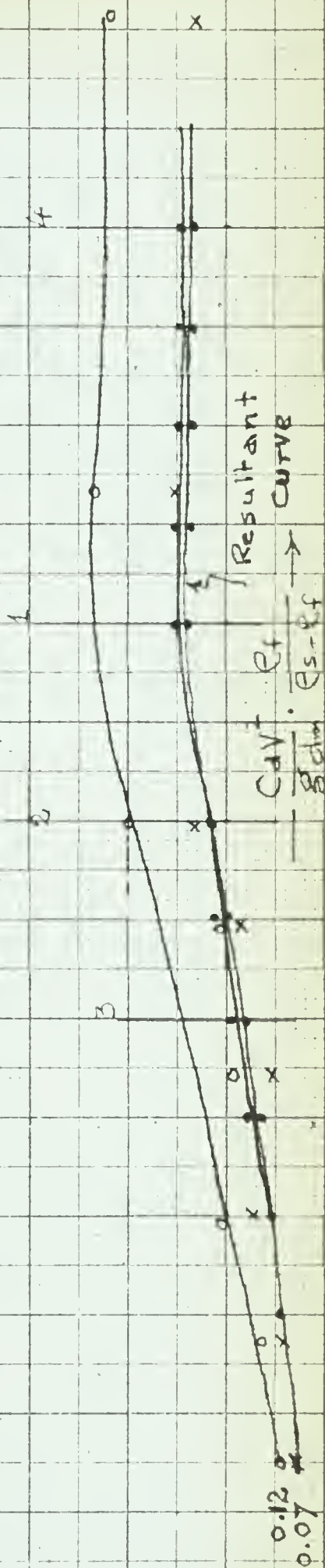
$$d_m = 1.56 \text{ mm}$$

$$d = 0.90'$$

$$\frac{d}{p} \left( \frac{B}{M} \right)^{1/8}$$

0.5 5

FIGURE 4 16







LIGHT WT. BED MATERIAL

CONSIDERING THE EFFECT OF VARIABLE W/B

FOR  
 $d_m = 1.56 \text{ mm}$   
 $d = 0.95'$

$\frac{C_d V^2}{g d_m} \frac{e_f}{e_s - e_f}$

$\frac{C_d V^2}{g d_m} \frac{e_f}{e_s - e_f}$

0.5 5

2 3

Resultant Curve 2

$\frac{C_d V^2}{g d_m} \frac{e_f}{e_s - e_f}$

0.12  
0.075

10

15

20

FIGURE 4.17



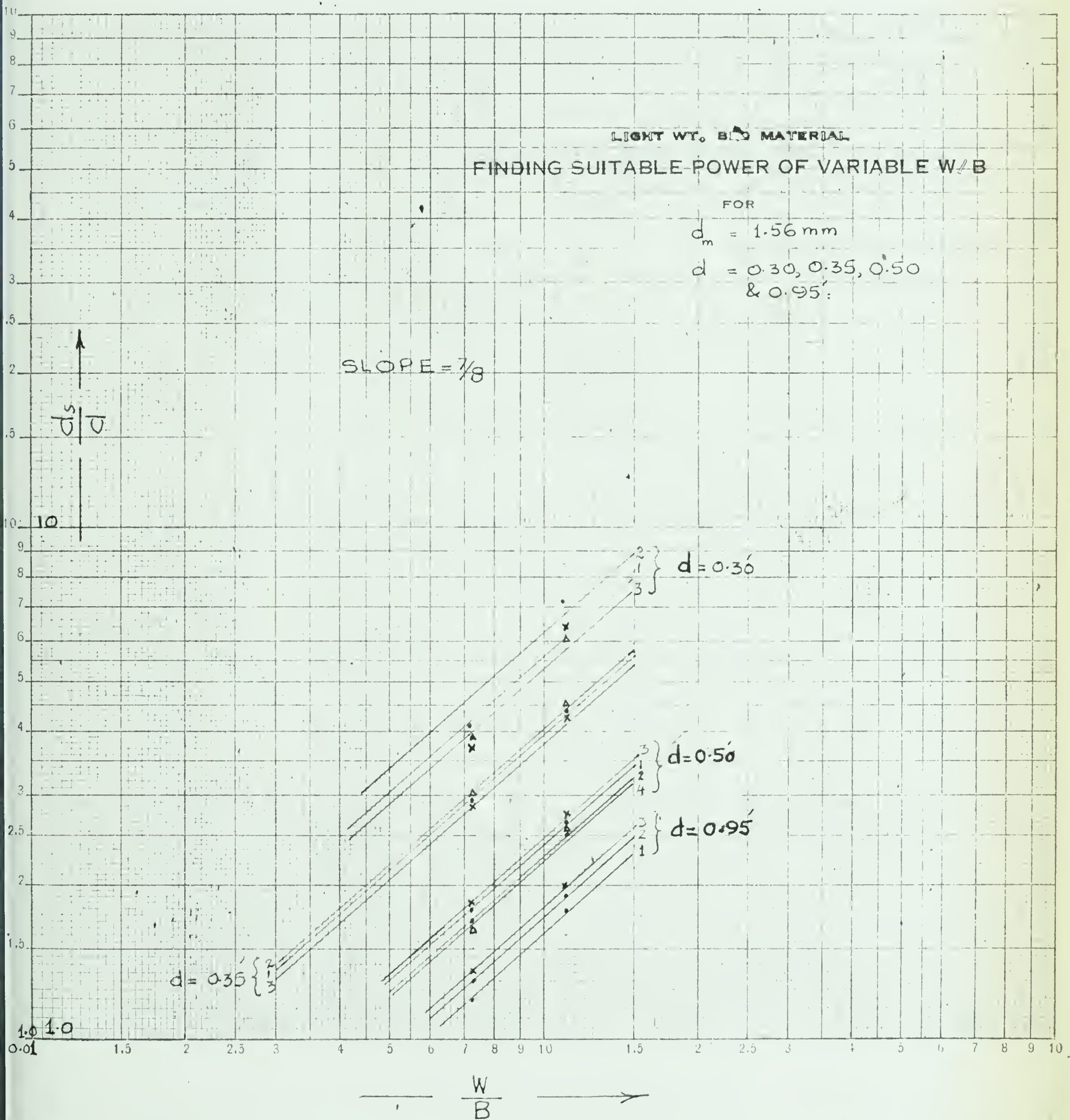


FIGURE 4, 18





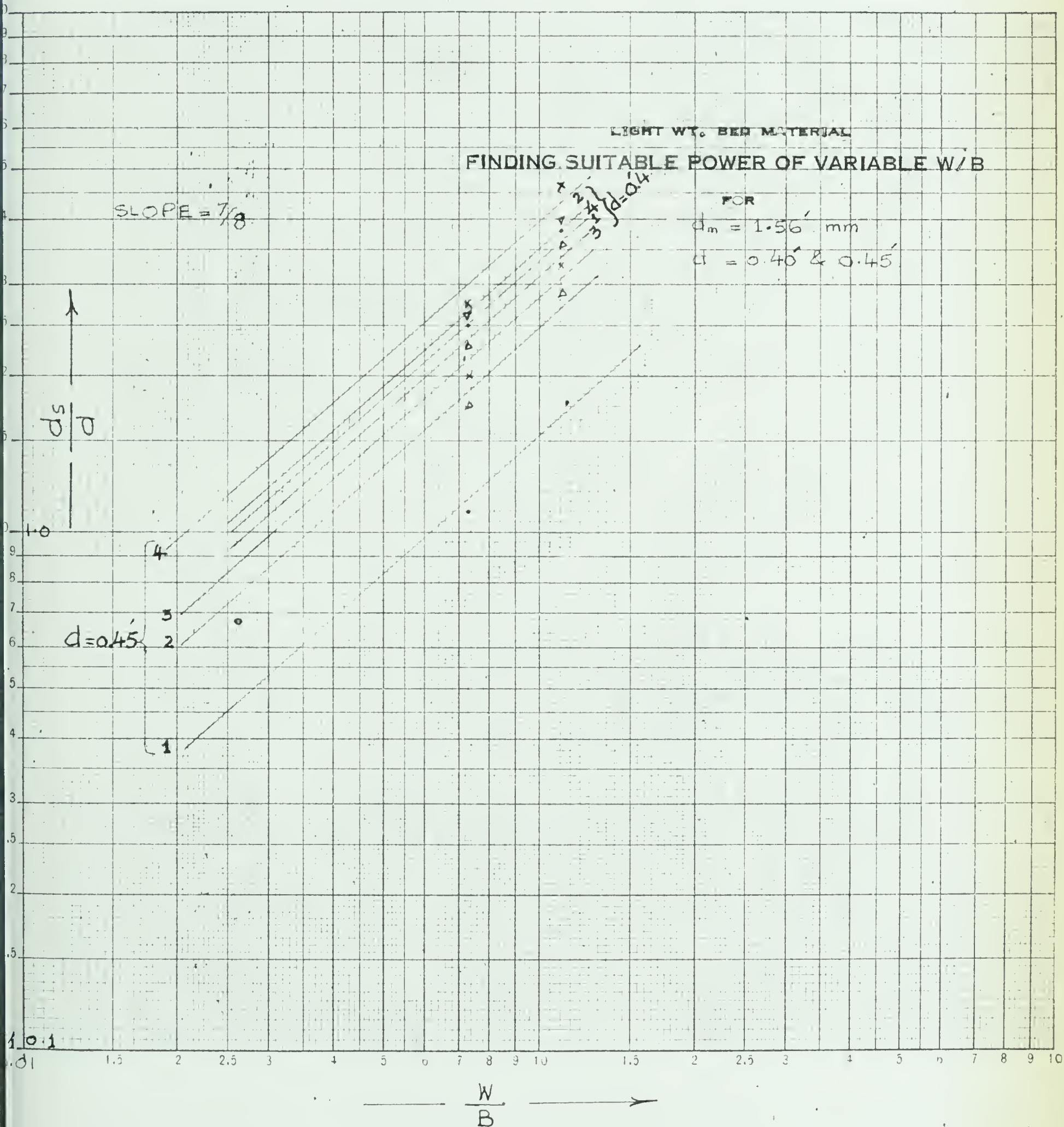


FIGURE 4.19



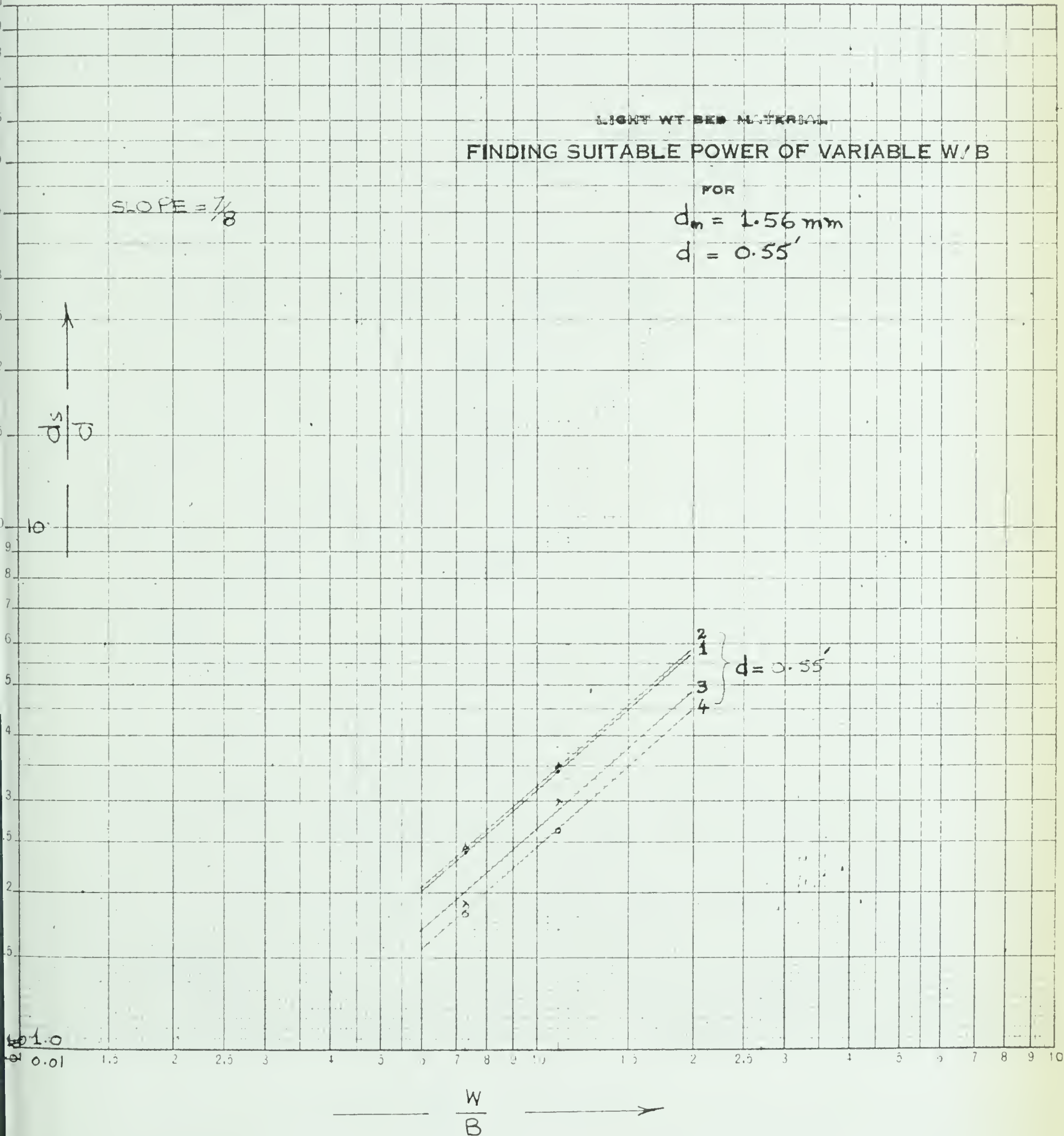


FIGURE 4.20





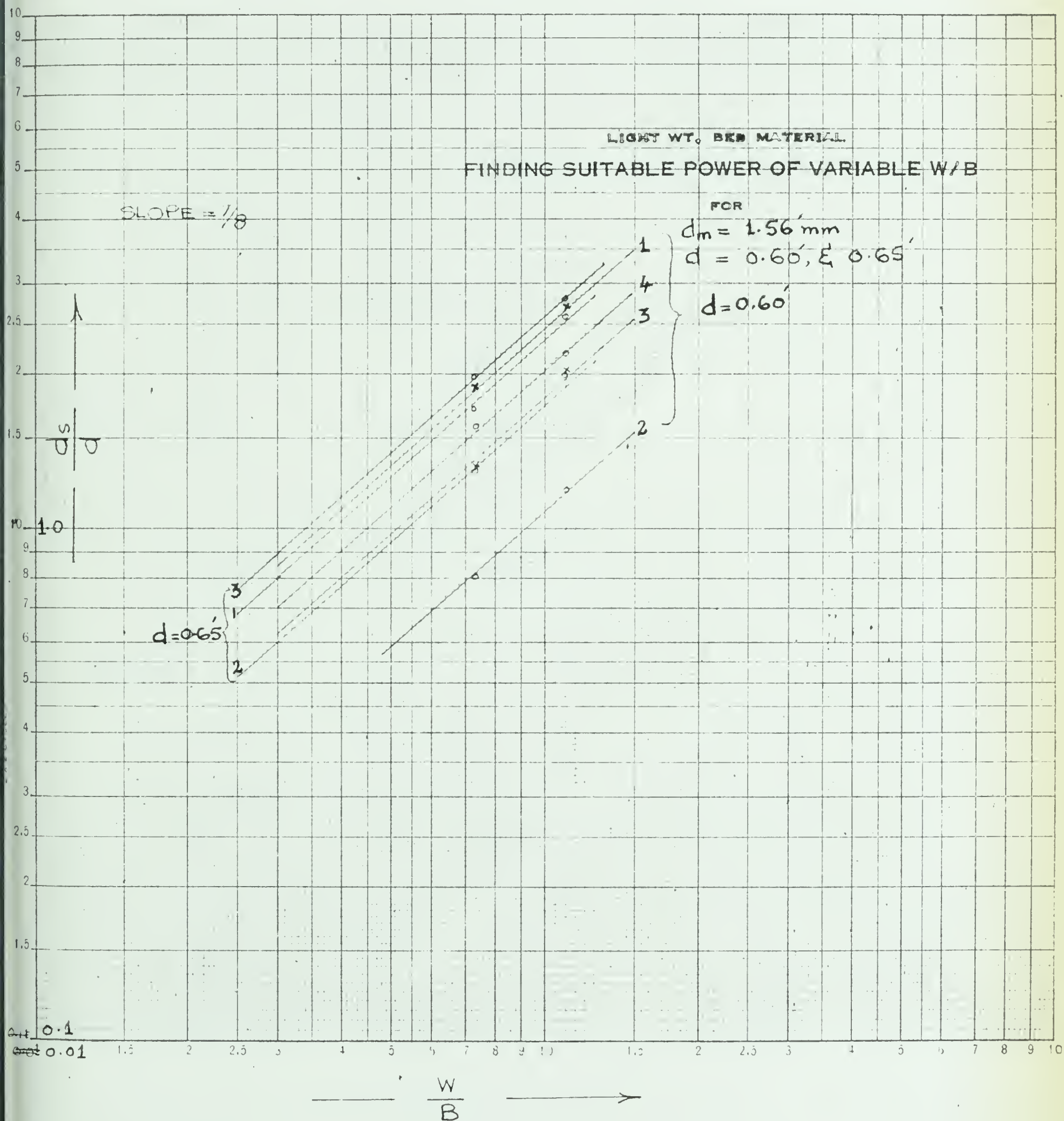


FIGURE 4.21





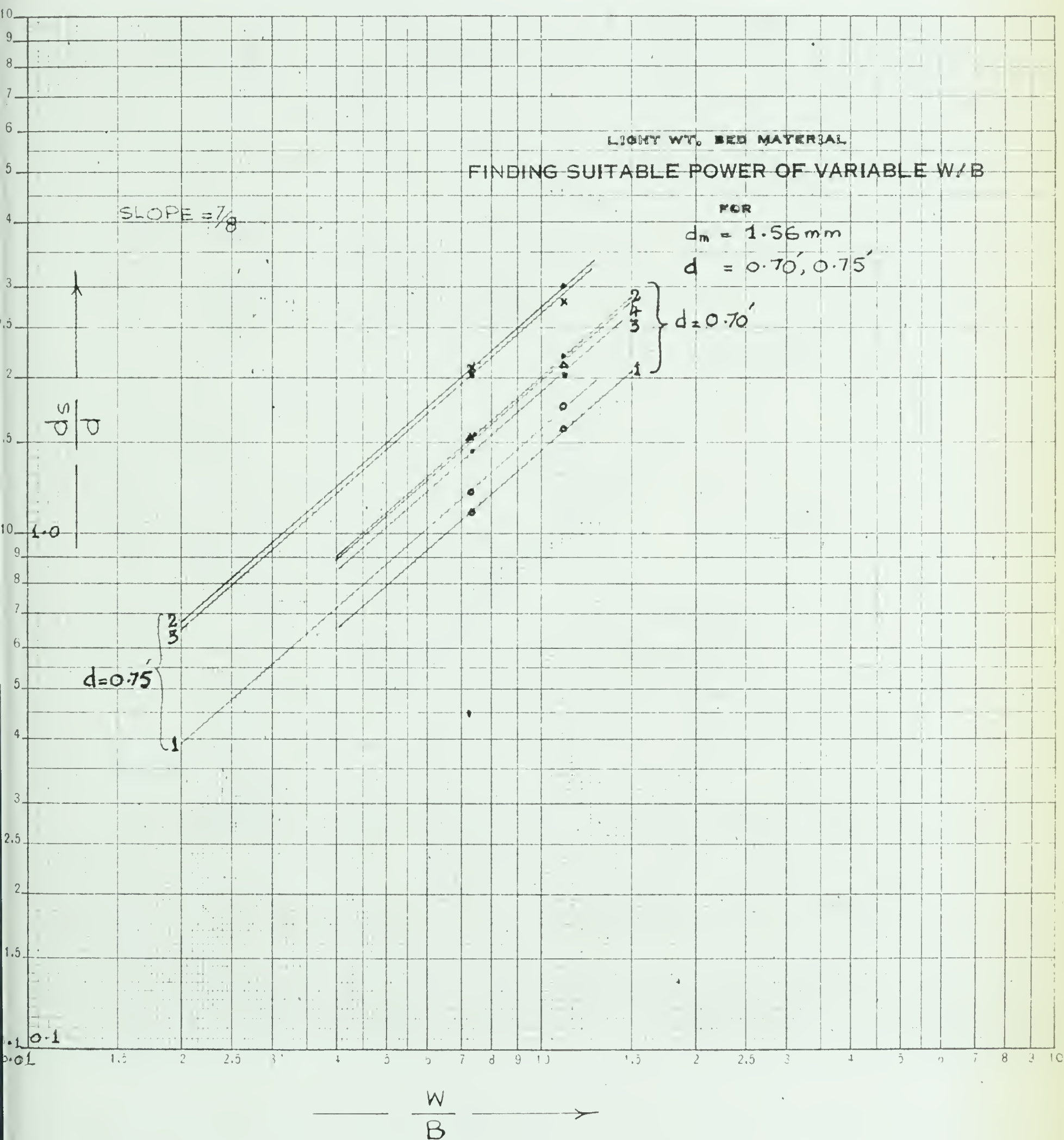


FIGURE 4.22



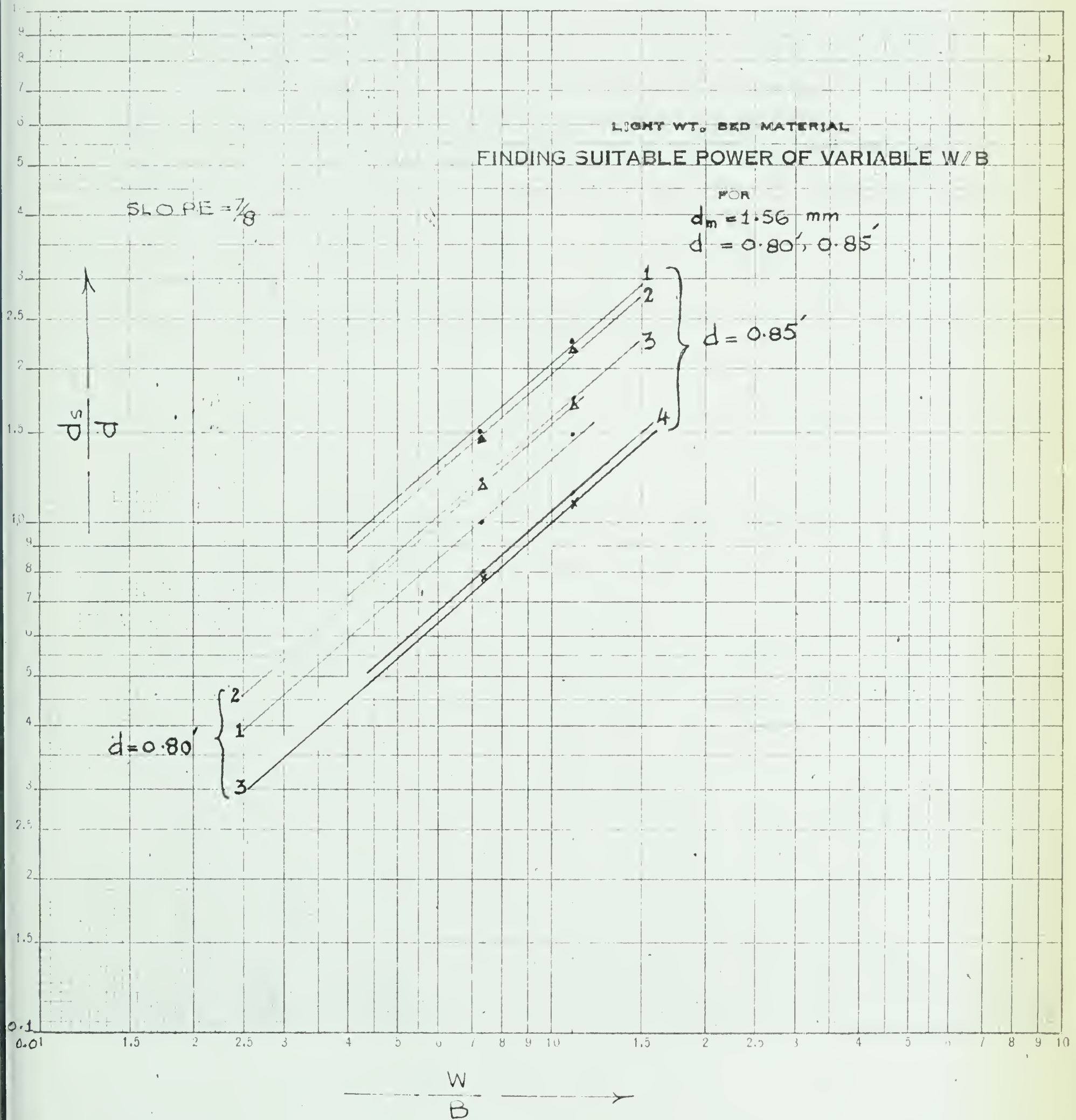


FIGURE 4.23





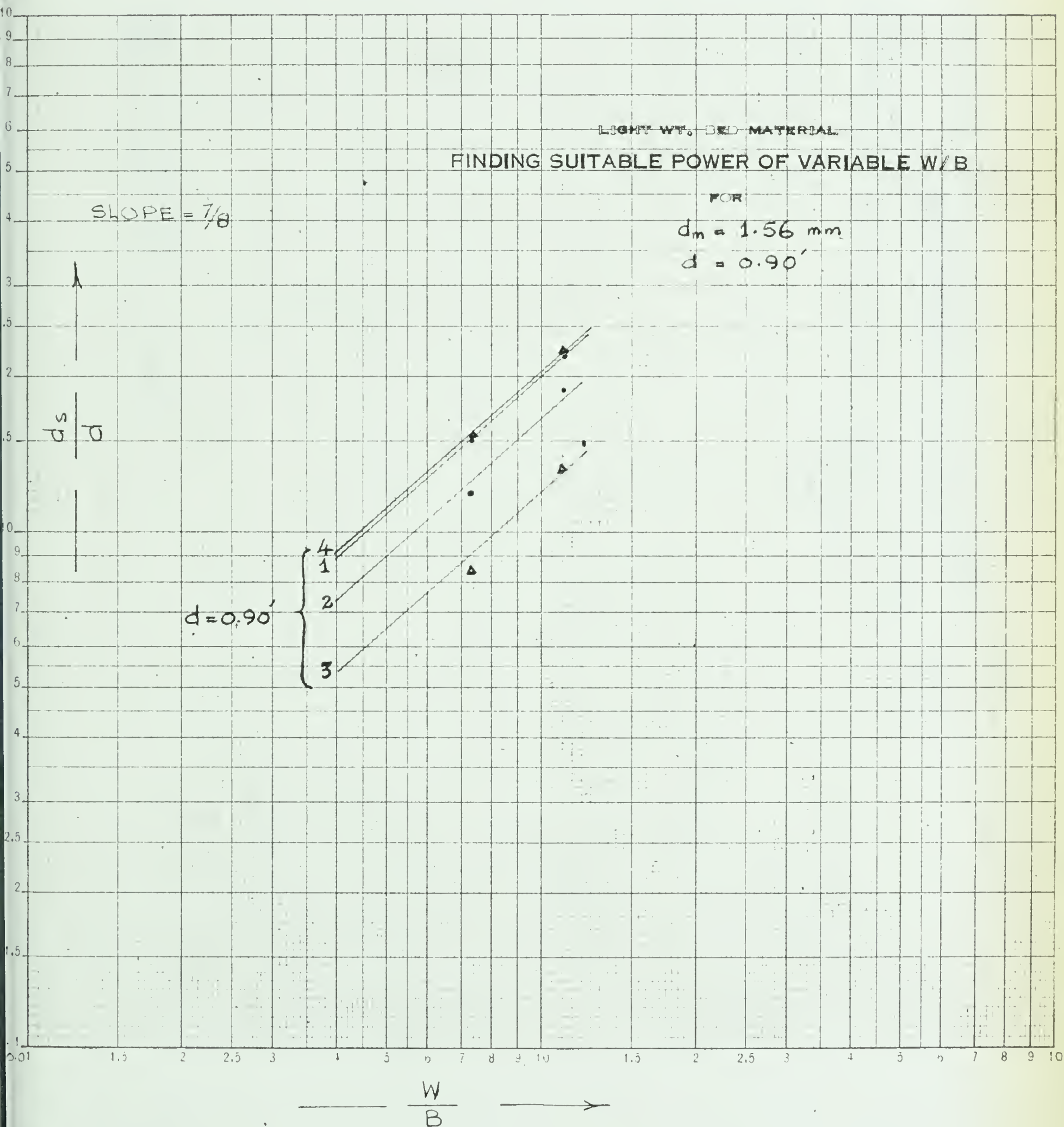


FIGURE 4.24



LIGHT WT. BED MATERIAL  
 VARIATION OF  $\left[\frac{d_s}{d} \left(\frac{W}{B}\right)^{1/8}\right]$  WITH  $\left[\frac{C_d V^2}{g_{dm}} \cdot \frac{\rho_f}{\rho_s - \rho_f}\right]$   
 [GRAVEL RANGE]

1.0

←

$\frac{8}{1} \left(\frac{W}{B}\right)^{1/8}$

←

$\frac{p}{s}$

—

0.5

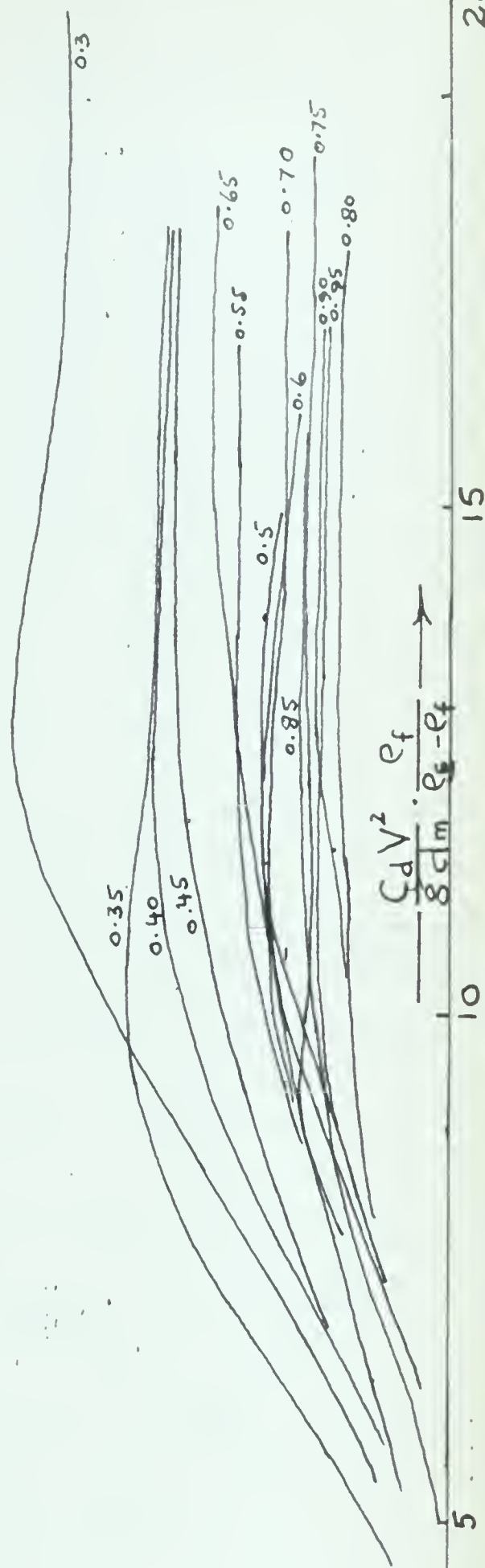


FIGURE 4.25





LIGHT WT. BED MATERIAL

# CONSIDERING THE EFFECT OF VARIABLE $d/B$

FOR  
GRAVEL RANGE

$\frac{d_s}{d} \left( \frac{B}{W} \right)^{1/2}$  ———  
Resultant Curve  $\left( \frac{d}{B} \right)^{1/2}$

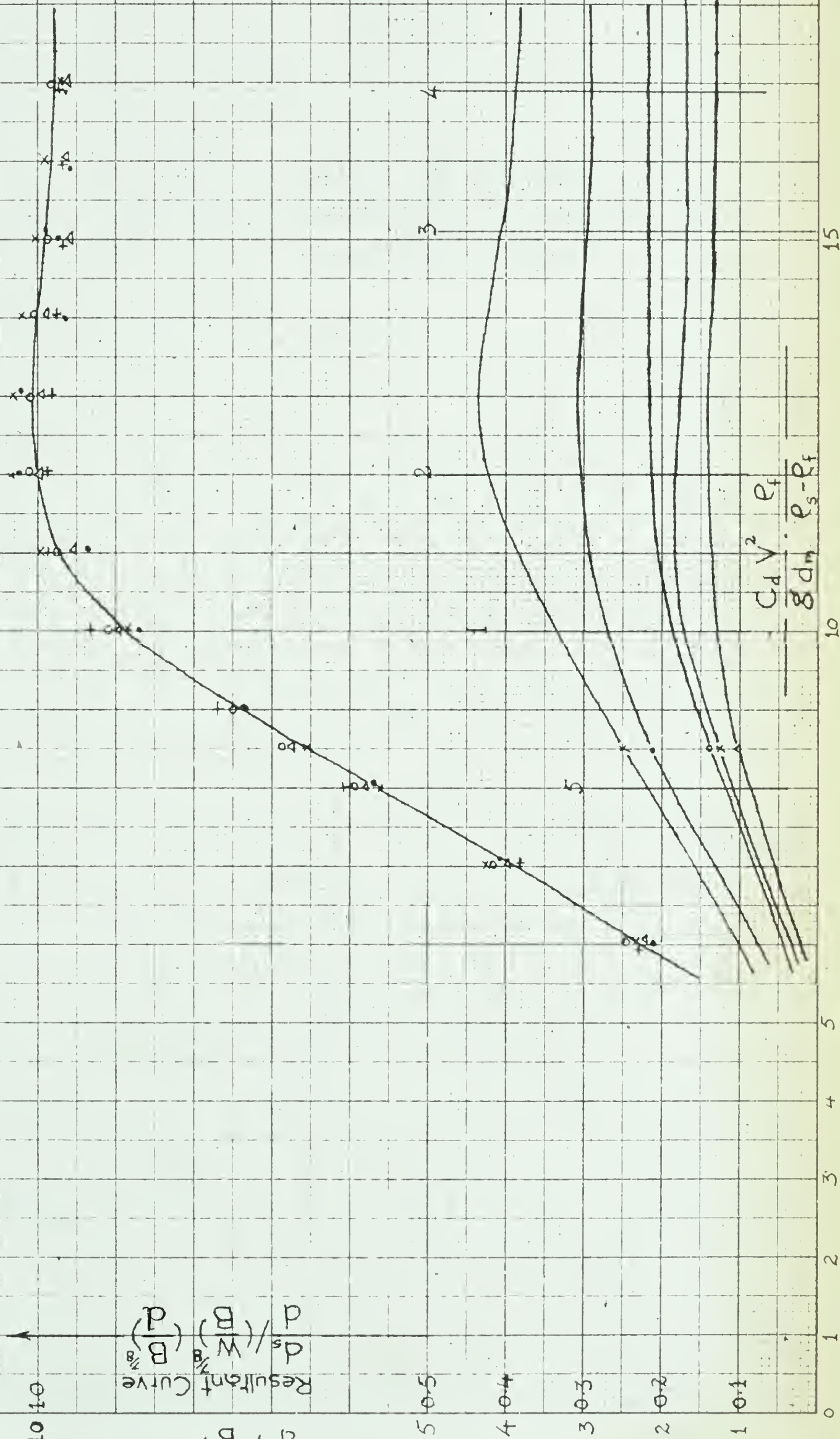


FIGURE 4.26





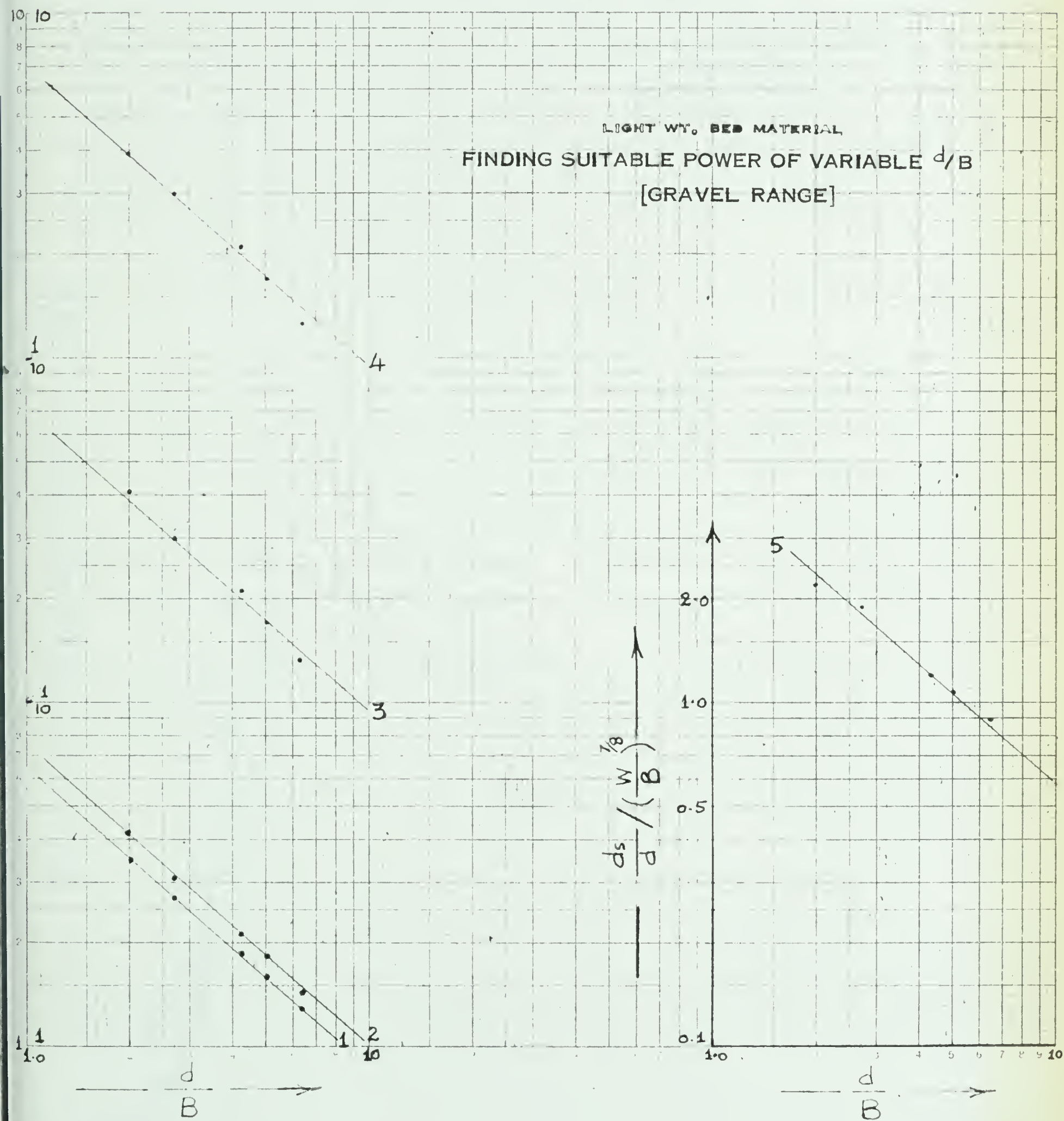


FIGURE 4.27



LIGHT WT. BED MATERIAL

VARIATION OF SCOUR DEPTH WITH VELOCITY

FOR  
 $W = 0.18, d = 0.30', 0.35', 0.40', 0.45'$   
[GRAVEL RANGE]

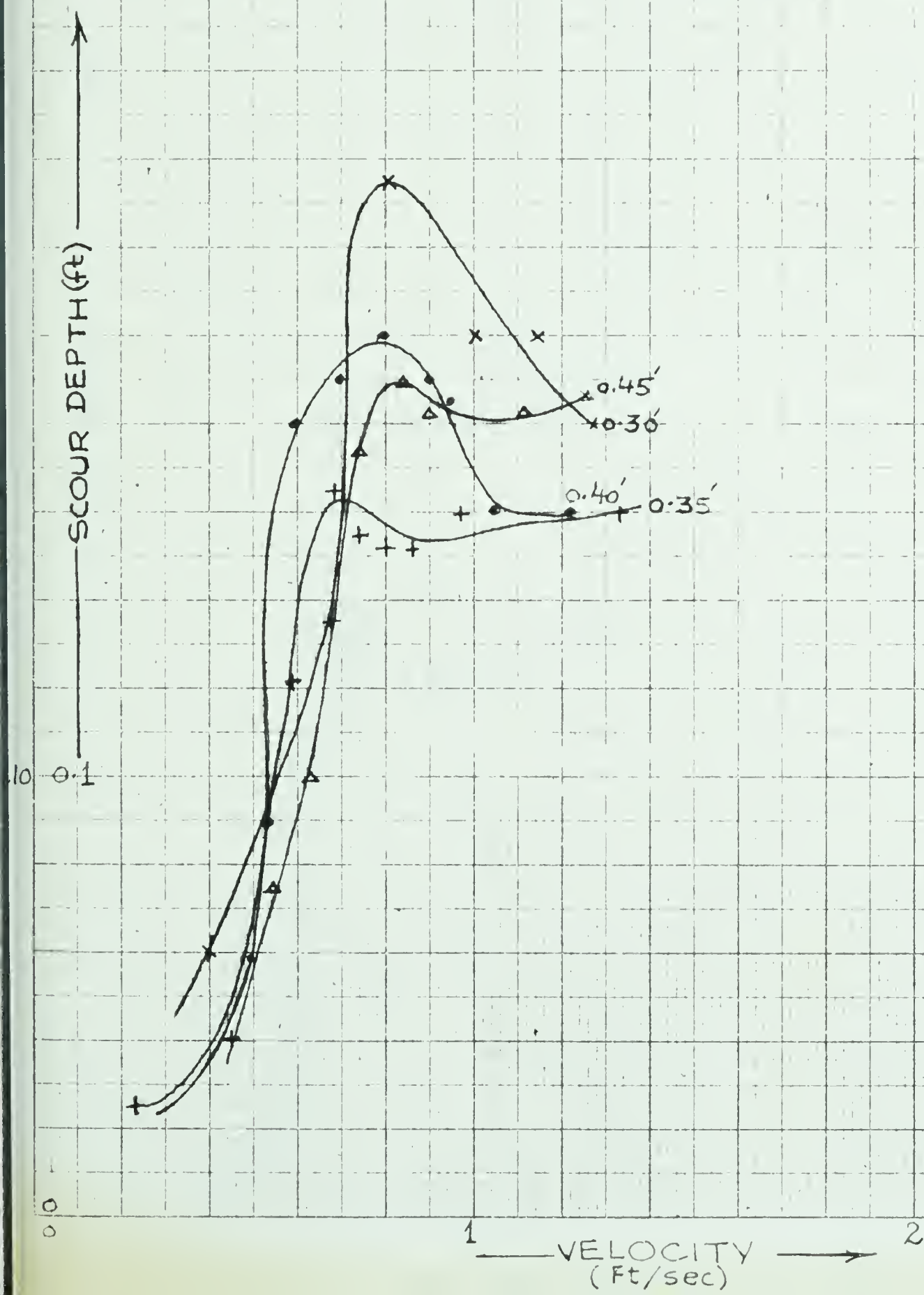


FIGURE 4.28





LIGHT WT. BED MATERIAL

VARIATION OF SCOUR DEPTH WITH VELOCITY

FOR

$$W = 0.18', \quad d = 0.50', 0.55', 0.60', 0.65'$$

[GRAVEL RANGE]

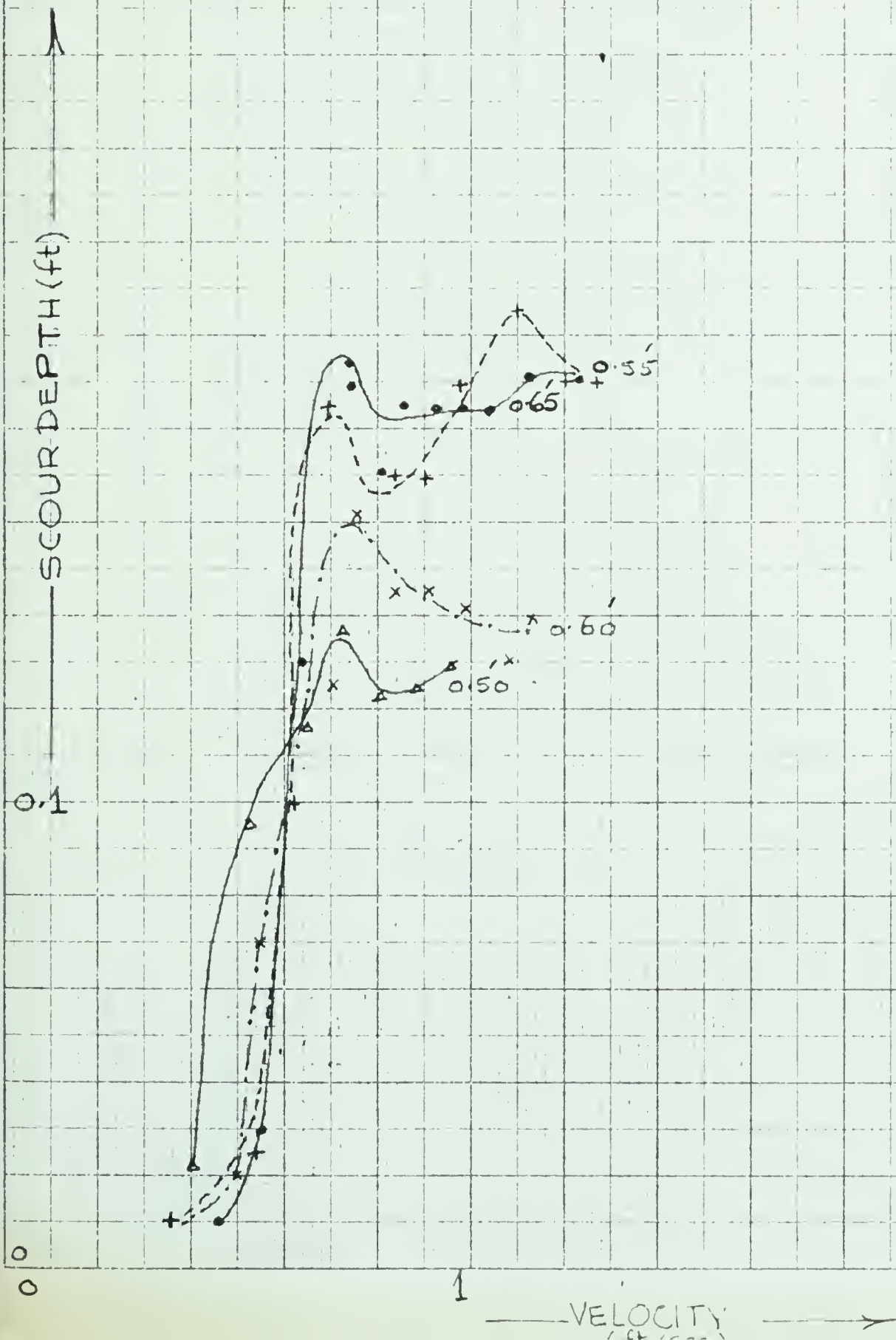


FIGURE 4.29



LIGHT WT. BED MATERIAL

VARIATION OF SCOUR DEPTH WITH VELOCITY

$W=0.19$ ,  $d = 0.70', 0.75', 0.80', 0.85'$   
[GRAVEL RANGE]

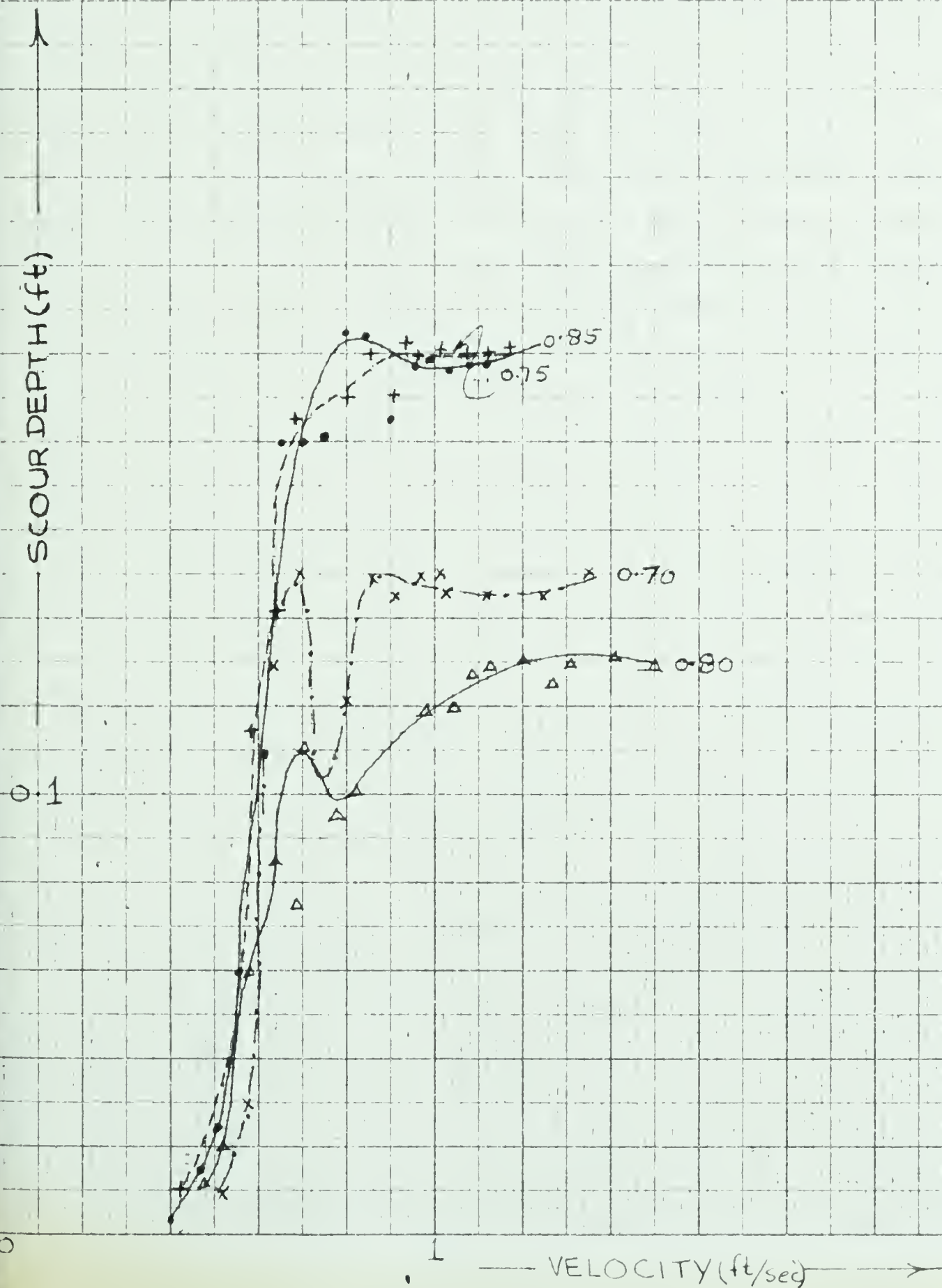


FIGURE 4.30





LIGHT WT. BED MATERIAL  
 VARIATION OF SCOUR DEPTH WITH VELOCITY

FOR  
 $W = 0.18$ ,  $d = 0.90 \text{ to } 0.95$   
 [GRAVEL RANGE]

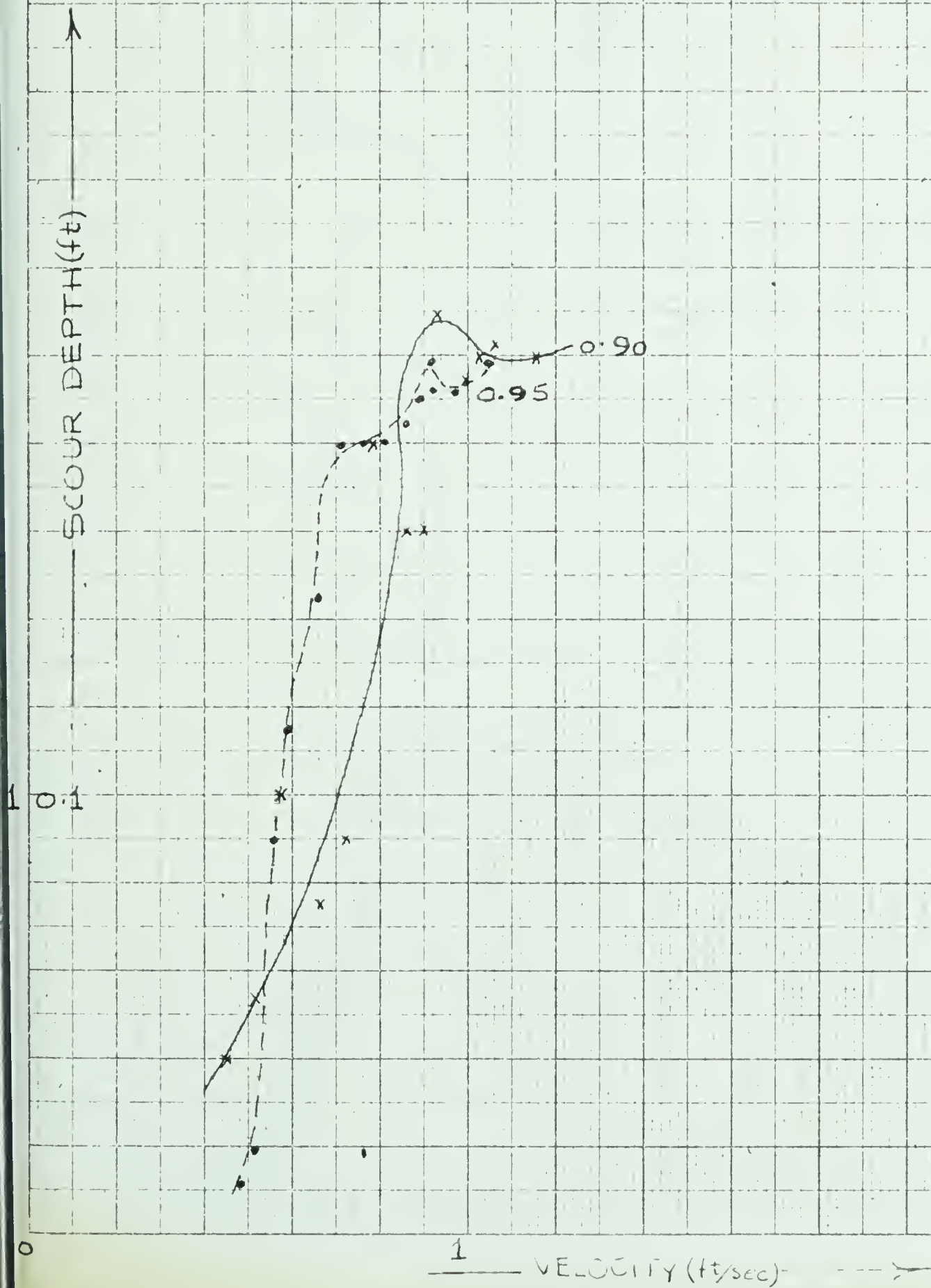


FIGURE 4.31





LIGHT WT. BED MATERIAL

VARIATION OF SCOUR DEPTH WITH VELOCITY

FOR

$W = 0.11'$ ,  $d = 0.30', 0.35', 0.40' \text{ \& } 0.45'$

[GRAVEL RANGE]

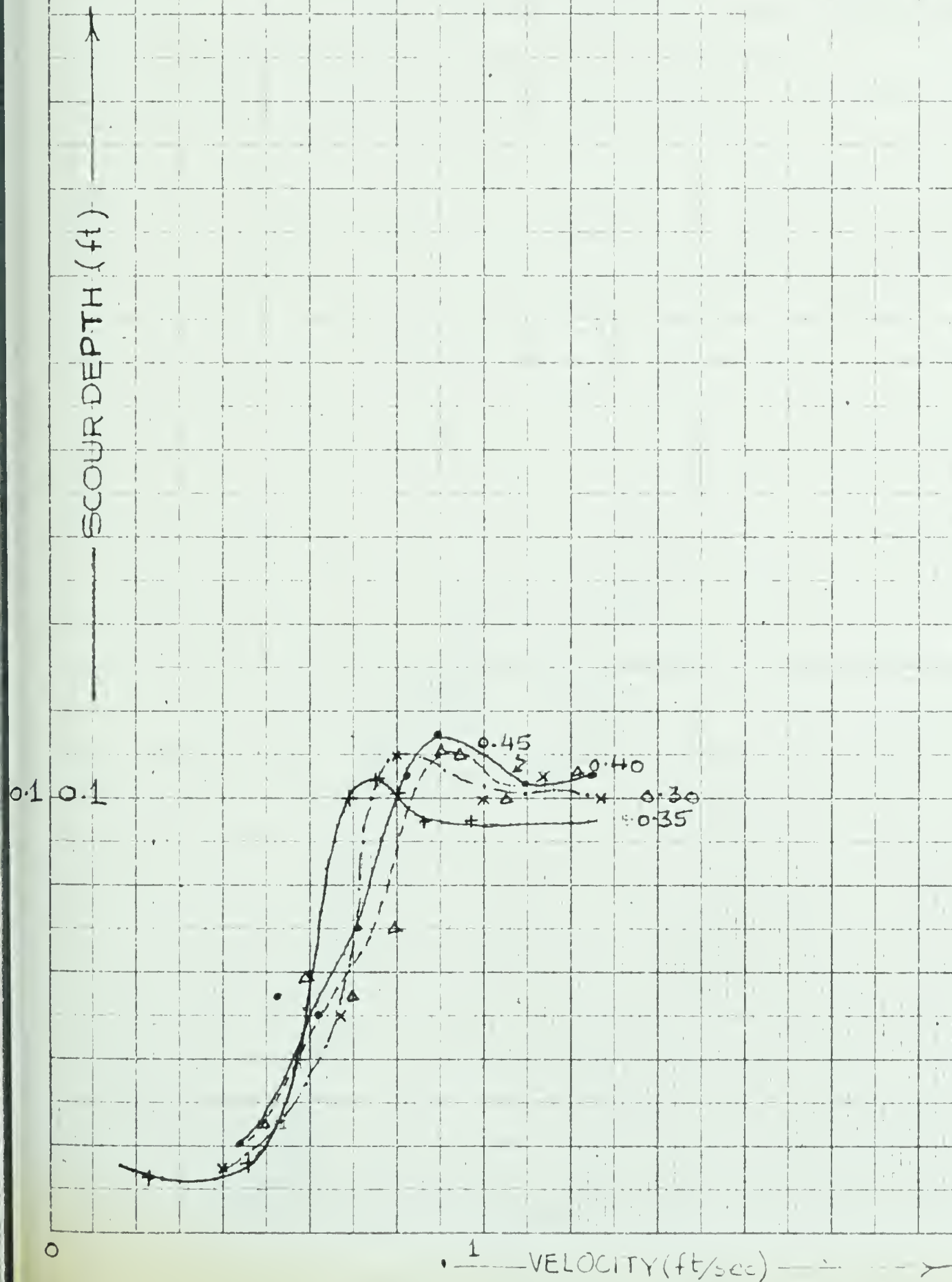


FIGURE 4.32



LIGHT WT. BED MATERIAL

VARIATION OF SCOUR DEPTH WITH VELOCITY

FOR  
 $W=0.11'$ ,  $d=0.50', 0.55', 0.60' \text{ \& } 0.65'$

[GRAVEL RANGE]

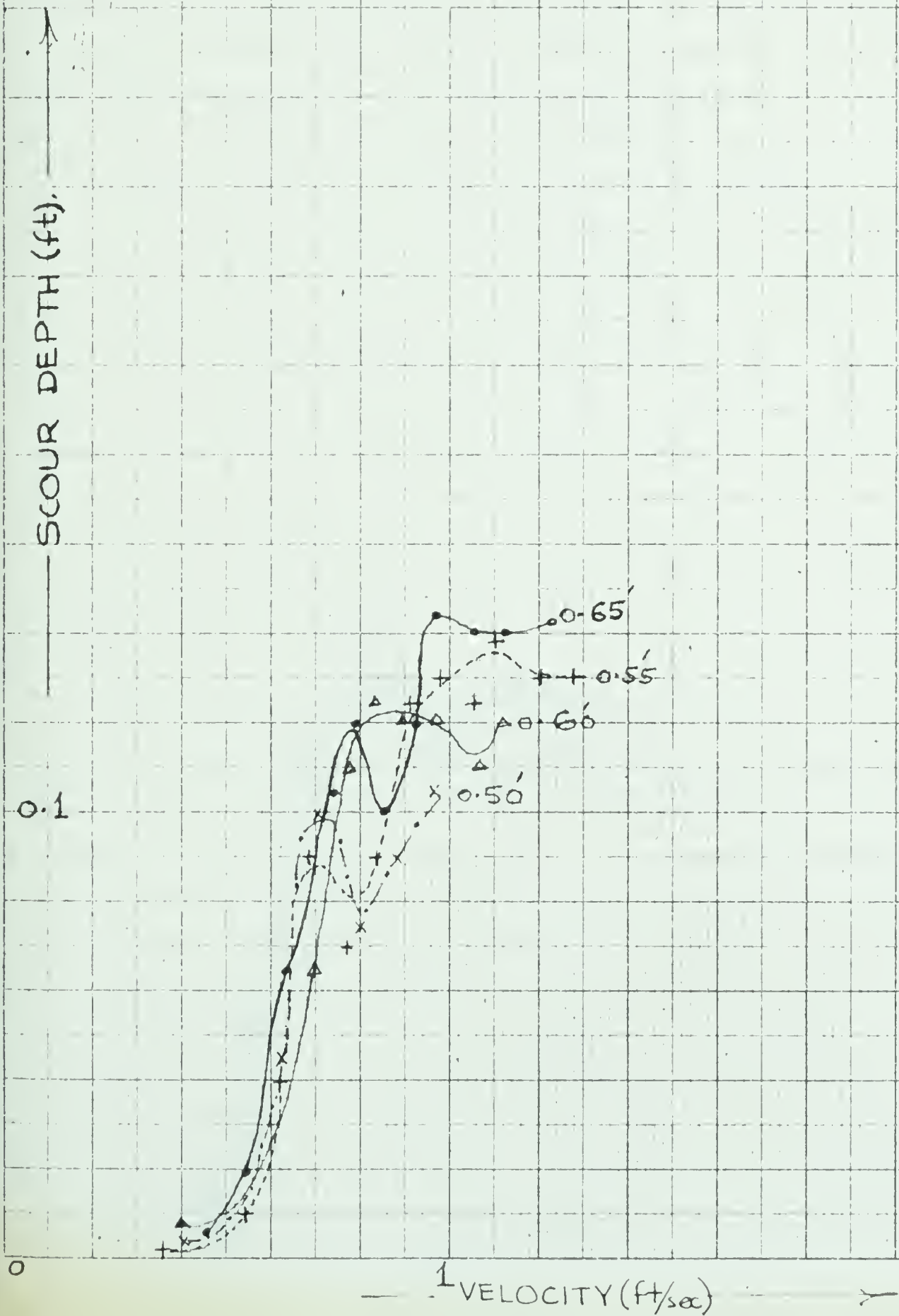


FIGURE 4.33









LIGHT WT. BED MATERIAL

VARIATION OF SCOUR DEPTH WITH VELOCITY

FOR  $W = 0.11$ ,  $d = 0.90$  AND  $0.95$

[GRAVEL RANGE]

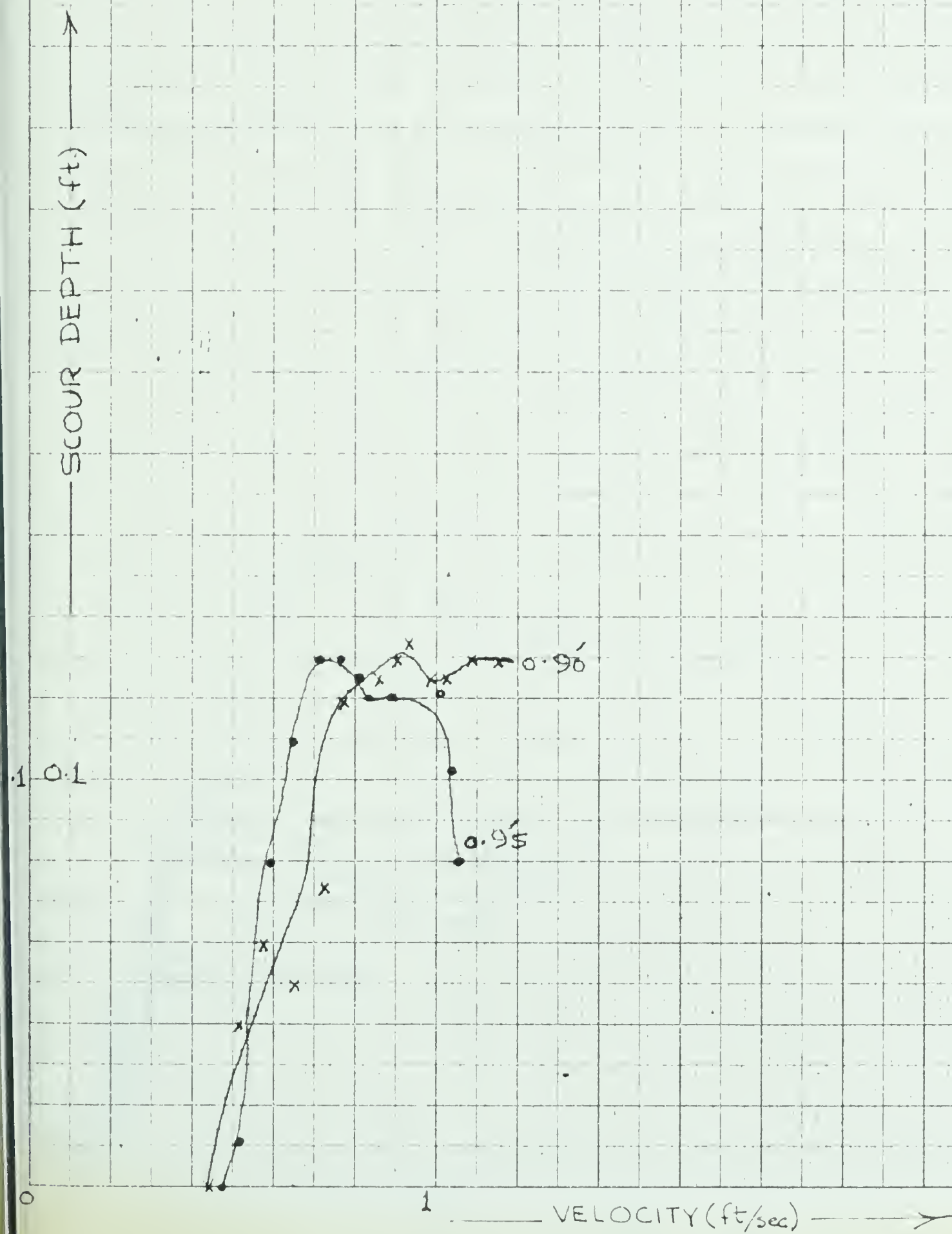


FIGURE 4.35





LIGHT WT. BED MATERIAL

VARIATION OF  $\frac{ds}{d}$  WITH FROUDE NO.

FOR  $W=0.18$ ;  $d=0.3', 0.35', 0.4', 0.45', 0.55'$

[GRAVEL RANGE]

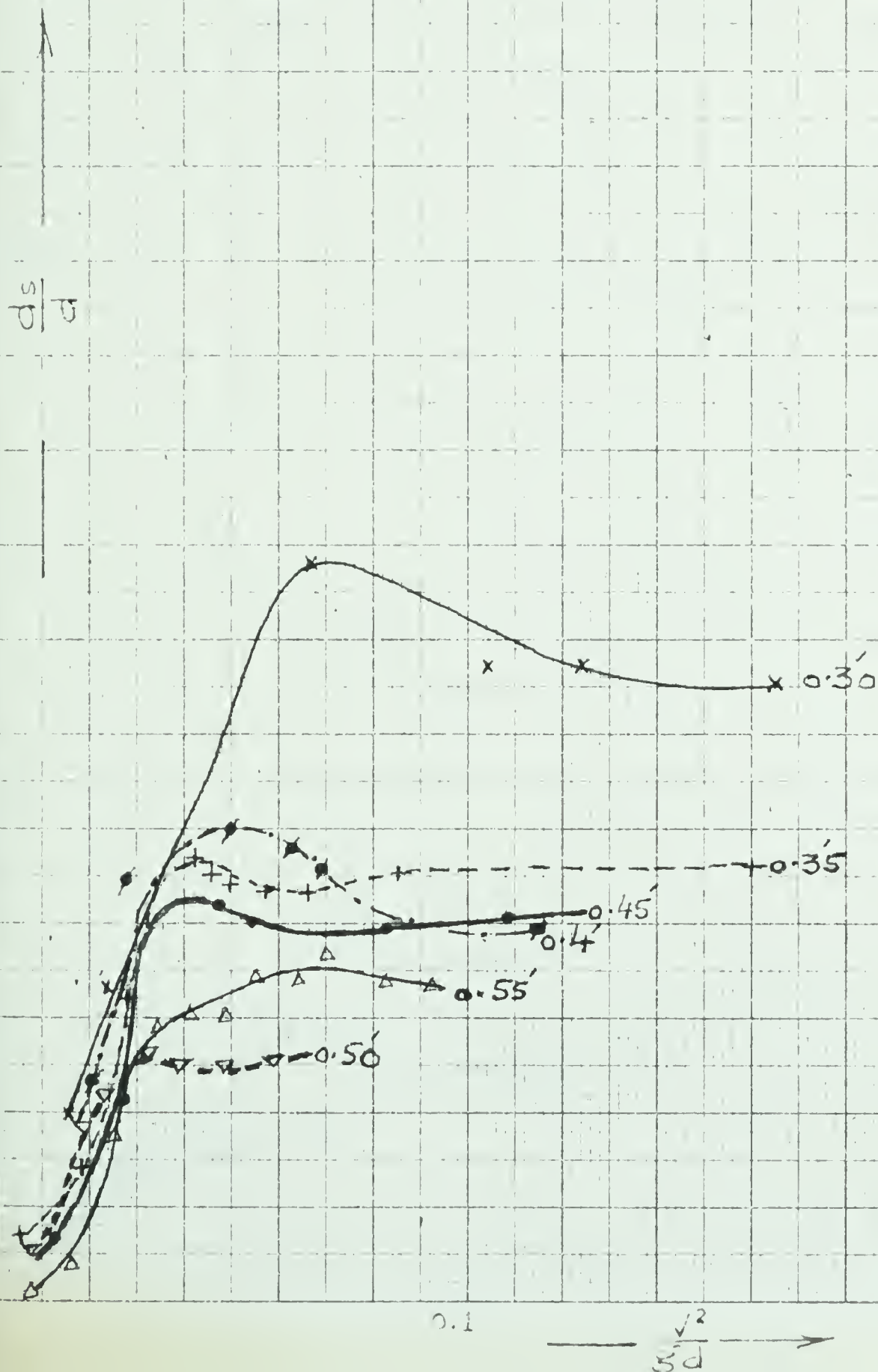


FIGURE 4.36





LIGHT WT. BED MATERIAL

VARIATION OF  $P/sp$  WITH FROUDE NO.

FOR  
 $W = 0.11'$ ,  $d = 0.30', 0.35', 0.40', 0.45'$

[GRAVEL RANGE]

$\frac{P}{sp}$

5

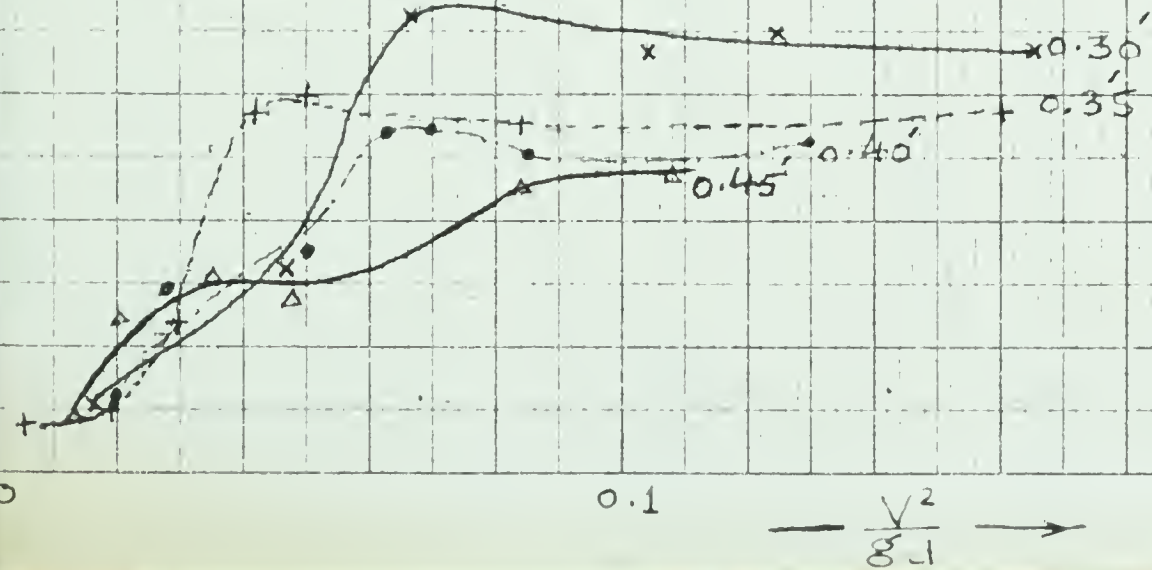


FIGURE 4.37



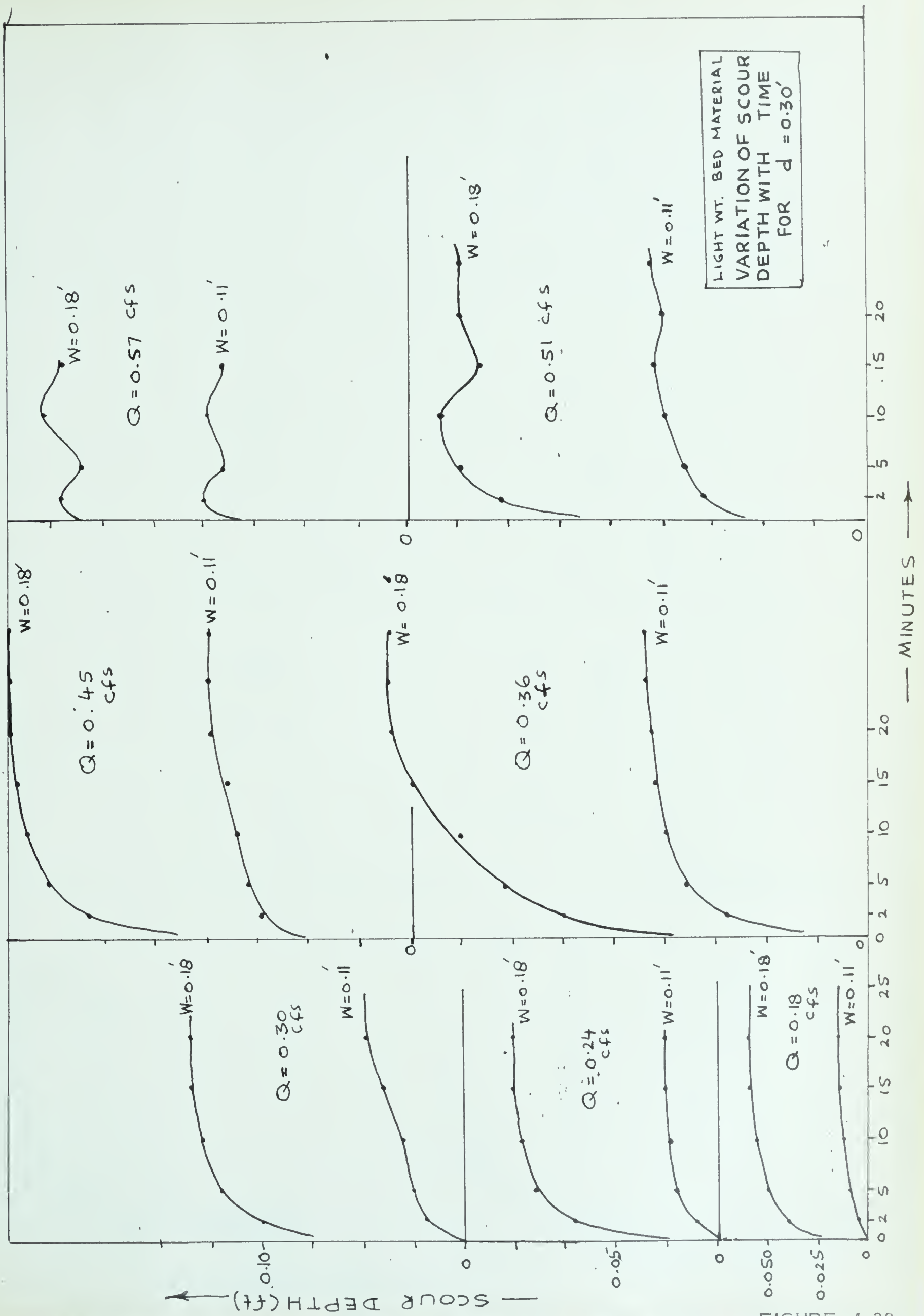


FIGURE 4.38





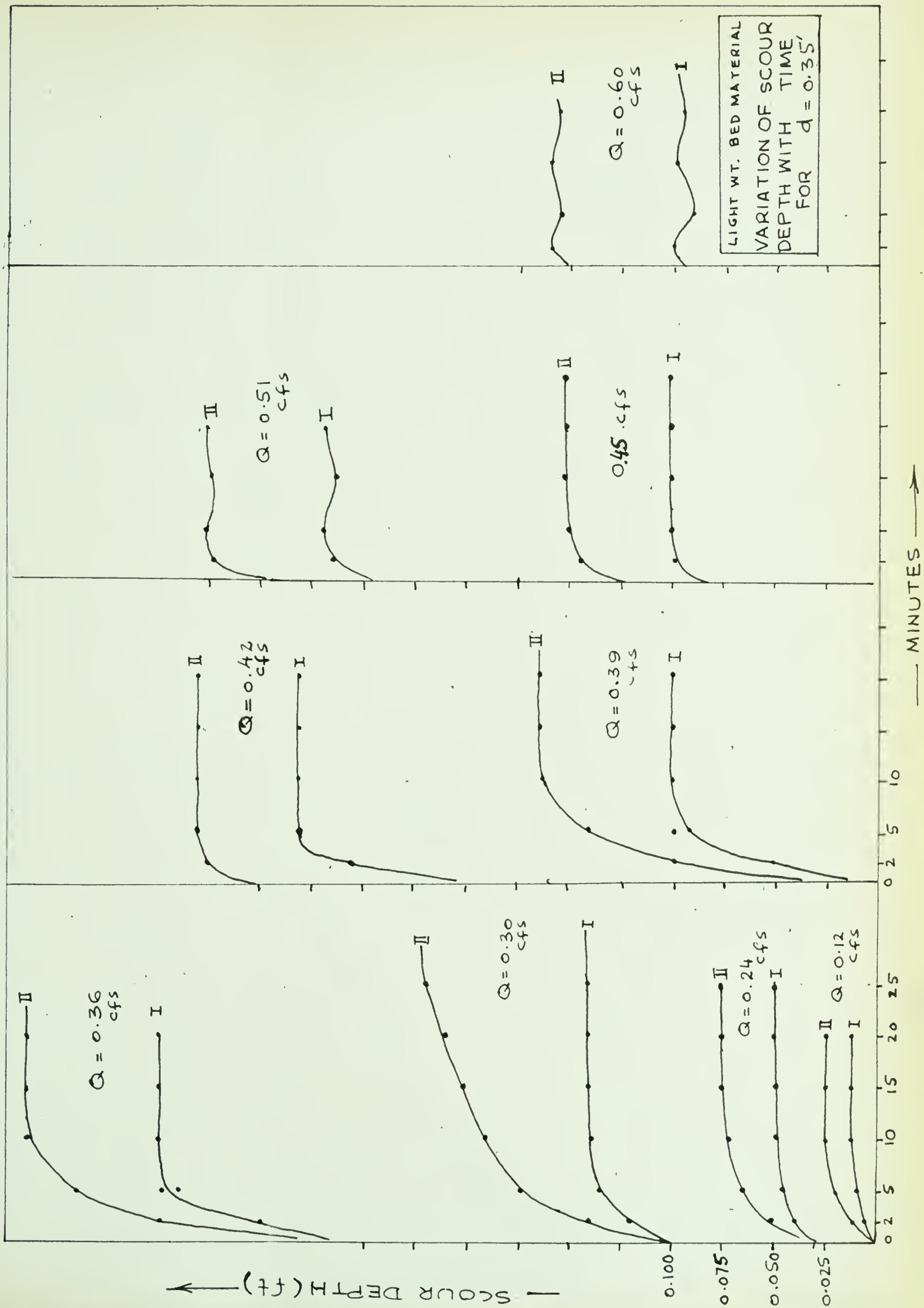


FIGURE 4.39



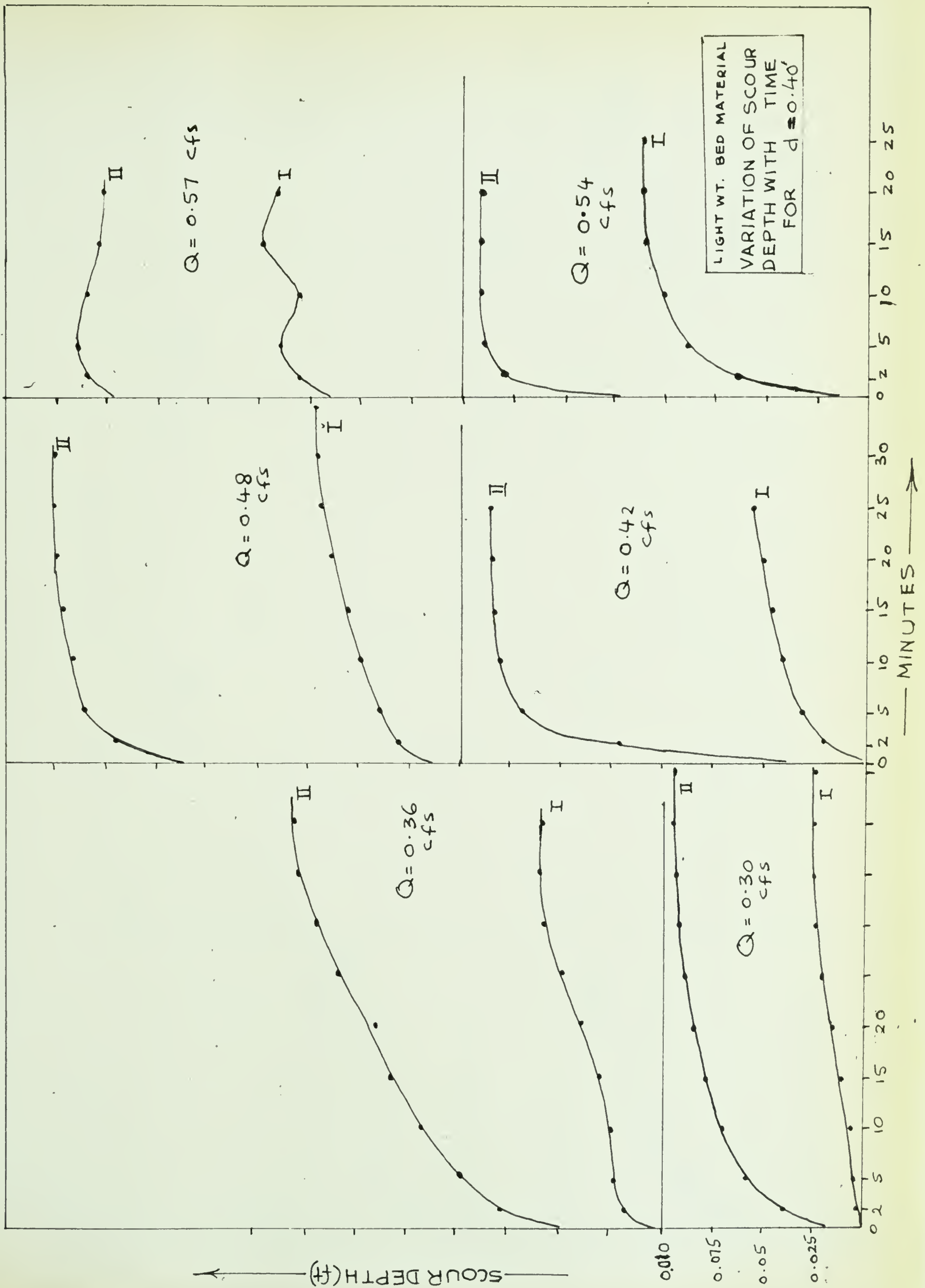


FIGURE 4.40



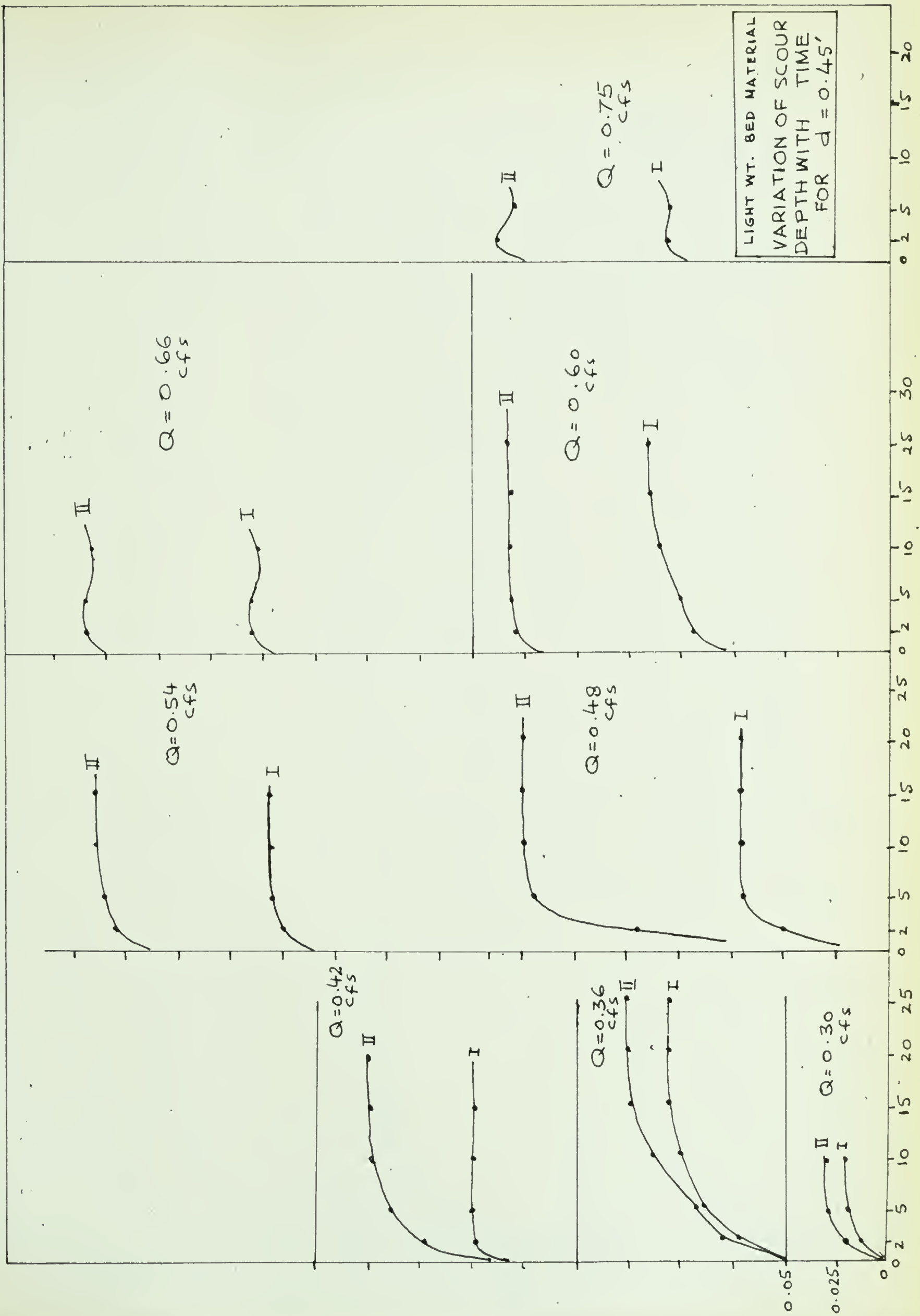


FIGURE 4. 41





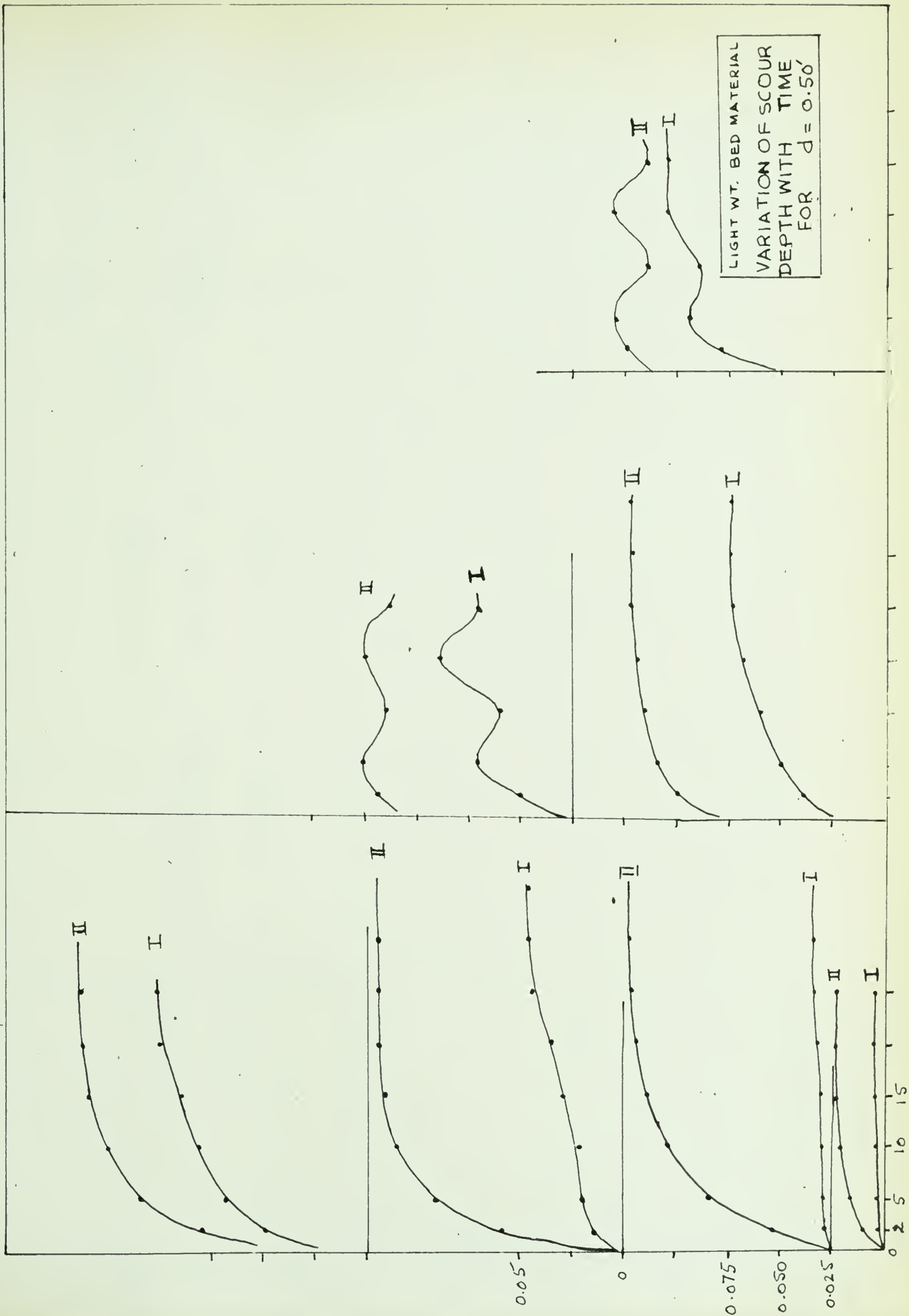


FIGURE 4. 42



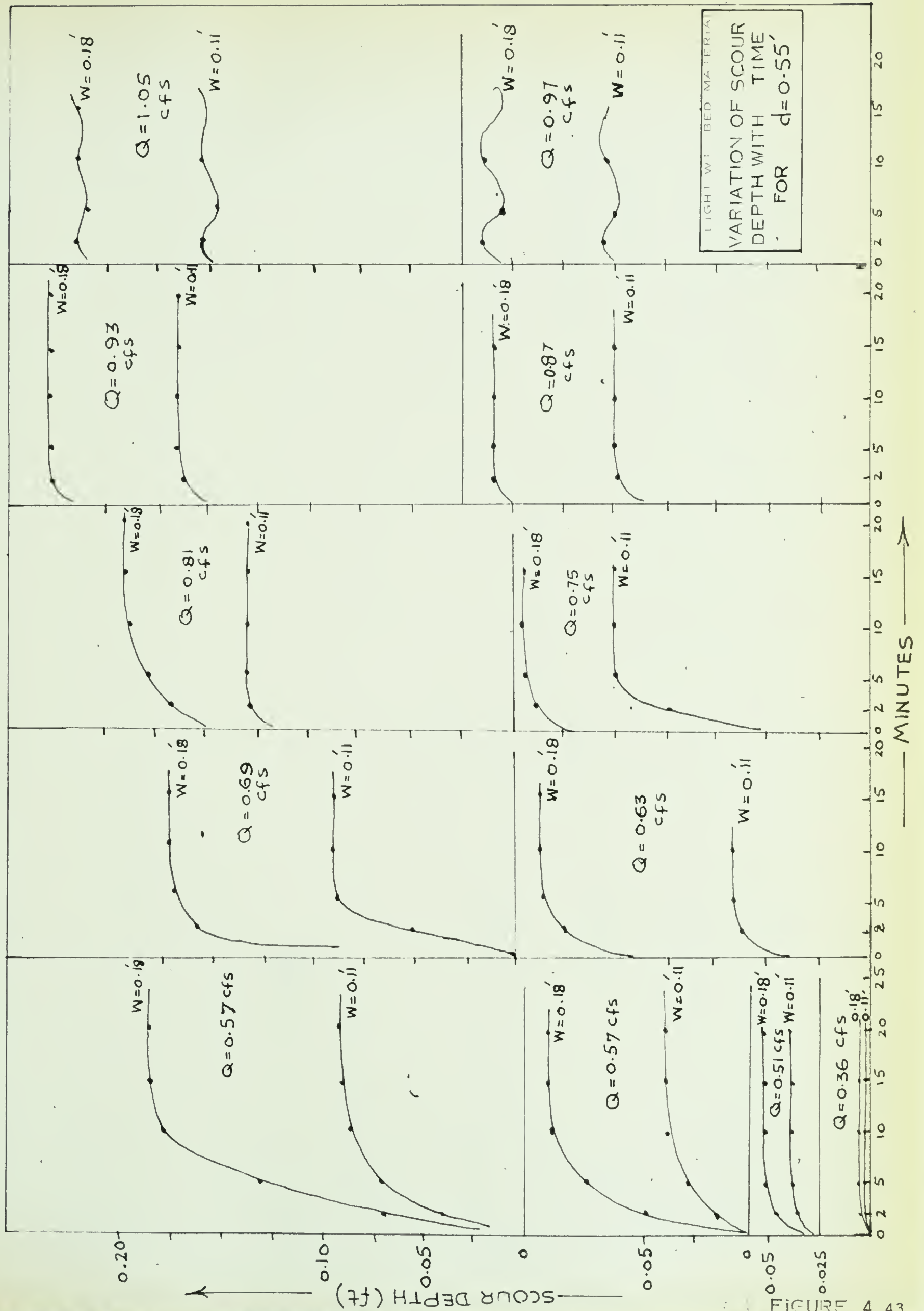


FIGURE 4.43





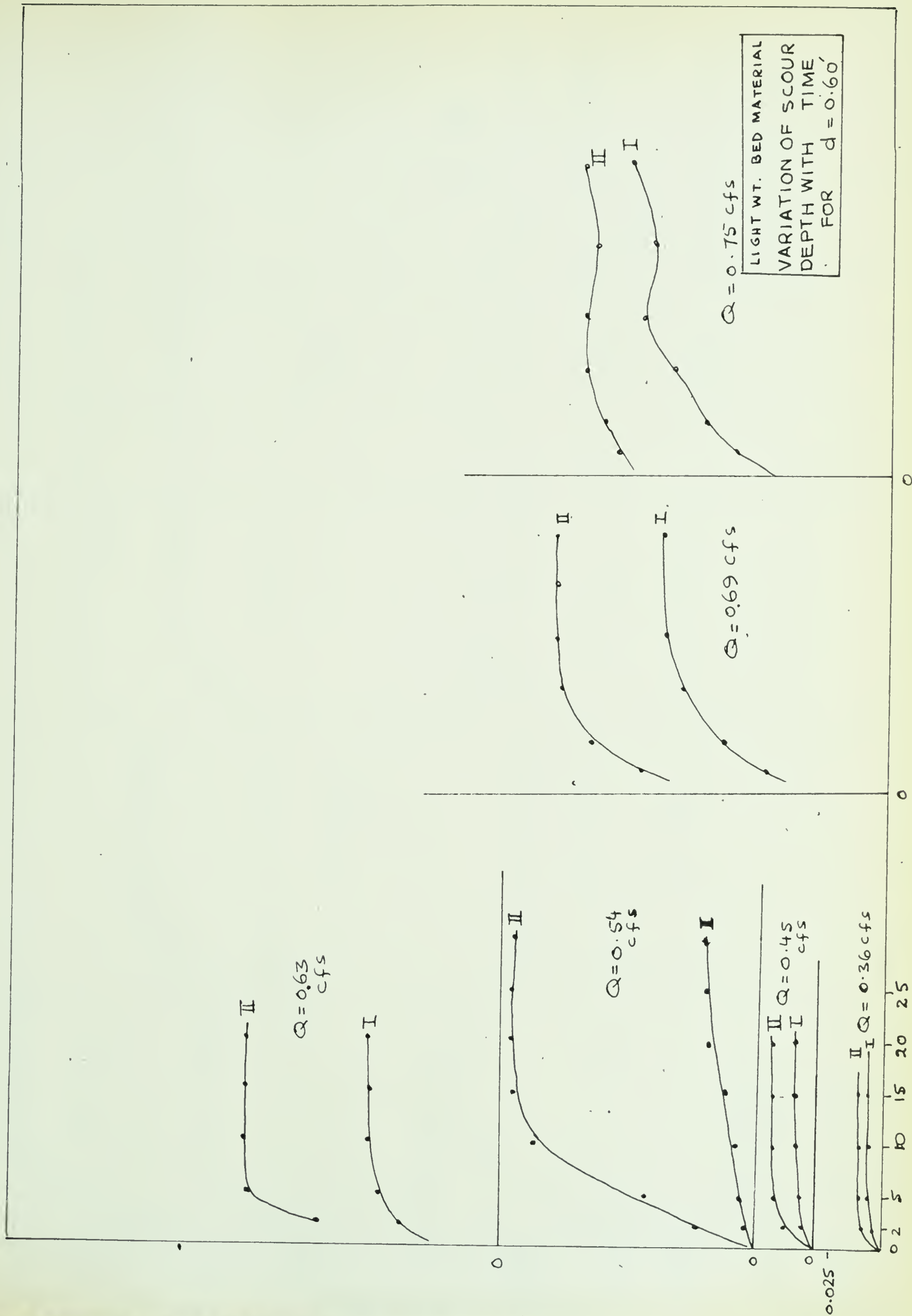


FIGURE 4 44



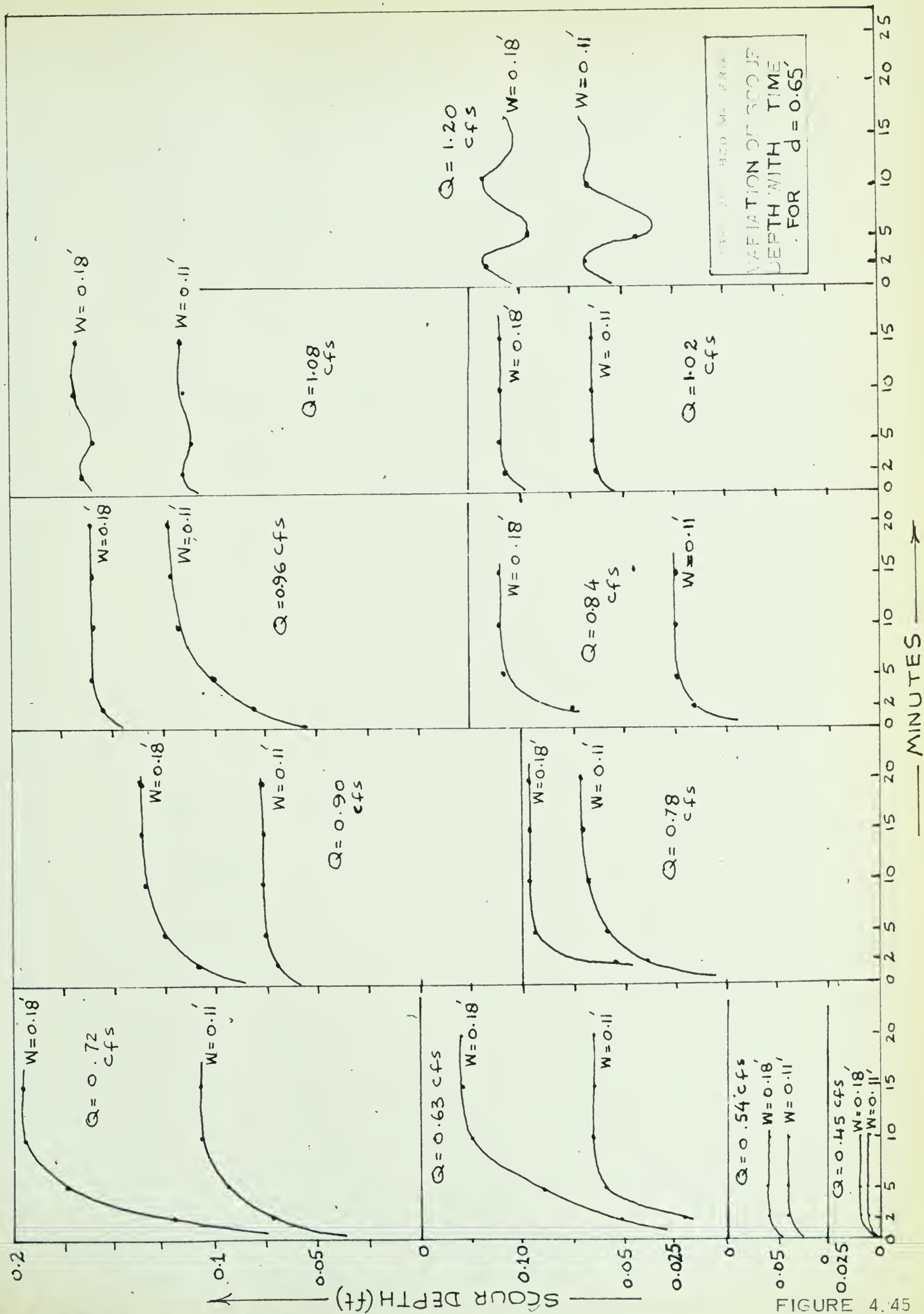


FIGURE 4.45



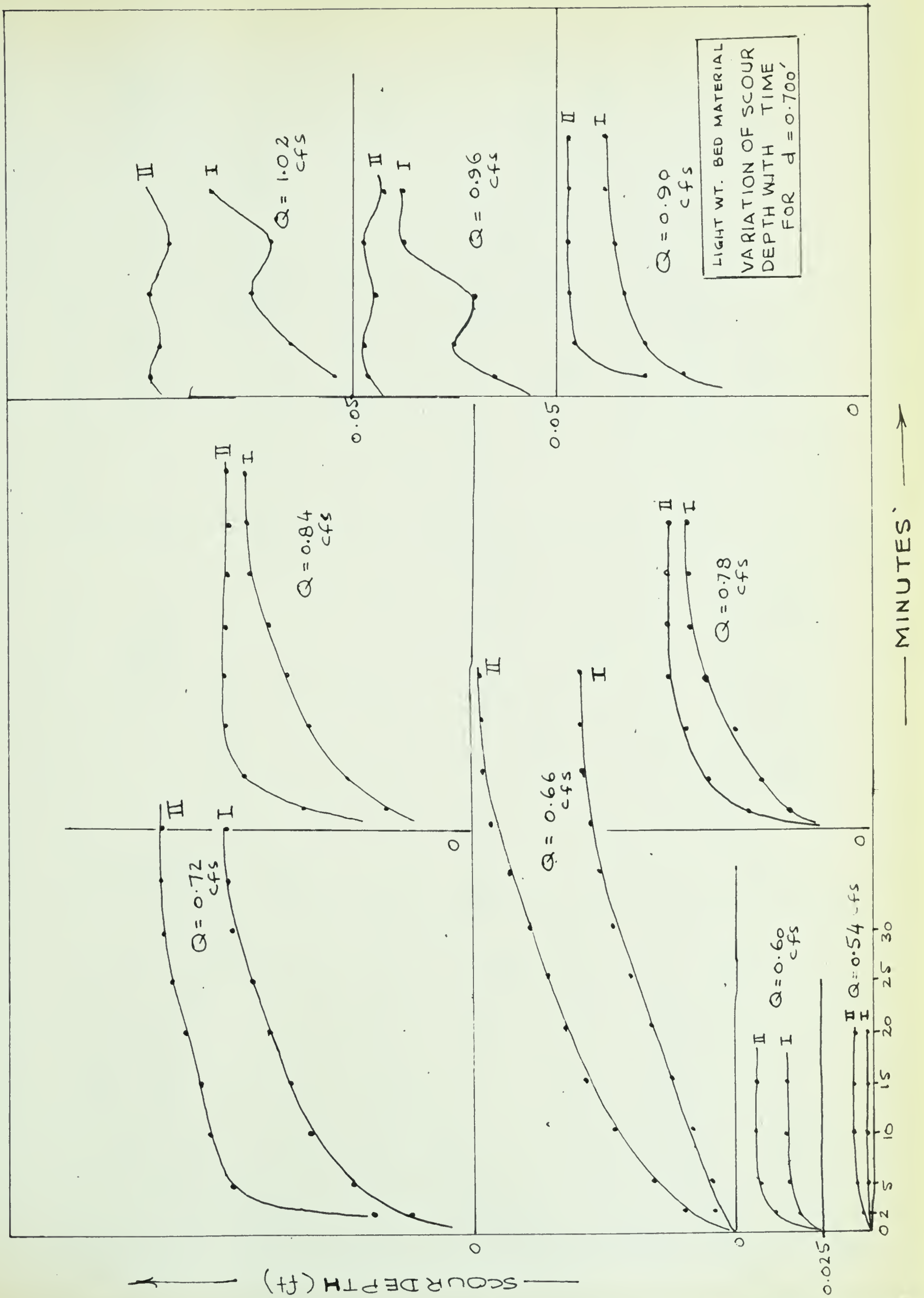


FIGURE 4.46





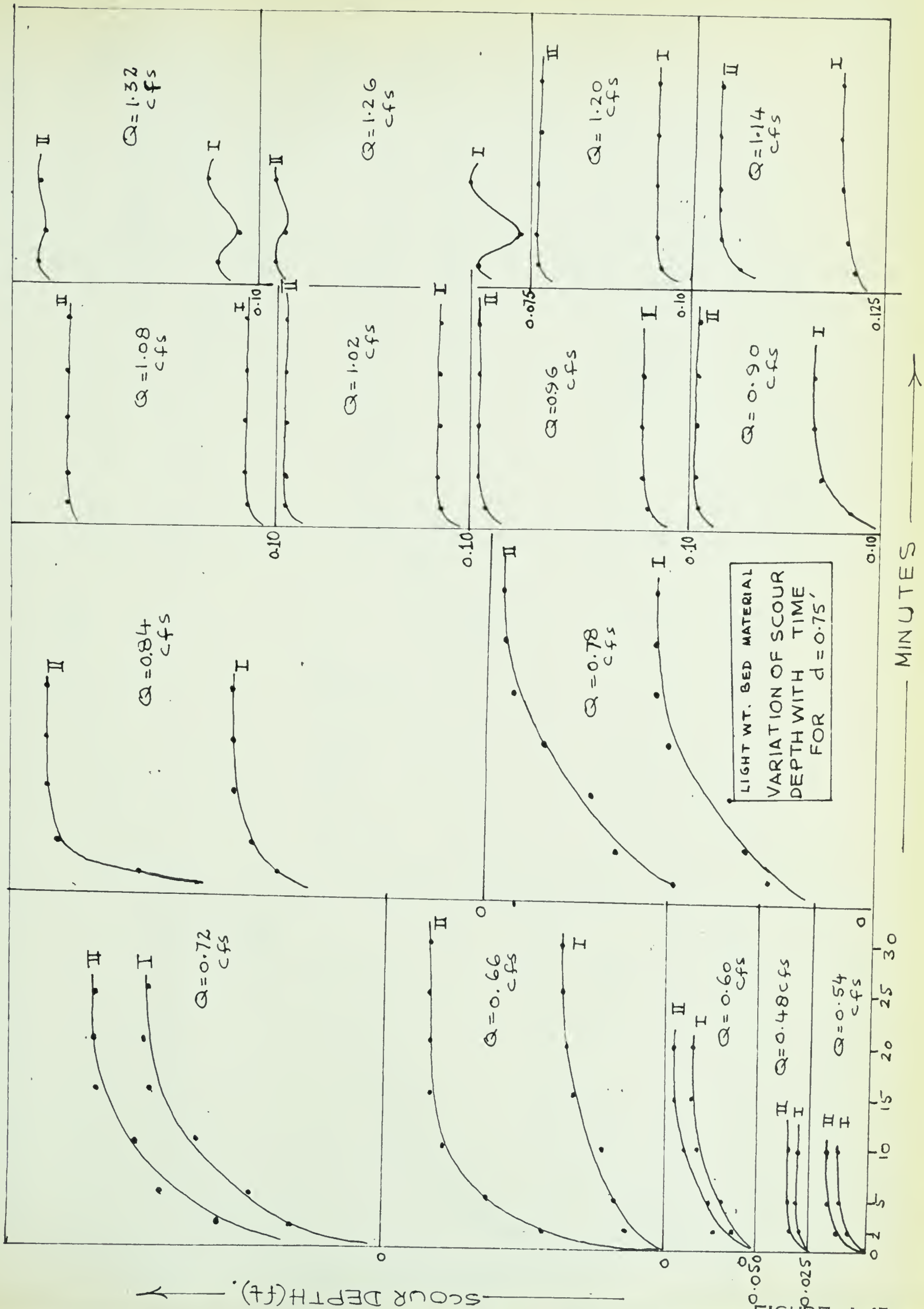


FIGURE 4.47









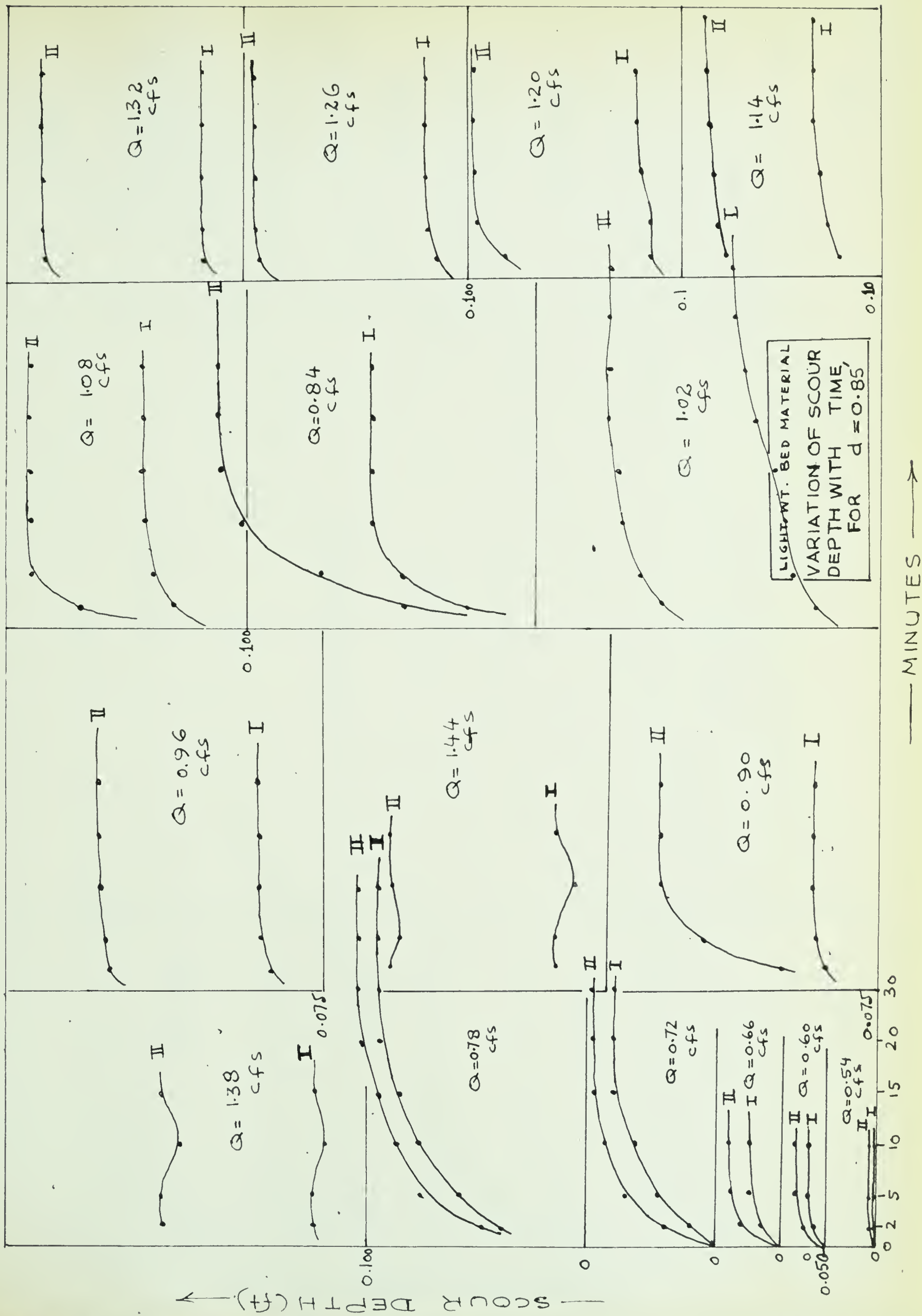


FIGURE 4.49



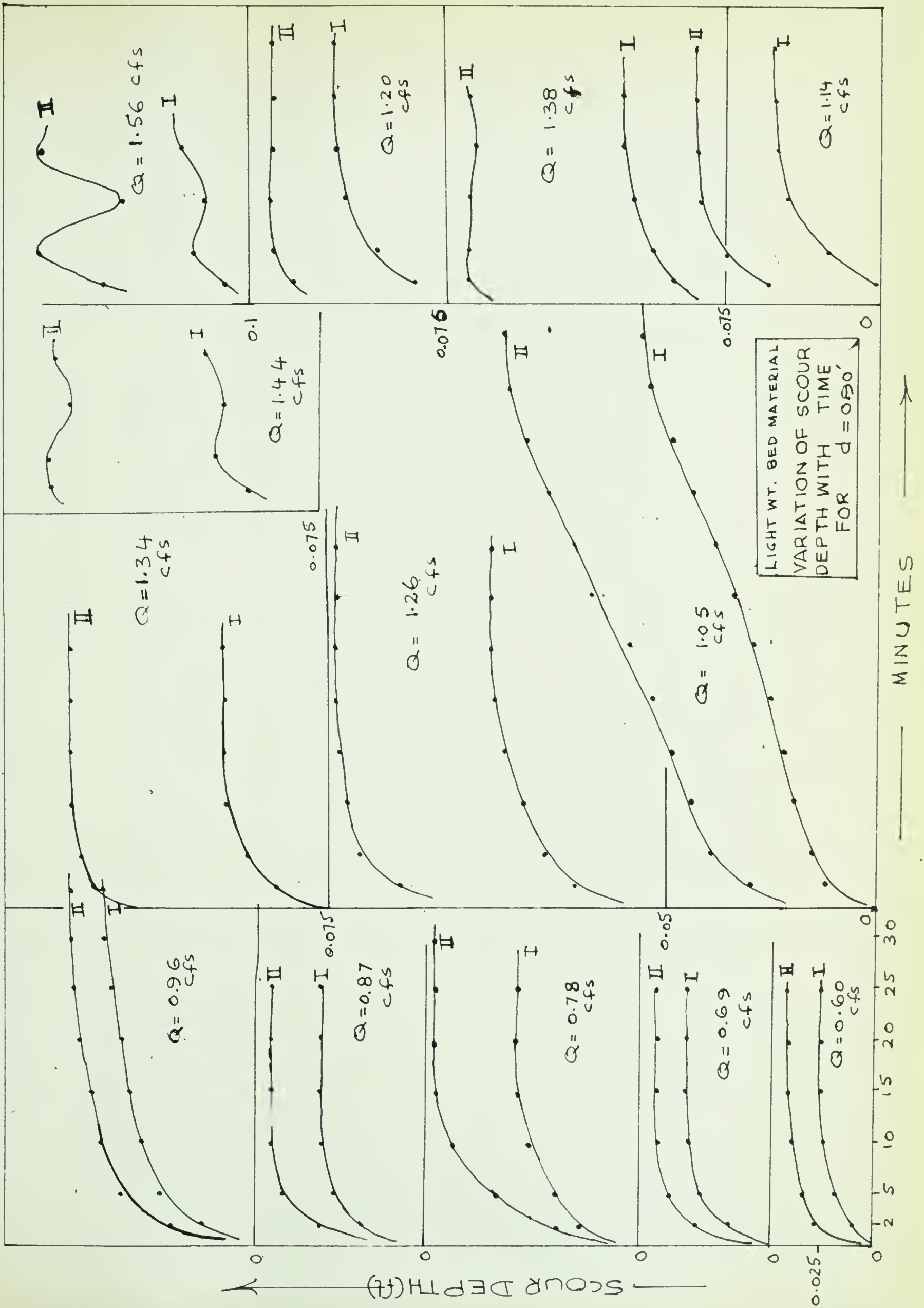


FIGURE 4.50



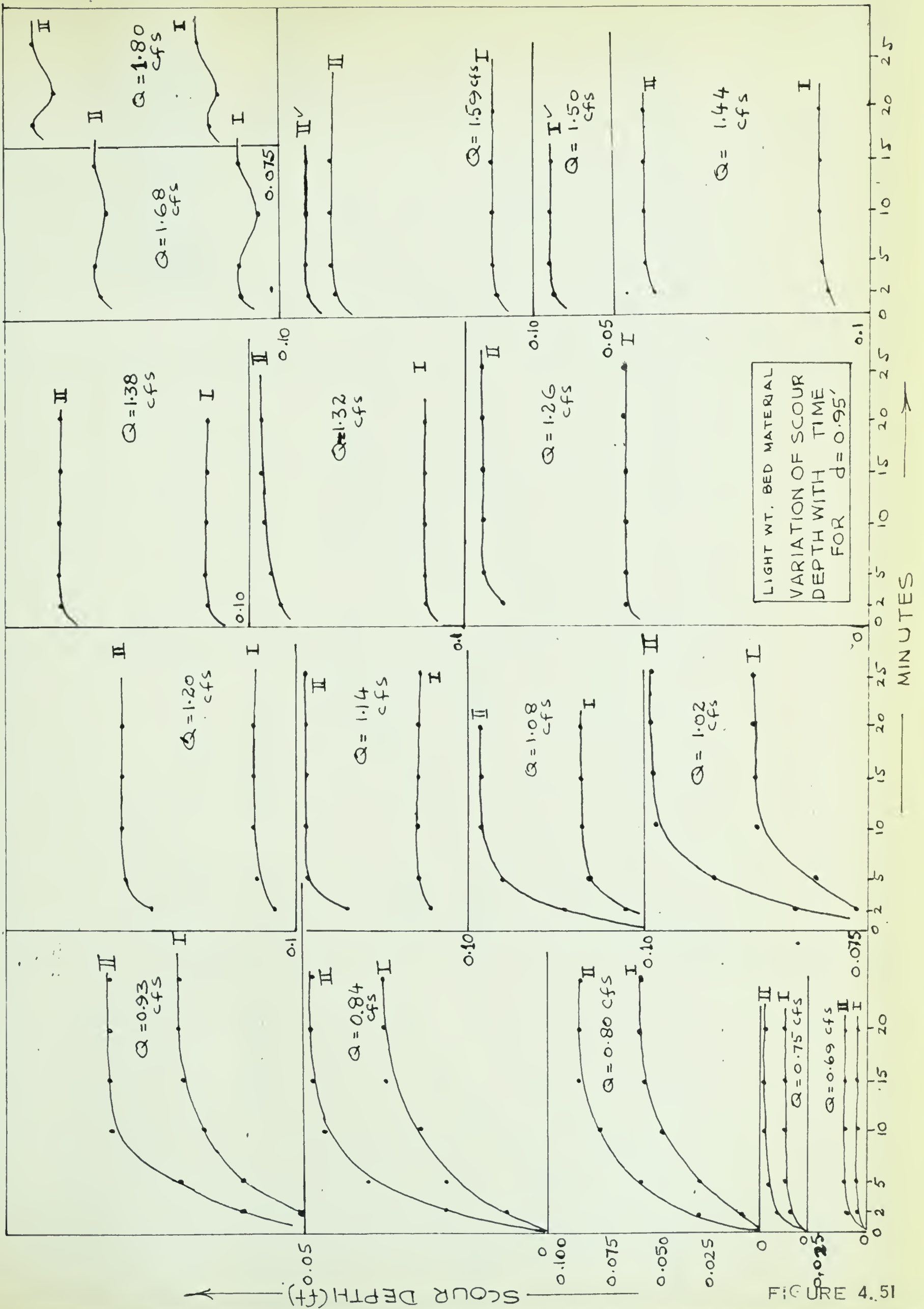


FIGURE 4.51





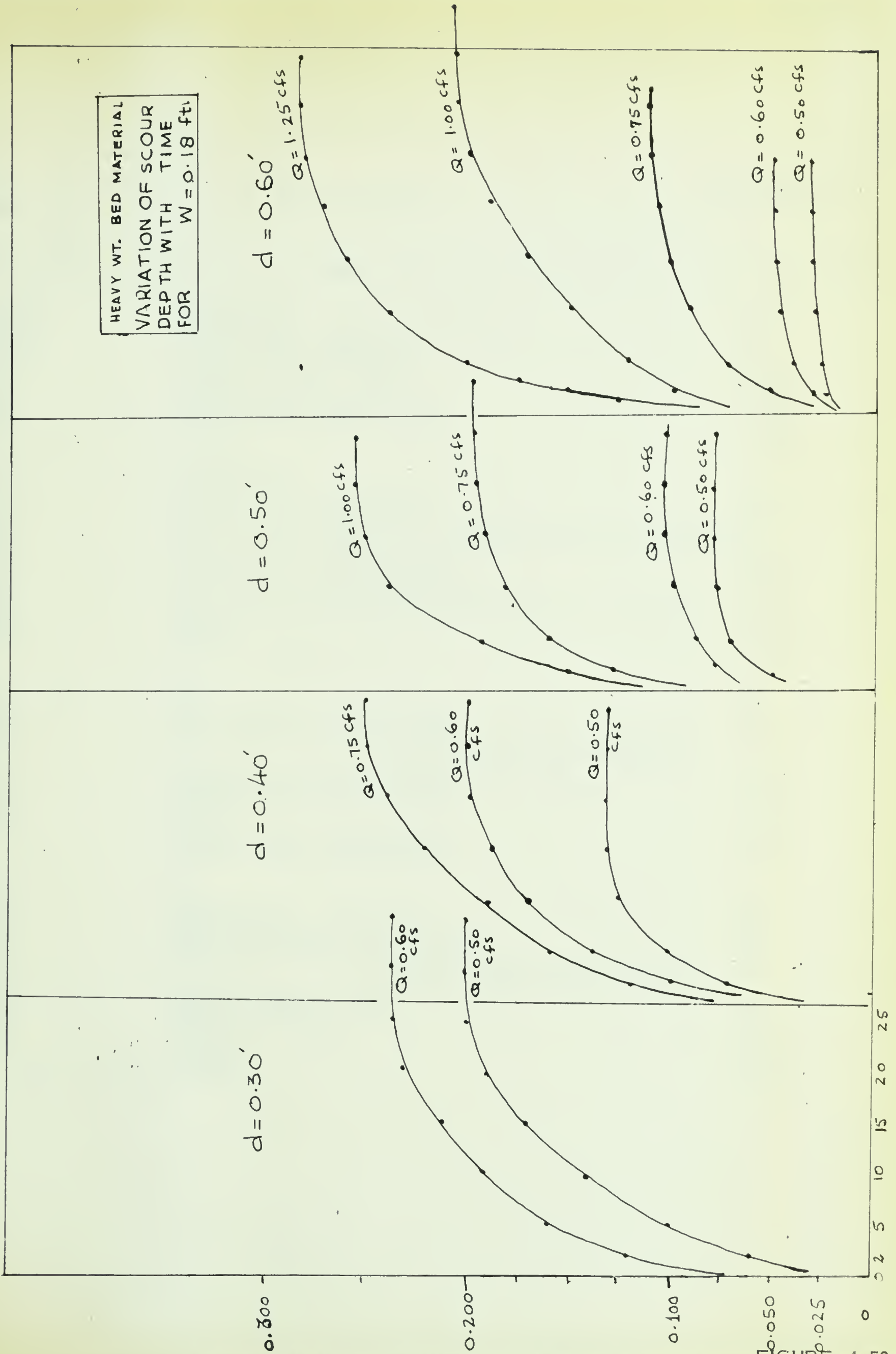


FIGURE 4.52



Table 5

SCOUR DATA (WRITER)

$$\text{S.G.} = 1.25$$

$$d_m = 1.56 \text{ mm}$$

Exp. No.	d (ft)	S (%)	Q (cusecs)	V (ft/sec)	d <sub>s</sub> (ft)		T sec	d <sub>s</sub> /d		d <sub>s</sub> /W		v <sup>2</sup> gd <sub>m</sub> (p <sub>f</sub> p <sub>s</sub> -p <sub>f</sub> )	R= v <sub>d</sub> v	C <sub>d</sub>	C <sub>d</sub> v <sup>2</sup> gd <sub>m</sub> (p <sub>f</sub> p <sub>s</sub> -p <sub>f</sub> )	v <sup>2</sup> gd	Bed Activity	Bed Material Feeding
					Pier I dia=0.18'	Pier II dia=0.11'		Pier I	Pier II									
1	2	3	4	5	6	7	8	9	10	11	12	13	14	15	16	17	18	19
301	0.30	1	0.18	0.40	0.06	0.015	20	0.200	0.050	0.332	0.136	3.84	170	0.97	3.73	0.0166	Inactive	No
2	0.30	1	0.24	0.53	0.10	0.025	20	0.334	0.085	0.555	0.227	6.80	228	0.91	6.15	0.0235	Particles mostly quivering	No
3	0.30	1	0.30	0.67	0.135	0.05	20	0.450	0.167	0.75	0.454	10.7	280	0.084	9.00	0.0465	Particles hopping	No
4	0.30	1	0.36	0.80	0.235	0.110	20	0.785	0.367	1.31	1.00	15.0	340	0.76	11.30	0.066	Slight sheet flow	Yes
5	0.30	1	0.45	1.0	0.20	0.10	20	0.670	0.334	1.11	0.91	24.0	425	0.64	15.40	0.104	Medium sheet flow	Yes
6	0.30	1	0.51	1.14	0.20	0.105	20	0.670	0.350	1.11	0.955	32.0	490	0.56	16.80	0.124	Vigorous sheet flow	Yes
7	0.30	1	0.57	1.24	0.18	0.1	20	0.600	0.334	1.0	0.91	38.4	540	0.55	21.20	0.165	Dunes	Yes
3501	0.35	1	0.12	0.23	0.025	0.0125	20	0.0715	0.0348	0.139	0.114	1.25	100	1.01	1.26	0.005	Inactive	No
2	0.35	1	0.24	0.46	0.04	0.0175	20	0.114	0.050	0.254	0.159	5.0	200	0.94	4.70	0.019	Particles Quivering	No
3	0.35	1	0.30	0.58	0.121	0.04	20	0.346	0.114	0.665	0.364	7.8	250	0.88	6.85	0.029	Particles hopping & rolling short distances	No
4	0.35	1	0.36	0.69	0.165	0.10	20	0.472	0.286	0.91	0.910	11.3	300	0.81	9.16	0.042	More part.hopping & rolling short distances	No
5	0.35	1	0.39	0.74	0.155	0.105	19	0.443	0.300	0.81	0.950	13.4	320	0.78	10.4	0.050	Slight to medium sheet	Yes
6	0.35	1	0.42	0.80	0.153	0.101	19	0.435	0.288	0.86	0.92	15.5	340	0.76	12.0	0.057	Medium to vigorous sheet	Yes
7	0.35	1	0.45	0.86	0.153	0.095	19	0.435	0.272	0.86	0.865	17.8	370	0.71	12.65	0.066	Strictly vigorous sheet-tendency to dunes	Yes
8	0.35	0.5	0.51	0.98	0.16	0.095	19	0.457	0.272	0.89	0.865	22.8	420	0.64	14.6	0.084	Dunes	Yes
9	0.35	0.5	0.60	1.33	0.16	0.095	19	0.457	0.272	0.89	0.865	42.5	560	0.61	25.4	0.16	Faster dunes	Yes
401	0.40	1	0.30	0.50	0.095	0.025	19	0.238	0.062	0.53	0.228	6.0	220	0.905	5.45	0.02	No	No
2	0.40	1	0.36	0.60	0.18	0.06	20	0.45	0.15	1.00	0.46	8.6	260	0.865	7.45	0.028	Quivering and hopping	No
3	0.40	1	0.42	0.70	0.185	0.055	19	0.462	0.137	1.03	0.50	11.7	300	0.810	9.46	0.038	Few part. rolling short distance-tendency	No
4	0.40	1	0.48	0.80	0.20	0.07	19	0.50	0.175	1.11	0.64	15.1	340	0.755	11.4	0.05	to slight sheet flow	
5	0.40	1	0.54	0.9	0.19	0.110	19	0.475	0.274	1.06	1.0	19.5	380	0.71	13.9	0.063	Slight to medium sheet	Yes
6	0.40	1	0.57	0.95	0.185	0.110	19	0.462	0.274	1.03	1.0	22.0	400	0.68	14.9	0.07	Vigorous sheet-tendency to dunes	Yes
7	0.40	1	0.63	1.05	0.16	0.10	19	0.400	0.250	0.85	0.91	26.5	450	0.615	16.3	0.085	Dunes	Yes
8	0.40	1	0.72	1.22	0.16	0.105	19	0.400	0.262	0.85	0.96	36.0	520	0.55	19.8	0.115	Dunes fully developed	Yes
4501	0.45	1	0.30	0.44	0.03	0.02	19.5	0.067	0.043	0.067	0.182	4.7	190	0.950	4.46	0.014	No	No
2	0.45	1	0.36	0.53	0.075	0.055	19.5	0.167	0.122	0.420	0.5	6.8	230	0.905	6.15	0.020	Occasional quivering	No
3	0.45	1	0.42	0.62	0.10	0.05	19.5	0.222	0.111	0.555	0.464	9.4	270	0.84	7.9	0.027	More frequent quivering	No
4	0.45	1	0.48	0.71	0.175	0.07	19.5	0.390	0.156	0.97	0.64	12.5	310	0.820	10.2	0.035	Hopping & rolling short distances-almost	No
5	0.45	1	0.54	0.83	0.190	0.105	19.5	0.424	0.234	1.055	0.96	16.5	350	0.745	12.3	0.047	slight sheet flow	
6	0.45	1	0.60	0.90	0.182	0.115	19.5	0.404	0.256	1.01	1.05	19.2	380	0.71	13.6	0.0545	Medium sheet flow	Yes
7	0.45	1	0.66	1.10	0.1825	0.1025	19.5	0.405	0.230	1.015	0.93	19.4	470	0.58	11.3	0.083	Vigorous sheet	Yes
8	0.45	1	0.75	1.25	0.1875	0.105	19.5	0.416	0.234	1.04	0.96	38.0	540	0.55	20.9	0.108	Dunes	Yes
																	Dunes	Yes





S.G. = 1.25

 $d_m = 1.56 \text{ mm}$ 

Exp. No.	d (ft)	S (%)	Q (cusecs)	V (ft/sec)	$d_s$ (ft)		c	$d_s/d$		$d_s/W$		$\frac{V^2}{gd_m} \left( \frac{\rho_f}{\rho_s - \rho_f} \right)$	$R = \frac{Vd_m}{v}$	$C_d$	$\frac{C_d V^2}{gd_m} \left( \frac{\rho_f}{\rho_s - \rho_f} \right)$	$\frac{V^2}{gd}$	Bed Activity	Bed Material Feeding
					Pier I dia.=0.18'	Pier II dia.=0.11'		Pier I	Pier II	Pier I	Pier II							
					6	7		9	10	11	12						18	19
1	2	3	4	5	6	7	8	9	10	11	12	13	14	15	16	17		
501	0.50	1.0	0.30	0.40	0.0225	0.004	19	0.045	0.008	0.125	0.036	3.85	170	0.97	3.74	0.0099	Inactive	No
2	0.50	1.0	0.39	0.52	0.0975	0.0095	19	0.195	0.019	0.541	0.087	6.5	220	0.905	5.87	0.0185	Quivering	No
3	0.50	1.0	0.48	0.64	0.1175	0.045	19	0.235	0.090	0.65	0.41	9.8	270	0.84	8.2	0.0255	Hopping	No
4	0.50	1.0	0.54	0.72	0.1375	0.10	19	0.274	0.20	0.765	0.91	12.5	310	0.820	10.3	0.032	Slight sheet	No
5	0.50	1.0	0.60	0.80	0.1225	0.075	19	0.245	0.150	0.68	0.68	15.5	340	0.755	9.7	0.0396	Medium sheet	Yes
6	0.50	1.0	0.66	0.88	0.125	0.09	19	0.250	0.180	0.695	0.82	18.5	380	0.71	13.1	0.048	Vigorous sheet, tendency to dunes	Yes
7	0.50	1.0	0.72	0.96	0.130	0.105	19	0.260	0.210	0.72	0.955	22.0	410	0.67	14.7	0.058	Dunes	Yes
5501	0.55	1.0	0.36	0.364	0.005	0.001	19	0.009	0.002	0.028	0.091	3.25	160	0.99	3.22	0.0076	Inactive	No
2	0.55	1.0	0.45	0.55	0.025	0.011	19	0.046	0.020	0.139	0.10	7.15	230	0.905	6.45	0.0168	Quivering small particles	No
3	0.55	1.0	0.51	0.62	0.10	0.04	19	0.182	0.073	0.556	0.36	9.3	260	0.865	8.05	0.0225	More often quivering	No
4	0.55	1.0	0.57	0.69	0.185	0.09	19	0.34	0.164	1.03	0.82	11.5	290	0.820	9.40	0.028	More particles hopping	No
5	0.55	1.0	0.63	0.77	0.16	0.065	19	0.292	0.118	0.89	0.59	14.10	326	0.775	10.9	0.034	V-slight sheet	No
6	0.55	1.0	0.69	0.84	0.172	0.091	19	0.312	0.166	0.955	0.83	16.70	360	0.735	12.3	0.041	Slight to medium sheet	Yes
7	0.55	1.0	0.75	0.91	0.17	0.125	19	0.31	0.227	0.945	1.14	20.0	390	0.690	13.8	0.048	Medium sheet	Yes
8	0.55	0.5	0.81	0.98	0.19	0.13	19	0.346	0.236	1.055	1.18	23.25	420	0.64	14.9	0.056	Vigorous sheet	Yes
9	0.55	0.5	0.87	1.05	0.185	0.125	19	0.347	0.227	1.14	1.14	26.5	450	0.615	16.3	0.064	V. vigorous sheet	Yes
10	0.55	0.5	0.93	1.10	0.205	0.14	19	0.374	0.255	1.055	1.27	29.0	470	0.58	16.8	0.070	Dunes	Yes
11	0.55	0.5	0.99	1.20	0.19	0.13	19	0.346	0.236	1.055	1.18	35.0	510	0.55	18.6	0.084	Faster dunes	Yes
12	0.55	0.5	1.05	1.27	0.19	0.13	19	0.346	0.236	1.01	1.18	39.0	540	0.55	21.5	0.0935	Faster dunes	Yes
601	0.60	1.0	0.36	0.40	0.0125	0.0075	19	0.021	0.013	0.0695	0.068	3.85	170	0.97	3.74	0.0083	Inactive	No
2	0.60	1.0	0.45	0.50	0.02	0.01	19	0.033	0.017	0.111	0.91	6.0	215	0.915	5.5	0.013	Quivering of small particles	No
3	0.60	1.0	0.54	0.60	0.12	0.025	19	0.20	0.042	0.666	0.23	8.70	256	0.875	7.6	0.0185	Few hopping	No
4	0.60	1.0	0.63	0.70	0.125	0.065	19	0.21	0.109	0.695	0.59	11.75	300	0.810	9.5	0.025	More parti. hopping, rolling	No
5	0.60	1.0	0.69	0.77	0.161	0.11	19	0.27	0.134	0.90	0.1	14.0	330	0.775	10.9	0.030	Slight sheet	Fed
6	0.60	0.5	0.75	0.83	0.145	0.125	19	0.242	0.208	0.805	1.14	16.75	360	0.795	12.3	0.036	Medium to vigorous sheet	Yes
7	0.60	0.5	0.81	0.90	0.145	0.12	19	0.242	0.200	0.805	1.09	19.9	385	0.70	13.9	0.042	Dunes	Yes
8	0.60	0.5	0.87	0.97	0.1425	0.12	19	0.237	0.200	0.795	1.09	22.5	425	0.64	14.4	0.049	Dunes	Yes
9	0.60	0.5	0.96	1.04	0.13	0.11	19	0.217	0.186	0.725	1.0	27.5	454	0.745	20.5	0.061	Dunes	Yes
10	0.60	0.5	1.02	1.14	0.14	0.12	19	0.234	0.200	0.78	1.09	44.0	490	0.56	24.6	0.068	Large dunes	Yes



S.G. = 1.25  
d<sub>m</sub> = 1.56 mm

Exp. No.	d (ft)	S (%)	Q (cusecs)	V (ft/sec)	d <sub>s</sub> (ft)			τ oc	d <sub>s</sub> /d			d <sub>s</sub> /w		V <sup>2</sup> gd <sub>m</sub>	V <sup>2</sup> gd <sub>m</sub>	C <sub>d</sub>	C <sub>d</sub> V <sup>2</sup> gd <sub>m</sub>	V <sup>2</sup> gd	Bed Activity	Bed Material Feeding
					τ				Pier			Pier								
					Pier I dia.=0.18'	Pier II dia.=0.11'	Pier II oc		Pier I	Pier II	Pier I	Pier II								
1	2	3	4	5	6	7	8	9	10	11	12	13	14	15	16	17	18	19		
6501	0.65	1.0	0.45	0.46	0.01	0.005	19.5	0.016	0.008	0.0556	0.0455	5.10	180	0.84	4.3	0.103	No	No		
2	0.65	1.0	0.54	0.56	0.03	0.02	19.5	0.046	0.031	0.167	0.182	7.40	240	0.885	6.65	0.15	Quivering	No		
3	0.65	1.0	0.63	0.65	0.130	0.065	19.5	0.20	0.100	0.725	0.59	10.0	275	0.84	8.4	0.20	More frequent quivering	No		
4	0.65	1.0	0.72	0.74	0.195	0.105	19.5	0.30	0.160	1.085	0.955	13.20	3.5	0.765	10.1	0.26	Rolling short distances	No		
5	0.65	1.0	0.78	0.80	0.17	0.12	19.5	0.262	0.175	0.95	1.09	15.5	340	0.755	11.7	0.31	V. slight sheet	No		
6	0.65	1.0	0.90	0.93	0.185	0.120	19.5	0.285	0.175	1.03	1.09	20.5	395	0.680	13.9	0.41	Medium sheet	Yes		
7	0.65	1.0	0.84	0.86	0.185	0.10	19.5	0.285	0.154	1.03	0.91	17.75	366	0.735	13.1	0.35	Slight to medium sheet	Yes		
8	0.65	1.0	0.96	0.99	0.185	0.145	19.5	0.285	0.223	1.03	1.32	23.30	410	0.670	15.6	0.465	Medium to vigorous sheet	Yes		
9	0.65	1.0	1.02	1.05	0.185	0.14	19.5	0.285	0.216	1.03	1.27	26.5	434	0.63	16.7	0.53	V. vigorous sheet-dune tendency	Yes		
10	0.65	1.0	1.08	1.11	0.1925	0.14	19.5	0.30	0.216	1.04	1.27	29.9	460	0.605	18.1	0.59	Faster dunes	Yes		
11	0.65	1.0	1.20	1.23	0.191	0.1425	19.5	0.294	0.22	1.06	1.30	36.5	510	0.54	19.7	0.73	Faster dunes	Yes		
701	0.70	1.0	0.45	0.43	-	-	19.5	-	-	-	-	4.35	204	0.94	4.08	0.08	No	No		
2	0.70	1.0	0.52	0.51	0.01	0.025	19.5	0.0143	0.004	0.0556	0.0227	6.35	220	0.905	5.75	0.117	No	No		
3	0.70	1.0	0.60	0.57	0.0305	0.025	19.5	0.044	0.036	0.17	0.227	7.80	244	0.88	6.86	0.145	Quivering	No		
4	0.70	1.0	0.66	0.63	0.1225	0.075	19.5	0.16	0.108	0.68	0.68	9.5	276	0.84	7.95	0.175	Hopping	No		
5	0.70	1.0	0.72	0.69	0.1525	0.12	19.5	0.218	0.173	0.85	1.09	11.30	294	0.810	9.15	0.21	More particles rolling, jumping	No		
6	0.70	1.0	0.78	0.74	0.10	0.09	19.5	0.146	0.129	0.555	0.82	13.30	320	0.775	10.3	0.25	All sizes rolling for short distance	No		
7	0.70	1.0	0.84	0.80	0.121	0.11	19.5	0.173	0.157	0.67	1.00	15.6	340	0.755	12.1	0.284	Slight sheet	Yes		
8	0.70	1.0	0.90	0.86	0.1475	0.13	19.5	0.210	0.186	0.82	1.18	17.8	365	0.72	12.8	0.325	Vigorous-tendency to dunes	Yes		
9	0.70	1.0	0.96	0.92	0.145	0.125	19.5	0.207	0.179	0.805	1.135	20.4	415	0.65	13.3	0.375	Dunes	Yes		
10	0.70	1.0	1.02	0.98	0.15	0.12	19.5	0.214	0.172	0.835	1.09	23.0	435	0.63	14.5	0.42	Dunes	Yes		
11	0.70	1.0	1.08	1.02	0.15	0.11	19.5	0.214	0.157	0.835	1.0	25.0	460	0.605	15.1	0.46	Large dunes	Yes		
12	0.70	1.0	1.20	1.12	0.145	0.11	19.5	0.207	0.157	0.805	1.0	30.0	510	0.50	15.0	0.56	Adv. dune stage	Yes		
13	0.70	1.0	1.32	1.26	0.145	0.115	19.5	0.207	0.164	0.805	1.14	38.5	560	0.45	17.6	0.71	Adv. dune stage	Yes		
14	0.70	1.0	1.44	1.35	0.15	0.12	19.5	0.214	0.172	0.835	1.09	44.0	575	0.45	19.8	0.82		Yes		
7501	0.75	1.0	0.56	0.48	0.02	0.015	19.5	0.027	0.020	0.111	0.136	5.55	170	0.97	5.3	0.096	No	No		
2	0.75	1.0	0.48	0.43	0.01	0.005	19.5	0.0135	0.007	0.056	0.046	4.35	200	0.94	4.1	0.076	Occasional quivering	No		
3	0.75	1.0	0.60	0.53	0.04	0.03	19.5	0.054	0.04	0.222	0.272	6.85	230	0.905	6.2	0.118	More frequent quivering	No		
4	0.75	1.0	0.66	0.59	0.115	0.050	19.5	0.153	0.07	0.64	0.46	8.35	250	0.875	7.3	0.144	More frequent quivering	No		
5	0.75	1.0	0.72	0.64	0.141	0.115	19.5	0.187	0.153	0.79	1.04	9.80	272	0.84	8.2	0.17	Short distance rolling	No		
6	0.75	1.0	0.84	0.75	0.185	0.125	19.5	0.247	0.147	1.03	1.00	11.5	296	0.810	9.2	0.20	V. small particles, rolling	No		
7	0.75	1.0	0.90	0.80	0.215	0.13	19.5	0.285	0.167	1.06	1.14	13.5	320	0.775	10.5	0.233	Small particles rolling continuously	No		
8	0.75	1.0	0.96	0.85	0.19	0.1225	19.5	0.254	0.163	1.13	1.11	15.5	340	0.755	11.7	0.266	Slight sheet	No		
9	0.75	1.0	1.02	0.91	0.2025	0.115	19.5	0.254	0.153	1.06	1.045	17.5	365	0.735	12.9	0.304	Slight to medium sheet	Yes		
10	0.75	0.5	1.08	0.96	0.19	0.115	19.5	0.270	0.153	1.13	1.045	20.0	390	0.690	13.8	0.345	Medium	Yes		
11	0.75	0.5	1.14	1.01	0.205	0.145	19.5	0.274	0.194	1.14	1.32	22.25	430	0.775	14.9	0.04	Vigorous sheet	Yes		
12	0.75	0.25	1.20	1.07	0.20	0.1425	19.5	0.267	0.190	1.11	1.3	24.6	455	0.61	16.5	0.047	Dunes	Yes		
13	0.75	0.25	1.26	1.12	0.20	0.105	19.5	0.267	0.140	1.11	0.96	30.0	470	0.58	17.4	0.0525	Faster dunes	Yes		
14	0.75	0.25	1.32	1.18	0.2075	0.125	19.5	0.276	0.167	1.15	1.14	33.5	500	0.55	13.4	0.0575		Yes		





$$S.G. = 1.25$$

$$d_m = 1.56 \text{ mm}$$

Exp. No.	d (ft)	S (%)	Q (cusecs)	V (ft/sec)	d <sub>s</sub> (ft)		d <sub>s</sub> /w		$\frac{v^2}{gd_m}(\frac{\rho_f}{\rho_s-\rho_f})$	$R=\frac{Vd_m}{v}$	C <sub>d</sub>	$C_d \frac{v^2}{gd_m}(\frac{\rho_f}{\rho_s-\rho_f})$	$\frac{v^2}{gd}$	Bed Activity		Bed Material Feeding
					Pier I dia.=0.18'	Pier II dia.=0.11'	Pier I	Pier II						17	18	
1				5	6	7										19
801	0.80	1.0	0.57	0.48	0.0125	0.0025	0.016	0.003	0.070	0.027	0.94	5.16	0.0087	No	Almost inactive	No
2	0.80	1.0	0.48	0.40	0.005	0.001	0.006	0.001	0.029	0.009	0.97	3.74	0.0062	Quivering		No
3	0.80	1.0	0.63	0.53	0.0225	0.01	0.028	0.013	0.125	0.09	0.905	6.06	0.0107	Rolling for short distance		No
4	0.80	1.0	0.69	0.58	0.0625	0.05	0.078	0.063	0.35	0.46	0.875	7.0	0.0135	More particles rolling short distance		No
5	0.80	1.0	0.75	0.63	0.085	0.065	0.106	0.081	0.47	0.59	0.850	8.1	0.015	More particles rolling short distance		No
6	0.80	1.0	0.81	0.68	0.075	0.065	0.094	0.081	0.42	0.59	0.820	9.1	0.0176	Rolling continuously-small size		No
7	0.80	1.0	0.87	0.73	0.111	0.10	0.139	0.125	0.62	0.91	0.80	10.1	0.0205	Slight sheet		Yes
8	0.80	1.0	0.93	0.78	0.095	0.08	0.119	0.100	0.53	0.73	0.775	11.4	0.0232	Medium sheet		Yes
9	0.80	1.0	0.99	0.83	0.10	0.09	0.125	0.123	0.55	0.82	0.745	12.4	0.0265	Medium to vigorous sheet		Yes
10	0.80	1.0	1.05	0.88	0.135	0.11	0.158	0.138	0.75	1.0	0.71	13.3	0.030	Vigorous sheet		Yes
11	0.80	0.5	1.11	0.93	0.125	0.10	0.150	0.125	0.69	0.91	0.65	15.0	0.037	Very vigorous sheet-dune tendency		Yes
12	0.80	0.5	1.17	0.98	0.12	0.11	0.151	0.125	0.67	0.91	0.625	16.2	0.042	Dunes		Yes
13	0.80	0.5	1.245	1.04	0.121	0.1	0.160	0.131	0.71	0.96	0.605	16.9	0.045	Faster Dunes		Yes
14	0.80	0.5	1.29	1.08	0.1275	0.105	0.163	0.131	0.72	0.96	0.58	17.4	0.049	Faster Dunes		Yes
15	0.80	0.5	1.35	1.12	0.130	0.105	0.163	0.135	0.72	0.98	0.58	20.0	0.056	Faster Dunes		Yes
16	0.80	0.5	1.44	1.20	0.13	0.1075	0.163	0.135	0.72	0.98	0.55	20.6	0.0595	Advanced dune stage		Yes
17	0.80	0.5	1.5	1.25	0.125	0.105	0.156	0.131	0.69	0.96	0.55	23.4	0.068	Advanced Dune stage		Yes
18	0.80	0.5	1.59	1.33	0.13	0.105	0.163	0.131	0.72	0.96	0.55	33.0	0.076	Advanced Dune stage		Yes
19	0.80	0.5	1.68	1.40	0.1325	0.105	0.165	0.131	0.735	0.96	0.55	29.8	0.087	Advanced Dune stage		Yes
20	0.80	0.5	1.8	1.50	0.13	0.105	0.163	0.131	0.72	0.96	0.55					
8501	0.85	1.0	0.59	0.43	0.0021	0.001	0.003	0.001	0.012	0.009	0.97	4.22	0.0061	No	Very rare quivering	No
2	0.85	1.0	0.60	0.47	0.015	0.0075	0.018	0.009	0.095	0.068	0.94	4.98	0.0080	More frequent quivering		No
3	0.85	1.0	0.66	0.51	0.025	0.015	0.029	0.017	0.139	0.136	0.915	5.8	0.0096	Quivering		No
4	0.85	1.0	0.72	0.57	0.06	0.05	0.071	0.059	0.332	0.46	0.885	6.85	0.0117	Quivering and jumping		No
5	0.85	1.0	0.78	0.61	0.11	0.10	0.129	0.118	0.61	0.91	0.865	7.8	0.0137	Rolling small distance		No
6	0.85	1.0	0.84	0.66	0.18	0.105	0.212	0.124	1.00	0.96	0.840	8.8	0.0158	More particles rolling short distance		No
7	0.85	1.0	0.90	0.71	0.18	0.105	0.212	0.124	1.00	0.96	0.810	9.7	0.0183	V. slight sheet		No
8	0.85	1.0	0.96	0.75	0.1825	0.105	0.215	0.124	1.01	0.96	0.775	10.7	0.0208	V. Slight sheet		No
9	0.85	1.0	1.02	0.80	0.205	0.145	0.242	0.176	1.14	1.32	0.755	11.7	0.0232	Slight sheet flow		Yes
10	0.85	1.0	1.08	0.84	0.205	0.15	0.242	0.176	1.14	1.36	0.735	12.5	0.026	Medium sheet		Yes
11	0.85	1.0	1.14	0.89	0.185	0.1325	0.218	0.155	1.03	1.20	0.69	12.9	0.033	Strictly vigorous		Yes
12	0.85	1.0	1.20	0.94	0.20	0.12	0.236	0.141	1.11	1.09	0.68	14.9	0.0345	Very vigorous		Yes
13	0.85	0.25	1.26	0.99	0.2025	0.12	0.24	0.141	1.12	1.09	0.64	15.0	0.036	Dunes		Yes
14	0.85	0.50	1.32	1.04	0.1975	0.12	0.232	0.141	1.10	1.09	0.55	14.3	0.038	Faster dunes		Yes
15	0.85	0.25	1.38	1.08	0.20	0.125	0.236	0.147	1.11	1.14	0.605	17.0	0.0394	Faster dunes		Yes
16	0.85	0.25	1.44	1.14	0.2050	0.125	0.242	0.147	1.14	1.14	0.57	17.7	0.0414			Yes





S.G. = 1.25  
d<sub>m</sub> = 1.56 mm

Exp. No.	d (ft)	S (%)	Q (cusecs)	V (ft/sec)	d <sub>s</sub> (ft)		T °C	d <sub>s</sub> /d			d <sub>s</sub> /W		Vd <sub>m</sub> R= $\frac{v}{v}$	C <sub>d</sub>	CdV <sup>2</sup> gd <sub>m</sub> $\left(\frac{\rho_f}{\rho_s-\rho_f}\right)$	V <sup>2</sup> gd	Bed Activity		Bed Material
					Pier I dia.=0.18'	Pier II dia.=0.11'		Pier I	Pier II	Pier I	Pier II	18					19		
1		2	3	4	5	6	7	8	9	10	11	12	13	14	15	16	17		
901	0.90	1.0	0.60	0.44	0.0425	0.03	19.5	0.033	0.047	0.033	0.24	0.274	4.74	190	0.95	4.50	0.0068	No	No
2	0.90	1.0	0.69	0.51	0.055	0.04	19.5	0.044	0.061	0.044	0.306	0.364	16.3	218	0.905	5.70	0.0091	Small particles quivering	No
3	0.90	1.0	0.78	0.58	0.10	0.06	19.5	0.067	0.111	0.067	0.556	0.55	8.0	245	0.875	7.0	0.0115	Small particles rolling short distance	No
4	0.90	1.0	0.87	0.65	0.075	0.05	19.5	0.056	0.083	0.056	0.42	0.46	10.0	275	0.840	8.4	0.0145	More particles rolling short distance	No
5	0.90	1.0	0.96	0.71	0.09	0.075	19.5	0.083	0.10	0.083	0.50	0.684	12.3	305	0.805	9.9	0.0175	V. Slight sheet	No
6	0.90	1.0	1.05	0.78	0.18	0.12	19.5	0.133	0.20	0.133	1.00	1.09	14.5	330	0.775	10.9	0.021	Slight sheet	No
7	0.90	1.0	1.14	0.85	0.1625	0.125	19.5	0.139	0.18	0.139	0.90	1.14	17.5	360	0.735	12.9	0.0255	Slight to medium sheet	Yes
8	0.90	1.0	1.20	0.90	0.161	0.13	19.5	0.144	0.179	0.144	0.895	1.18	19.5	385	0.70	13.7	0.028	Medium sheet flow	Yes
9	0.90	1.0	1.26	0.94	0.211	0.135	19.5	0.15	0.235	0.15	1.175	1.23	21.0	400	0.68	14.3	0.0304	Medium to vigorous sheet flow	Yes
10	0.90	1.0	1.335	0.99	0.195	0.125	19.5	0.139	0.216	0.139	1.08	1.14	23.5	420	0.64	15.1	0.034	Vigorous sheet flow	Yes
11	0.90	1.0	1.38	1.02	0.20	0.125	19.5	0.139	0.222	0.139	1.11	1.14	25.0	434	0.765	19.1	0.036	Tendency to dunes	Yes
12	0.90	1.0	1.44	1.07	0.2025	0.13	19.5	0.144	0.226	0.144	1.125	1.18	27.5	455	0.615	16.9	0.0394	Dunes	Yes
13	0.90	1.0	1.56	1.16	0.20	0.13	19.5	0.144	0.222	0.144	1.11	1.18	32.0	490	0.56	17.9	0.046	Faster Dunes	Yes
9501	0.95	1.0	0.69	0.49	0.011	0.005	20.0	0.005	0.012	0.005	0.061	0.046	5.7	206	0.94	5.35	0.0077	No	No
2	0.95	1.0	0.75	0.53	0.0201	0.0101	20.0	0.011	0.021	0.011	0.112	0.091	6.7	225	0.905	6.05	0.0092	Occasional quivering	No
3	0.95	1.0	0.80	0.56	0.09	0.06	20.0	0.063	0.095	0.063	0.50	0.55	7.5	240	0.885	6.65	0.0103	Frequent quivering	No
4	0.95	1.0	0.84	0.59	0.115	0.08	20.0	0.084	0.121	0.084	0.64	0.73	8.5	250	0.875	7.44	0.0115	More frequent quivering	No
5	0.95	1.0	0.93	0.65	0.145	0.11	20.0	0.116	0.153	0.116	0.81	1.00	10.05	290	0.800	8.4	0.014	Mostly quivering	No
6	0.95	1.0	1.02	0.71	0.18	0.13	20.0	0.137	0.190	0.137	1.00	1.18	12.0	300	0.810	9.72	0.0167	Rolling short distances	No
7	0.95	1.0	1.08	0.77	0.18	0.13	20.0	0.137	0.190	0.137	1.00	1.18	14.1	325	0.775	10.9	0.0193	More particles rolling short distance	No
8	0.95	1.0	1.14	0.81	0.18	0.125	20.0	0.132	0.190	0.132	1.00	1.14	15.7	345	0.745	11.7	0.0216	V. slight sheet flow	No
9	0.95	1.0	1.20	0.84	0.185	0.12	20.0	0.126	0.195	0.126	1.03	1.09	17.0	360	0.735	12.5	0.0232	Slight sheet	No
10	0.95	1.0	1.26	0.89	0.19	0.12	20.0	0.126	0.200	0.126	1.06	1.09	18.7	375	0.71	13.2	0.026	Slight to medium sheet	Yes
11	0.95	1.0	1.32	0.93	0.20	0.12	20.0	0.126	0.210	0.126	1.11	1.09	20.4	395	0.68	13.9	0.028	Medium sheet	Yes
12	0.95	1.0	1.38	0.98	0.1925	0.121	20.0	0.127	0.203	0.127	1.07	1.1	23.0	415	0.65	15.0	0.031	Medium to vigorous sheet flow	Yes
13	0.95	1.0	1.44	1.01	0.21	0.1225	20.0	0.128	0.220	0.128	1.17	1.12	24.9	470	0.58	14.5	0.033	Vigorous sheet	Yes
14	0.95	1.0	1.5	1.05	0.20	0.08	20.0	0.084	0.210	0.084	1.11	0.73	27.0	460	0.605	16.3	0.036	Vigorous	Yes
15	0.95	1.0	1.59	1.13	0.20	0.12	20.0	0.126	0.21	0.126	1.11	1.09	30.5	480	0.58	17.7	0.0414	V. vigorous sheet	Yes
16	0.95	1.0	1.68	1.18	0.19	0.12	20.0	0.126	0.20	0.126	1.06	1.09	33.5	500	0.55	18.5	0.045	Extremely vigorous sheet & dune tendency	Yes
17	0.95	1.0	1.8	1.27	0.195	0.115	20.0	0.122	0.205	0.122	1.08	1.09	38.5	540	0.55	21.2	0.052	Dunes	Yes



## CHAPTER 5

### STUDY OF EFFECT OF BED MATERIAL DENSITY ON BRIDGE PIER SCOUR

#### Effect of Bed Material Density.

The two resultant plots in Figures 3.19 and 4.26 for heavy weight and light weight bed materials respectively, were transferred on one sheet in Figure 5.1. The only different feature for these two plots in Figure 5.1 was the parameter  $\frac{\rho_s - \rho_f}{\rho_f}$ , the value of which for stone and coal was 1.65 and 0.25 respectively.

An exponent of  $7/8$  for  $\frac{\rho_s - \rho_f}{\rho_f}$  was found in Figure 5.2, which made it possible to combine the two plots as in Figure 5.1. The resultant plot in Figure 5.1 which is coincident for stone and coal up to an approximate value of about 3.7 of abscissa, is between

$$\frac{d_s}{d} / \left(\frac{W}{B}\right)^{7/8} \times \left(\frac{B}{d}\right)^{7/8} \quad \text{and} \quad \frac{C_d V^2}{g d_m} \left(\frac{\rho_f}{\rho_s - \rho_f}\right) \left(\frac{\rho_s - \rho_f}{\rho_f}\right)^{7/8}.$$

Other Investigator's Data: Tables 7 to 9 list scour data for gravel range collected in laboratory by Inglis (Reference 6), Varzeliotis (Reference 7) and Neill (Reference 2). From the data of each of these investigators values of  $\frac{d_s}{d} / \left(\frac{W}{B}\right)^{7/8} \times \left(\frac{B}{d}\right)^{7/8}$  and  $\frac{C_d V^2}{g d_m} \left(\frac{\rho_f}{\rho_s - \rho_f}\right) \left(\frac{\rho_s - \rho_f}{\rho_f}\right)^{7/8}$  were found and plotted in Figure 5.1. The plotted points of these investigators fell fairly close to the heavy weight





bed material resultant curve in Figure 5.1. This shows the versatility of the parameters  $\frac{d_s}{d} / (\frac{W}{B})^{7/8} \times (\frac{B}{d})^{7/8}$  and

$$\frac{C_d V^2}{g d_m} \left( \frac{\rho_f}{\rho_s - \rho_f} \right) \left( \frac{\rho_s - \rho_f}{\rho_f} \right)^{7/8}.$$

### Log-log Plot.

The coincident portion of the resultant curve in Figure 5.1 was plotted on double log paper in Figure 5.3. The resulting straight line had the following equation:

$$\frac{d_s}{d} / \left( \frac{W}{B} \right)^{7/8} \times \left( \frac{B}{d} \right)^{7/8} = 1 \cdot \left\{ \frac{C_d V^2}{g d_m} \cdot \left( \frac{\rho_f}{\rho_s - \rho_f} \right) \left( \frac{\rho_s - \rho_f}{\rho_f} \right)^{7/8} \right\}^2$$

$$\frac{d_s}{d} / \left( \frac{W}{B} \right)^{7/8} \times \left( \frac{B}{d} \right)^{7/8} = \left\{ \left( \frac{\text{drag force}}{\text{buoyant weight}} \right) (S-1)^{7/8} \right\}^2$$

The above relation has the following limitations:

- i) it is based on consideration of two different gravel sized bed materials (stone and coal).
- ii) it is based on the consideration of only the coincident portion of total plot in Figure 5.1, i.e., up to a condition when  $\left[ \frac{\text{drag force}}{\text{buoyant weight}} \times \left( \frac{\rho_s - \rho_f}{\rho_f} \right)^{7/8} \right]$  has a value of approximately 3.7, or, in terms of bed activity, up to a point when the bed is active.



## Conclusions

1) As observed from Figure 5.1, below a certain threshold value of  $\frac{\text{drag force}}{\text{buoyant weight}}$  there is no scour, for stone and coal. This value of  $\frac{\text{drag force}}{\text{buoyant weight}}$  is much higher for coal ( $\simeq 5$ ) than for stone ( $\simeq 0.5$ ).

2) In Figure 5.1 the plots for coal and stone coincide up to the point P. Looking at actual experiments, the point P signifies a stage when approach bed is moving in the form of sheet flow (stage earlier than dunes) for the case of stone and in slightly more developed sheet flow form for coal. In general we can say that for both types of bed materials, point P shows a threshold of active bed activity. If there are two models, in stone and coal as bed materials, for one prototype, then the two models should give the same results as long as the forces parameter

$\frac{C_d V^2}{g d_m} \cdot \left( \frac{\rho_f}{\rho_s - \rho_f} \right) \left( \frac{\rho_s - \rho_f}{\rho_f} \right)^{7/8}$  remains the same for the models and prototype. It must be noted that the foregoing conclusion has the limitation of being based on the use of only two different bed material, i.e., stone and coal, of gravel size, and up to a stage of active transport.



3) As we enter the stage of fair to very active bed activity the plots for coal and stone do not coincide for the same ordinates. This means that when we are working with models with fairly active transport the density of the bed material has to be considered as we may get different results with different bed material in the models.

4) The non-coincidence of two plots beyond point P for coal and stone in active to very active stage of the bed activity may lead one to conjecture that there may be some additional non-dimensional density parameter, which may have still remained unaccounted for. But for stone and coal beyond the point P, besides the density of bed material the bed activity is not, in a strict sense, of similar nature. It is possible that some parameter characteristic of the bed transport for coal and stone remains unaccounted for. For active to very active bed activity range, the dimensionless equation (B) in Chapter 2, may perhaps be modified to the form:

$$\frac{d_s}{d} = \text{fn} \left[ \frac{C_d V^2}{g d_m} \cdot \frac{\rho_s - \rho_f}{\rho_f}, \frac{W}{B}, \frac{V d_m}{\nu}, \frac{d_m}{d}, \frac{d}{B}, \text{ some} \right]$$

additional parameter or parameters which take care of transport phenomena.]

As to what these parameters are is being left for future research.





5) For a fixed particle size  $d_m$  and density  $\rho_s$ ,  
the term

$$\frac{C_d V^2}{g d_m} \left( \frac{\rho_f}{\rho_s - \rho_f} \right) \left( \frac{\rho_s - \rho_f}{\rho_f} \right)^{7/8} = \frac{\text{drag force}}{\text{buoyant weight}} \times \text{constant}$$

$$= \frac{\text{drag force}}{(\text{constant})} \times (\text{constant}) .$$

For a given  $d_m$  and  $\rho_s$  the abscissa is a measure of the drag on particle. Again, the ordinate term  $\frac{d_s}{d} / \left( \frac{W}{B} \right)^{7/8} \times \left( \frac{B}{d} \right)^{7/8}$  may be said to be, for a given depth, the measure of maximum scour depth. This means that for a given  $d_m$ ,  $\rho_s$ , and  $d$ , the scour depth both for coal and stone cases increases almost linearly with drag, as there is increase in velocity of flow. The above is true only up to the active bed stage. Beyond the latter range of bed activity,  $d_s$  varies differently with drag (no more a linear relationship), for both the bed materials.

6) From double log plot in Figure 5.3 we can deduce the following relation:

$$\left\{ \frac{d_s}{d} / \left( \frac{W}{B} \right)^{7/8} \times \left( \frac{B}{d} \right)^{7/8} \right\} = \left\{ \frac{C_d V^2}{g d_m} \cdot \left( \frac{\rho_f}{\rho_s - \rho_f} \right) \cdot \left( \frac{\rho_s - \rho_f}{\rho_f} \right)^{7/8} \right\}^2$$



or

$$\left[ \frac{d_s}{d} / \left(\frac{W}{B}\right)^{7/8} \times \left(\frac{B}{d}\right)^{7/8} \right] = \left\{ \left[ \frac{\text{drag force on particle}}{\text{buoyant wt. of particle}} \right] \left( \frac{\rho_s - \rho_f}{\rho_f} \right)^{7/8} \right\}^2$$

$$\left[ \frac{d_s}{d} / \left(\frac{W}{B}\right)^{7/8} \times \left(\frac{B}{d}\right)^{7/8} \right] = \left\{ \left( \frac{\text{drag force on particle}}{\text{buoyant wt. of particle}} \right) (S-1)^{7/8} \right\}^2$$

The above relation should be viewed with caution as it holds for below a certain definite state of bed activity, and is based on the data collected with only two different bed materials of gravel size.

The above relation shows that for all other factors remaining unchanged, the non-dimensional scour depth varies

- i) directly with  $7/8^{\text{th}}$  power of  $W/B$
- ii) inversely with  $7/8^{\text{th}}$  power of  $d/B$
- iii) directly with square of  $\frac{\text{drag}}{\text{buoyant weight}}$  ratio
- iv) directly with  $7/4^{\text{th}}$  power of  $\left( \frac{\rho_s - \rho_f}{\rho_f} \right)$ .

This shows that the parameters  $W/B$  and  $d/B$  are quite effective in scour phenomenon, but the effect of the parameter in (iii) is more as scour depends upon the square of this parameter. Again the scour depends upon the  $7/4$ , of the bed material density factor  $\left( \frac{\rho_s - \rho_f}{\rho_f} \right)$  or  $(S-1)$ , and





thus the effect of the density of bed material is almost twofold the effect the parameter  $W/B$  and  $d/B$  and is slightly less than that of the parameter  $\frac{\text{drag force}}{\text{buoyant weight}}$  ratio.

In Chapter 2, under dimensional analysis description, the importance of the parameter  $\frac{\text{drag force}}{\text{buoyant weight}}$  to the maximum scour around bridge pier has been stressed. Again, the plottings in Chapter 4 and Chapter 5 were initiated with the parameter  $\frac{\text{drag}}{\text{buoyant weight}}$ . Both these steps are justified as we have found in above paragraph that the relative effect of ratio of drag force and buoyant weight, is the maximum of all the other parameters in equation (B) of dimensional analysis in Chapter 2.

7) Data from laboratory experiments by Inglis, Varzeliotis, and Neill in Tables 7 to 9 fitted the resultant plot in Figure 5.1.

This shows the applicability of the parameters

$$\frac{d_s}{d} / \left(\frac{W}{B}\right)^{7/8} \times \left(\frac{B}{d}\right)^{7/8} \quad \text{and} \quad \frac{C_d V^2}{g d_m} \left(\frac{\rho_f}{\rho_s - \rho_f}\right) \left(\frac{\rho_s - \rho_f}{\rho_f}\right)^{7/8}$$

to the other investigator's scour data.



8) From the practical point of view, the maximum scours for coal and stone are roughly laid down as follows:

$$\frac{d_s}{d} = 1.5 \left(\frac{W}{d}\right)^{7/8} \quad (\text{stone gravel size})$$

$$\frac{d_s}{d} = \left(\frac{W}{d}\right)^{7/8} \quad (\text{coal gravel size})$$

The first expression for stone (gravel size) compares favourably with the expression  $\frac{d_s}{d} = 1.5 \left(\frac{W}{d}\right)^{0.7}$ , which has been attributed by Neill (Reference 4) to Laursen (Reference 11).

The parameter  $\frac{W}{d}$  varies from 0.14 to 1.5 for the case of first expression listed above. For the case of Laursen's expression the variation in  $\frac{W}{d}$  is from 0.71 to 3.

The above expression for stone checks reasonably well with data by Varzeliotis (Reference 7), given in Table 7, of (Reference 4). The parameter  $\frac{W}{d}$  varies between 0.33 and 0.71 for the case of data collected by Varzeliotis, for round nosed pier.

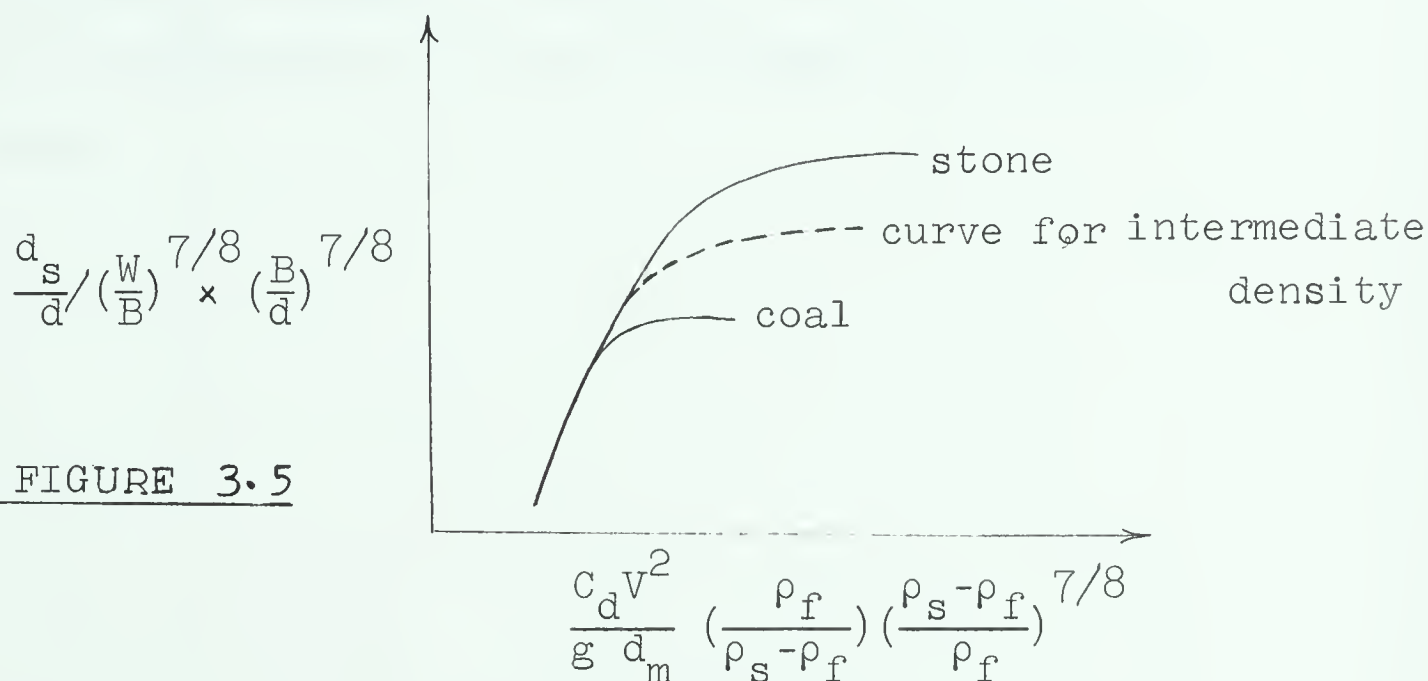
For the case of coal  $\frac{W}{d}$  varies between 0.116 and 0.6.



### Suggestions

1) More sizes of coal should be used as the present work is based on one coal size only.

2) The results have the limitations of consideration of only two different bed materials. More different bed materials may be tried, like gilsonite, amber and lignite, to make conclusions more sound. There is a possibility that an intermediate density bed material may fit in as shown by dotted lines in diagram.



SKETCH OF FIGURE 3.5

3) Effors should be made to find quantitative reasons for the bifurcation of the coal and stone plot beyond point P, by accounting for possibly the further effect of the density parameter, which may still have remained unaccounted for, or by taking into consideration the complex sediment transport phenomena.





4) By using a bigger flume, more depths of flow fairly apart could be considered without encountering too closely spaced plots as in Figure 4.25.

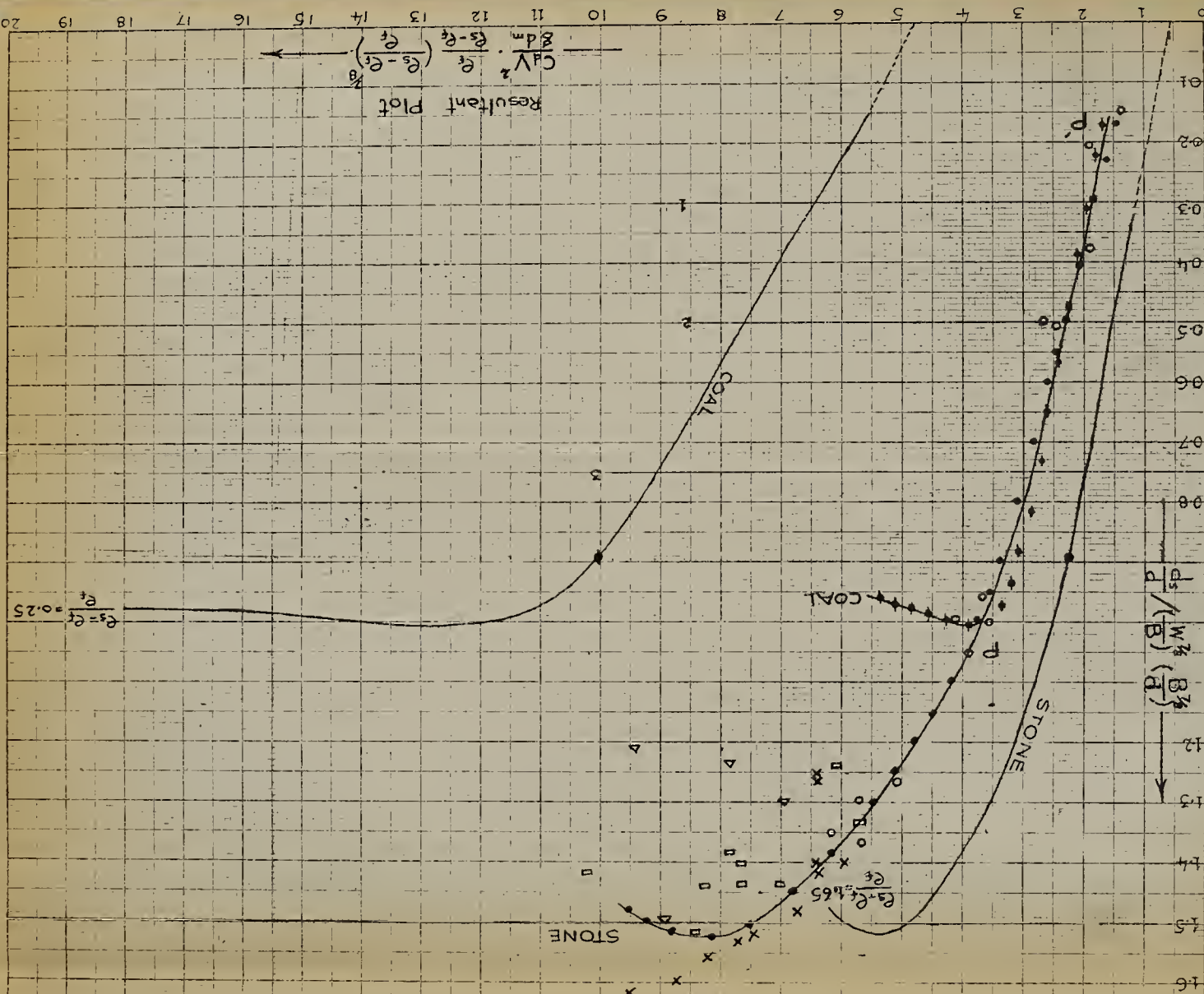
5) Different pier shapes may also be brought in.

6) Some method may be found to find mathematical form of bifurcating portions of the total plot in Figure 5.1.

7) Further research may be aimed at the study of the scour phenomenon in terms of transport of bed sediment, in order to investigate as to how the amount of transport affects scour.



FIGURE 5.1



CONSIDERING THE EFFECT OF VARIABLE  
GRAVEL RANGE

- STONE [S.G. 2.65]
- ♦ COAL [S.G. 1.25]
- SCOUR DATA [WRITER]
- × SCOUR DATA [VARZELIOTIS]
- △ SCOUR DATA [INGLIS]
- SCOUR DATA [NEILL]





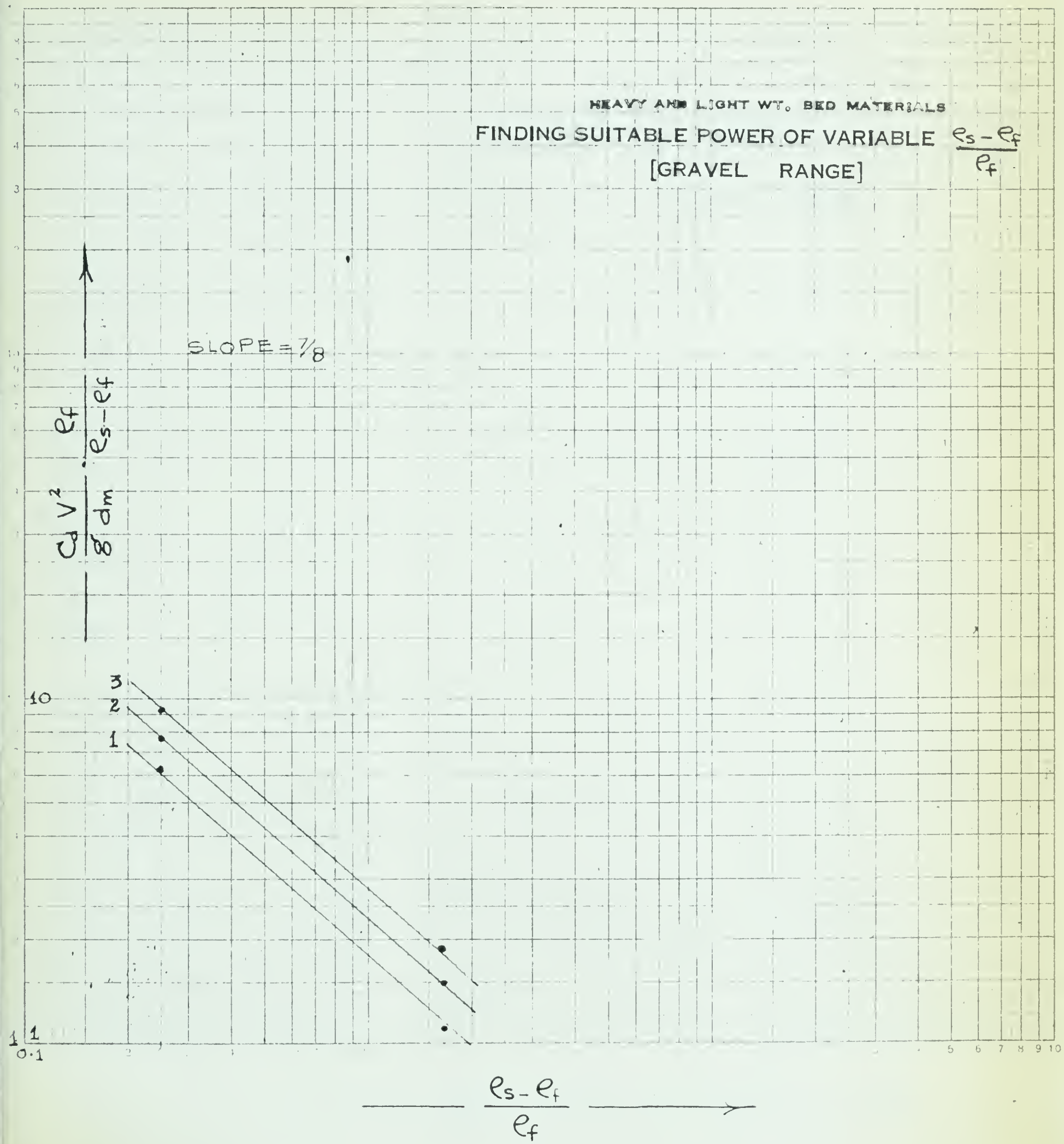


FIGURE 5.2



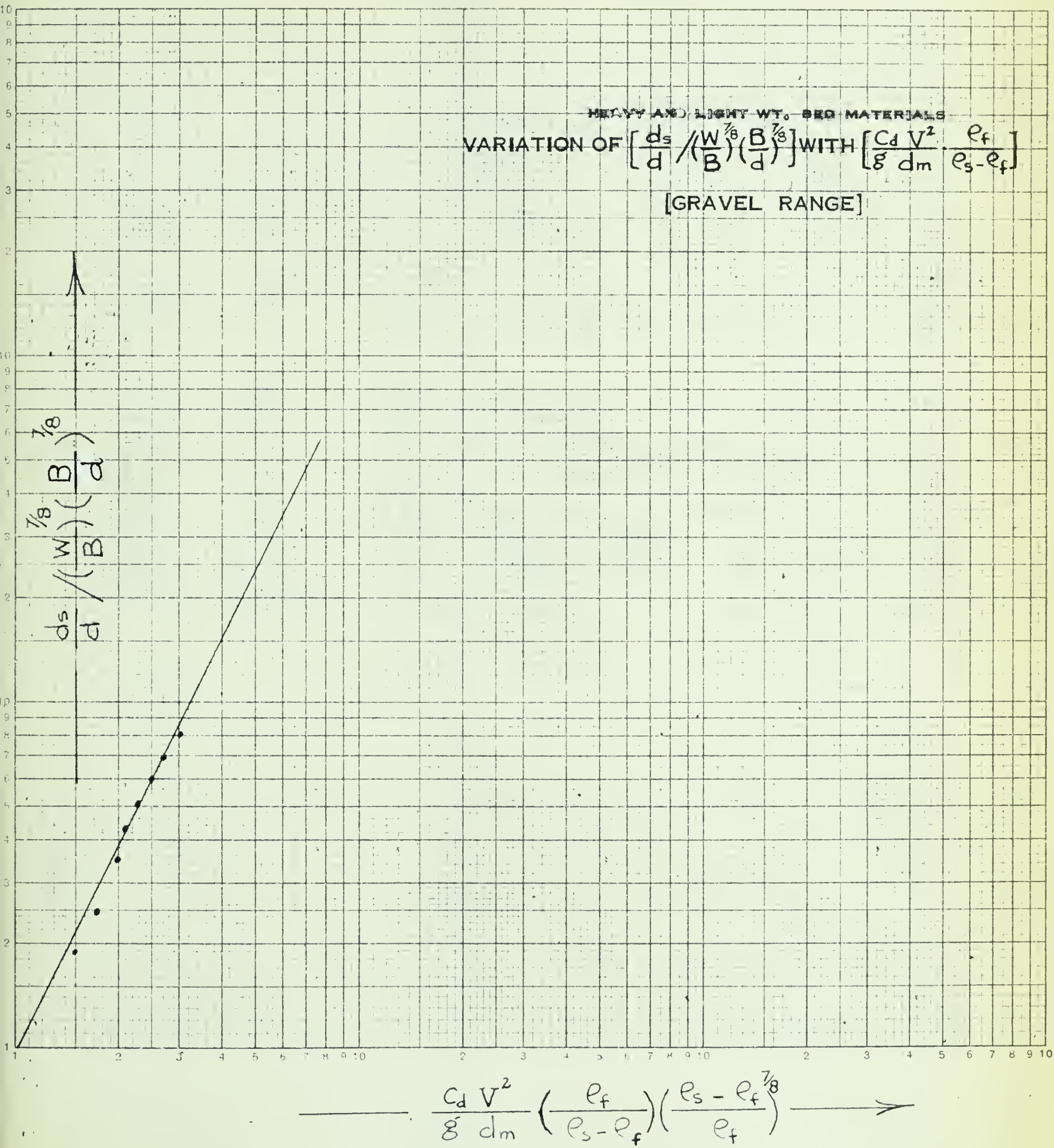


FIGURE 5.3





Table 6  
SCOUR DATA (WRITER)

S.G. = 2.65  
 $d_m = 1.56 \text{ mm}$

d (ft)	Q (cusecs)	V (ft/sec)	$d_s$ (ft)	$\frac{d_s}{d} \cdot \frac{W}{B} \cdot \left( \frac{B}{Q} \right)^{\frac{1}{3}}$	$R = \frac{V d_m}{v}$	$C_d$	$\frac{C_d V^2}{g d_m} \left( \frac{\rho_f}{\rho_s - \rho_f} \right)$	$\frac{\rho_s - \rho_f}{\rho_f}$	Bed Activity
1	2	3	4	5	6	7	8	9	
0.3	0.50	1.11	0.20	1.05	455	0.56	3.90		Hopping & jumping of small part., rolling
0.3	0.60	1.34	0.235	1.37	550	0.59	5.70		Slight sheet flow
0.4	0.50	0.835	0.130	0.66	340	0.65	2.68		Inactive
0.4	0.60	1.0	0.209	1.00	410	0.60	3.54		Quivering and hopping
0.4	0.75	1.26	0.250	1.26	510	0.55	5.15		Hopping and rolling short distances
0.5	0.50	0.67	0.0775	0.38	275	0.72	1.93		Inactive
0.5	0.60	0.80	0.1025	0.51	330	0.65	2.46		Quivering and hopping
0.5	0.75	1.00	0.195	0.96	410	0.60	3.54		Rolling and jumping
0.5	1.00	1.34	0.255	1.30	550	0.54	5.70		Small particle rolling continuously (slight sheet flow)
0.6	0.5	0.56	0.030	0.15	230	0.77	1.40		Inactive
0.6	0.60	0.67	0.0425	0.21	275	0.73	1.94		Rare quivering. Almost inactive
0.6	0.75	0.84	0.104	0.50	345	0.65	2.68		Small particles hopping.
0.6	1.00	1.10	0.205	1.00	450	0.575	4.14		Most of particles hopping, some rolling.
0.6	1.25	1.40	0.28	1.35	575	0.525	6.14		Slight sheet flow





TABLE 7

## SCOUR DATA (INGLIS)

$$S.G. = 2.65$$

$$d_m = 1.3 \text{ mm}$$

Round Nosed Pier

$W$ (ft)	$d$ (ft)	$q$ (cusecs/ft)	$V$ (ft/sec)	$d_s$ (ft)	$\frac{d_s}{d} \times \frac{W}{B}$	$R = \frac{V d_m}{\nu}$	$C_d$	$\frac{C_d V^2}{g d_m} \left( \frac{\rho_f}{\rho_s - \rho_f} \right) \left( \frac{\rho_s - \rho_f}{\rho_f} \right)^{\frac{7}{8}}$
1	2	3	4	5	6	7	8	9
0.57	0.82	1.12	1.37	0.78	1.30	494	0.55	6.95
0.57	0.98	1.47	1.46	0.76	1.24	525	0.54	7.8
0.57	1.25	1.99	1.58	0.95	1.50	570	0.525	8.9
0.57	1.57	2.56	1.63	0.79	1.21	586	0.52	9.4

TABLE 8

## SCOUR DATA (VARZELIOTIS)

$$S.G. = 2.65$$

$$d_m = 1.70 \text{ mm}$$

Round Nosed Pier

$W$ (ft)	$d$ (ft)	$V$ (ft/sec)	$d_s$ (ft)	$\frac{d_s}{d} \times \frac{W}{B}$	$R = \frac{V d_m}{\nu}$	$C_d$	$\frac{C_d V^2}{g d_m} \left( \frac{\rho_f}{\rho_s - \rho_f} \right) \left( \frac{\rho_s - \rho_f}{\rho_f} \right)^{\frac{7}{8}}$
1	2	3	4	5	6	7	8
0.08	0.35	1.56	0.12	1.25	480	0.50	6.35
0.17	0.35	1.56	0.26	1.40	480	0.50	6.35
0.25	0.35	1.56	0.37	1.40	480	0.50	6.35
0.33	0.35	1.56	0.42	1.26	480	0.50	6.35
0.17	0.24	1.32	0.25	1.40	350	0.65	5.90
0.17	0.30	1.46	0.27	1.47	400	0.60	6.65
0.17	0.35	1.58	0.29	1.53	430	0.59	7.70
0.17	0.40	1.66	0.30	1.56	450	0.57	8.2
0.17	0.44	1.74	0.31	1.60	470	0.56	8.7
0.17	0.48	1.82	0.32	1.63	490	0.55	9.5
0.17	0.52	1.89	0.33	1.67	510	0.54	10.1



Table 9  
SCOUR DATA (NEILL)

S.G. = 2.65

$d_m = 1.70$  mm

Round Nosed Pier

$d$ (ft)	$W$ (ft)	$V$ (ft/sec)	$ds$ (ft)	$\frac{ds}{d} / \left( \frac{W}{B} \right) \times \left( \frac{B}{d} \right)^{\frac{7}{8}}$	$R = \frac{Vd_m}{\nu}$	$C_d$	$\frac{C_d V^2}{g d_m} \left( \frac{\rho_f}{\rho_s - \rho_f} \right) \left( \frac{\rho_s - \rho_f}{\rho_f} \right)$
1	2	3	4	5	6	7	8
0.6	0.17	1.40	0.25	1.24	390	0.60	6.10
0.6	0.17	1.60	0.28	1.4	440	0.57	7.60
0.6	0.17	1.70	0.29	1.44	470	0.56	8.40
0.3	0.17	1.65	0.29	1.57	460	0.55	7.80
0.2	0.17	1.50	0.25	1.44	410	0.60	7.00
0.2	0.17	1.75	0.20	1.15	480	0.56	8.85
0.2	0.17	1.65	0.24	1.38	460	0.55	7.80
0.2	0.17	1.30	0.23	1.33	360	0.65	5.70
0.4	0.17	1.60	0.275	1.43	440	0.575	7.60
0.4	0.17	1.70	0.290	1.51	470	0.56	8.40
0.4	0.17	1.90	0.270	1.41	530	0.54	10.10





## BIBLIOGRAPHY



BIBLIOGRAPHYReference  
Number

- 1            T. Blench.    "Regime Behaviour of Canals and Rivers."  
Butterworth Scientific Publication (1957).
- 1A          T. Blench.    "Reprint from Butterworth Civil Engin-  
eering Reference Book," Second edition,  
(1961).
- 1B          T. Blench.    "Illustrated Notes on River Engineering,"  
(1961).
- 2            C. R. Neill.    Experimental data of July 1961,  
(unpublished).
- 3            C. R. Neill.    "Introduction to the Problem of  
scour at bridge pier," unpublished  
paper presented to the subcommittee  
on Bridge Pier scour of the Committee  
on Bridges and Structures, C.G.R.A.  
Winnipeg (October 1963).
- 4            C. R. Neill.    "Local Scour around Bridge Pier (a  
comparative analysis of model experi-  
ments and field data)", unpublished  
report, Alberta Joint Highway Research  
Program, (October 1963).
- 5            C. R. Neill.    "River Bed Scour," Technical Publi-  
cation No. 23, Canadian Good Roads  
Association, Ottawa, Canada (December 1964).
- 5A          C. R. Neill.    "Use of Echo Sounders to Measure Scour  
at Bridges," unpublished Report, Alberta  
Joint Highway Research Program, (1962).
- 6            C. C. Inglis.    "The Behaviour and Control of  
rivers and canals," Part II, Central  
Water Power Irrigation and Navigation  
Research Station, Poona, India (1949).



- 7        A. N. Varzeliotis. "Model studies of Scour  
around bridge pier and stone aprons,"  
M.Sc. Thesis, University of Alberta (1960).
- 8        P. Andru. "A study of scour at obstructions in  
Non-Cohesive Bed." M.Sc. Thesis (Un-  
published). University of Alberta (1956).
- 9        H. Rouse. "Engineering Hydraulics," (1949) and  
H. Rouse and J. W. Howe, "Basic Mechanics  
of Fluids" (1953), John Wiley and Sons, Inc.
- 10       M. Mushtaq. "Experiments on Design and Behaviour  
of Spur Dykes," Published in Proceed-  
ings of Minnesota Int. Hyd. Convention,  
(September 1 - 4, 1953).
- 11       E. M. Laursen and A. Toch. "Scour Around Bridge  
Pier and Abutments," Iowa Institute  
of Hydraulic Research, (May, 1956).
- 12       S. S. Karaki and R. M. Haynie. "Mechanics of  
Local Scour, Part II, Bibliography,"  
Civil Engineering Section, Colorado  
State University, Fort Collins,  
Colorado, (November 1963).
- 13       Chabert, J. and Engeldinger, P. "Etude des  
affouillements autour des piles des ponts,"  
Laboratoire National d'Hydraulique,  
Chatou, France (1956).
- 14       C. R. Neill. "English translation of 'Etude des  
affouillements autour des piles des  
ponts', Laboratoire National d'Hydrau-  
lique, Chatou, France" (July 1961), and  
Appendix III "Tables of Test data,"  
by E. A. Portfors (undated).
- 15       D. C. Ipsen. "Units, dimensions and dimensional  
numbers," McGraw-Hill Book Company, (1960).
- 16       R. J. Garde, K. Subramanya, and K. Nambudkipad.  
"Study of Scour around spur dikes,"  
A.S.C.E. Hydraulic Division, Proceedings  
(November 1961) (Proc. Paper 2978).





- 17 T. Blench. "Discussion on sediment transport paper by Yalin." Journal Hyd. Dn. A.S.C.E. (HY-2) March 1964, pages 371-377.
- 17A T. Blench. "Discussion on 'Scour at bridge pier crossing' by E.M. Laursen, Feb. 1960," Journal of Hyd. Dn. A.S.C.E., Vol. 86, No. HY-5, (May 1960), Pages 193, 194.
- 18 T. Blench. "Some points about dimensional analysis in bridge pier scour," unpublished paper (May 17, 1964).
- 19 E. M. Laursen. "Scour at bridge crossings," Bulletin No. 8, Iowa Highway Research Board, (1958).
- 20 E. M. Laursen. "An analysis of relief bridge scour," Proc. A.S.C.E., Vol. 89, No. HY-3, Pages 93-118.
- 21 F. M. Chang and V. M. Yevdjovich. "Analytical study of local scour," Civil Engineering Section of Colorado State University, Fort Collins, Colorado (April 1962).
- 22 Doddiah Dodiah, M. L. Abertson and R. K. Thomas. "Scour from jets," Proceedings International Association for Hydraulic Research, September 1-4, 1953, Pages 161-169, (1953).
- 23 T. Blench and M. A. Qureshi. "Practical regime analysis of river slopes," Journal of Hyrd. Dn. Proc. A.S.C.E., (March 1964).
- 24 P. G. Hubbard. "Field Measurement of bridge-pier scour," E. M. Laursen "Model-prototype comparison of bridge-pier scour," Proceedings of Highway Research Board, Vol. 34, Pages 184-192, (1955).



- 26 E. J. Sanden. "A method of measurement of scour at bridge piers," M.Sc. thesis, University of Alberta, (1960).
- 26A E. J. Sanden. "Scour around bridge piers and erosion of river banks," Proc. of Western Canadian Association of Canadian Highway Officials, (1960).
- 27 E. J. Sanden and C. R. Neill. "Measuring scour around bridge foundations in floods," Public Works in Canada, Vol. 11, No. 7, Pages 14-17, (1963).
- 28 D. B. Steinman and S. R. Watson. "Bridges and their builders," Dover, New York.
- 29 L. J. Tison. "Erosion autour des piles de ponts en riviere," Annales des travaux publics de Belgique, Vol. 41, No. 6, Pages 813-817, (1940).
- and
- Tison, L.J., "Local scour in rivers," Jour. Geophys. Research, Vol. 66, No. 12, Pages 4227-4232, (1961).
- 30 Posey, C. J., and Sybert, J. H., "Erosion protection of production structures," Proc. Int. Association for Hyd. Research, Ninth General Assembly, Dubrovnick, Pages 1157-1162, (1961).
- 31\* Bata, G. "Erozija Oko novo sadskog mostovskog (Siberian) (Scour around bridge pier)," Yugoslavia 1960. English Translation by Colorado State University, Civil Engineering Department by Markovic (1960).
- 32\* Engels, H., (Protection Against underscouring), (German). Zeitschrift für Bauwesen (1894).
- 33\* Flamment, A., "Affouillements qui en sont la consequence (French). (Scour around Bridge piers as a consequence of the reduction of section). Hydraulique, Chapter V, Paris (1900).

---

\* Summary translation in English given in Reference 12





- 34<sup>\*</sup> Keutner, Chr., "Stromungs vorgäng an strompfeilorn von verschiedenen Grundriss," (German), (The flow around bridge piers of different shapes and its effect on the river bed). Die Bautechnik, Volume ten, No. 12, (1932) March, (Translated by E.F. Wilsey, April 22, 1937, U. S. Bureau of Reclamation Report HYD-19, Translation No. 40).
- 35<sup>\*</sup> Ishihara, T., "Experimental study of scour at bridge piers," (Japanese). Trans. Japanese Soc. of Civil Engineers, Volume 24, No. 1, (1938).

---

\* Summary translation in English given in Reference I2



APPENDIX I

PLATES





PLATE I. OVERALL VIEW OF FLUME  
[LOOKING FROM DOWNSTREAM SIDE]







PLATE 2. SLOPE                      ADJUSTMENT                      DEVICE

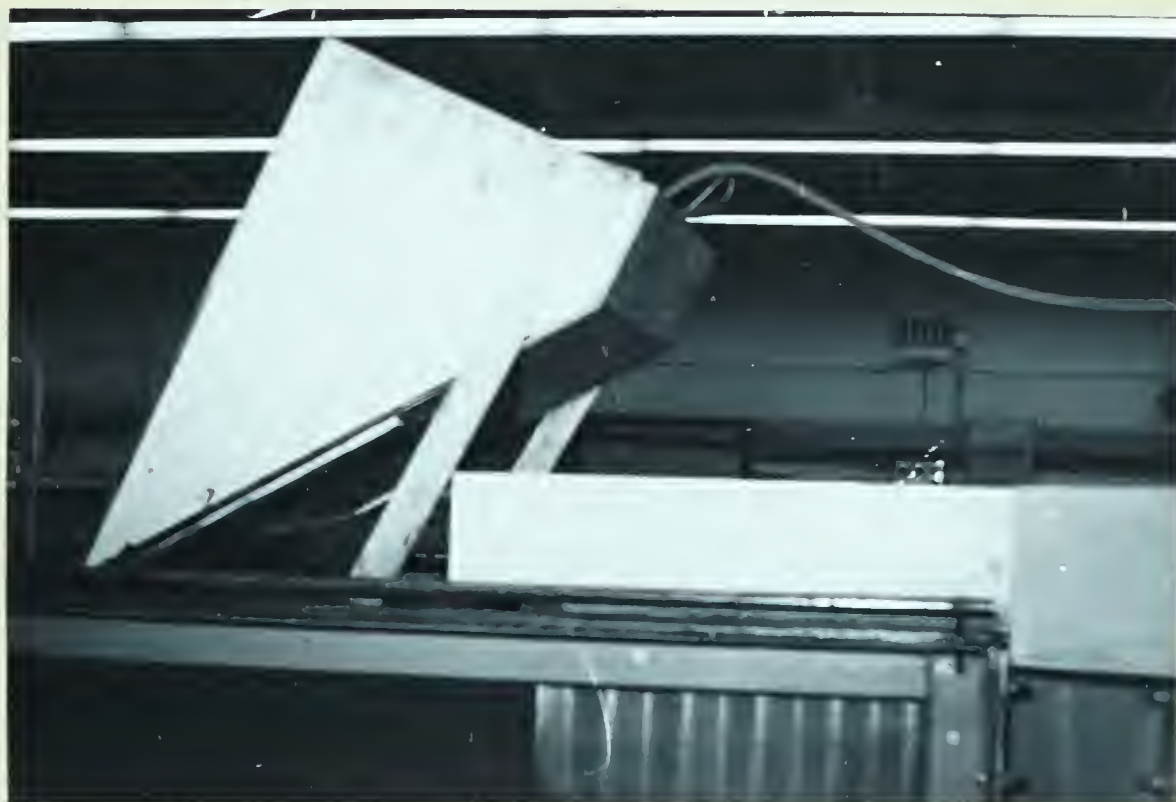


PLATE 3. HOPPER FOR BED MATERIAL    FEEDING



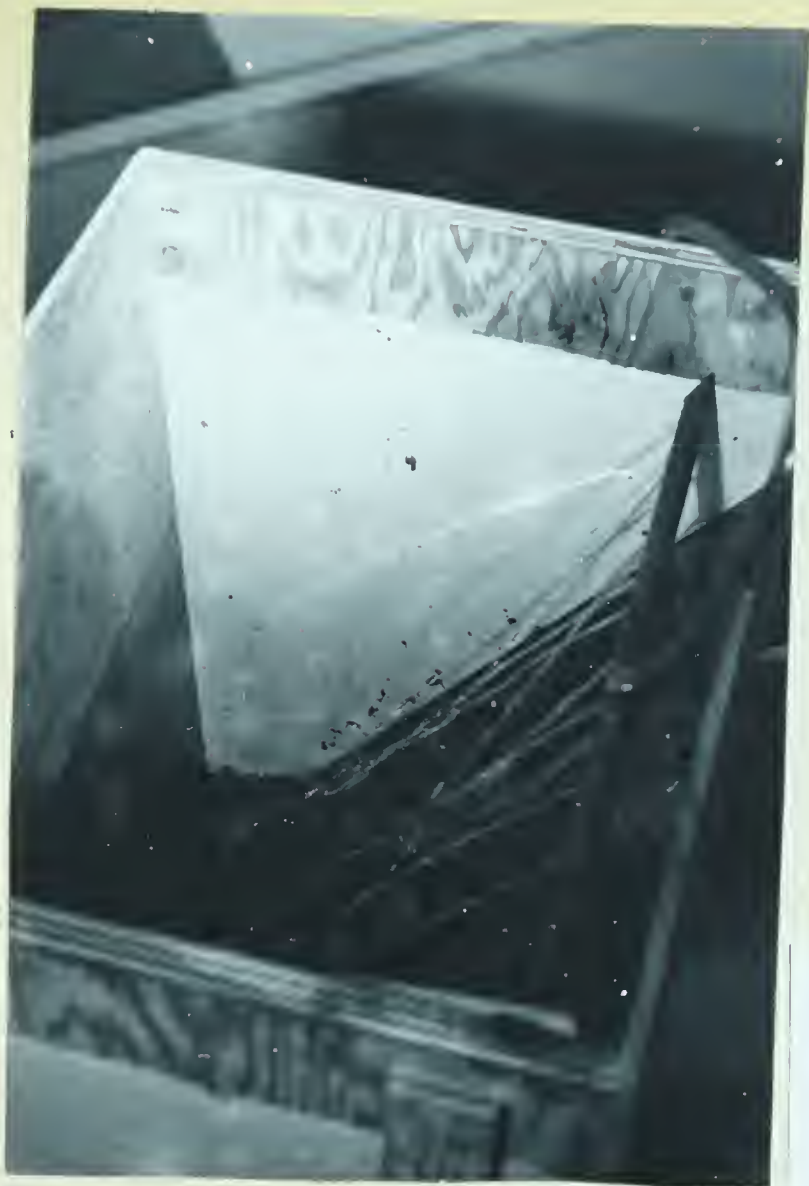


PLATE 4. WATER SPRAY FOR  
WASHING DOWN THE COAL IN  
THE HOPPER.



PLATE 5. SLIDING GATE DEVICE  
FOR ADJUSTING HOPPER OPENING.







PLATE 6. MAIN SUPPLY LINE  
WITH DISCHARGE REGULATING  
VALVE.



PLATE 7. FLOWMETER FOR  
DISCHARGE MEASUREMENT





PLATE 8. BAFFLES FOR ENERGY DISSIPATION

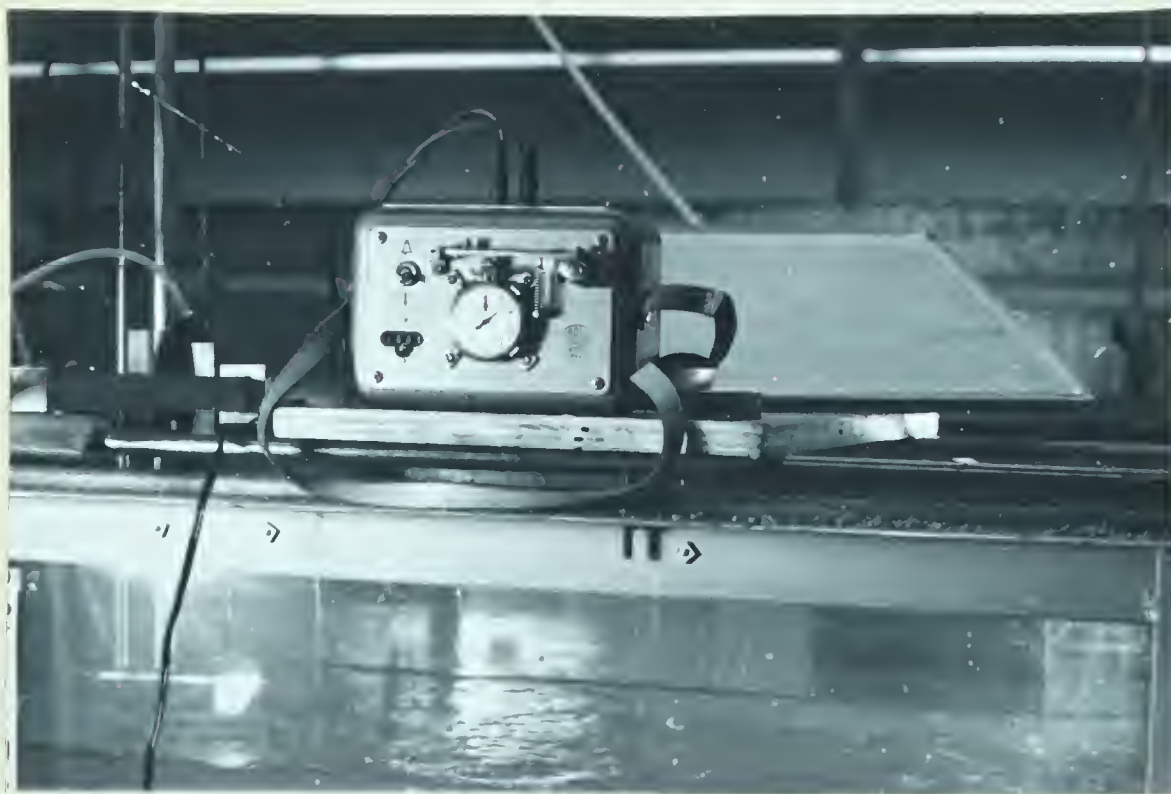
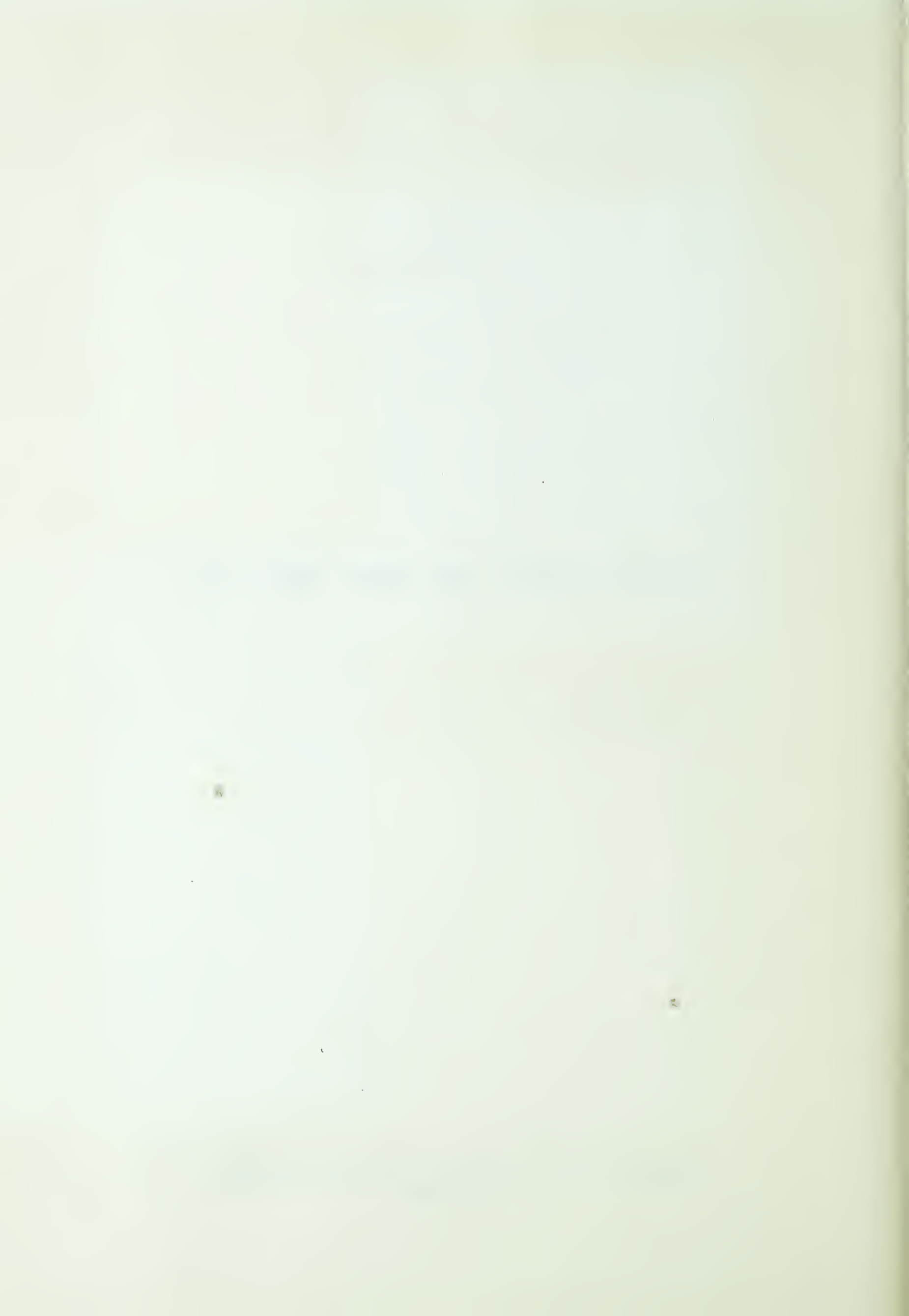


PLATE 9. OTT CURRENTMETER REVOLUTION  
COUNTER





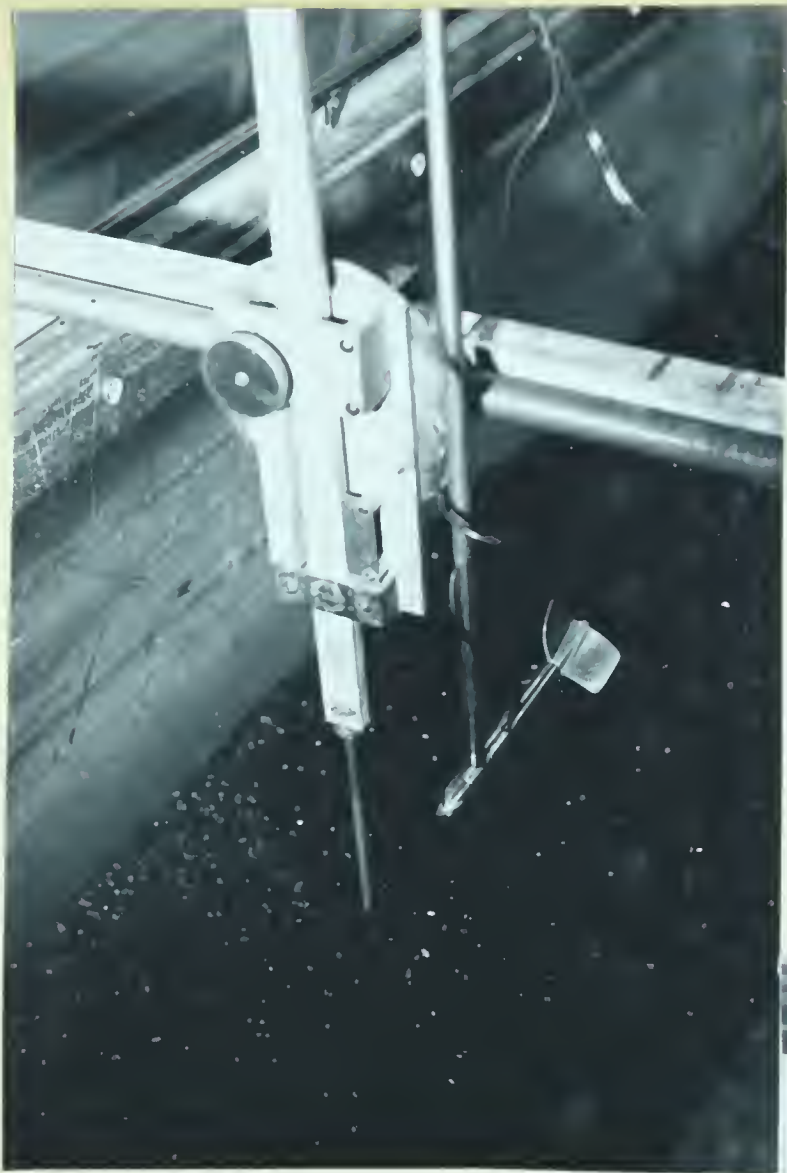


PLATE 10. OTT CURRENTMETER  
PROPELLER AND POINT GAUGE



PLATE 11. ARRANGEMENT FOR  
INITIAL WATER FEEDING FROM  
DOWNSTREAM SIDE OF FLUME.





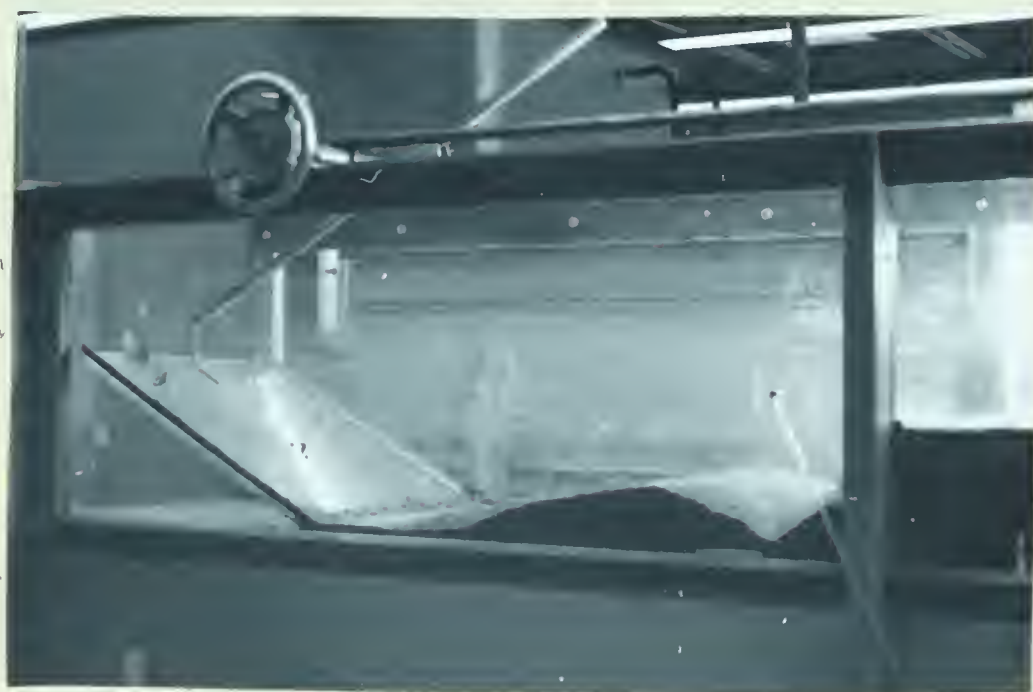


PLATE 12. TAIL GATE AND BED MATERIAL TRAP

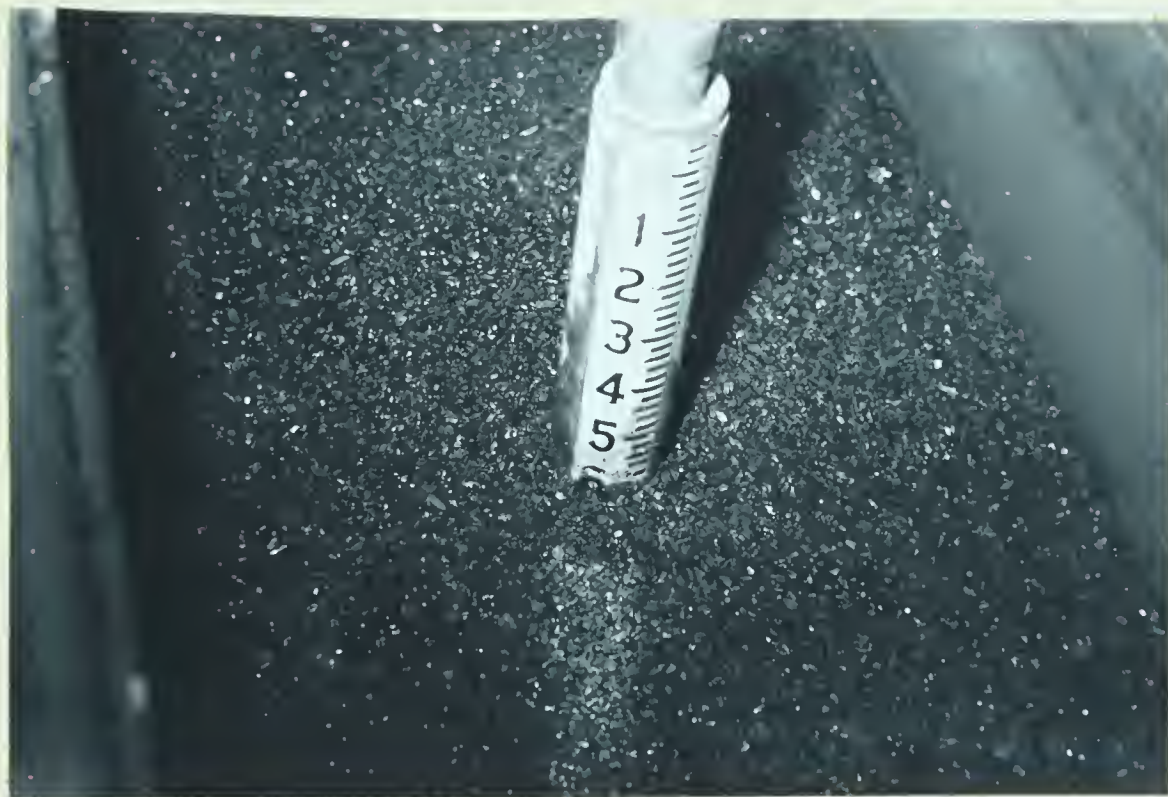


PLATE 13. PIER GRADUATION FOR SCOUR DEPTH  
BELOW GENERAL BED LEVEL.





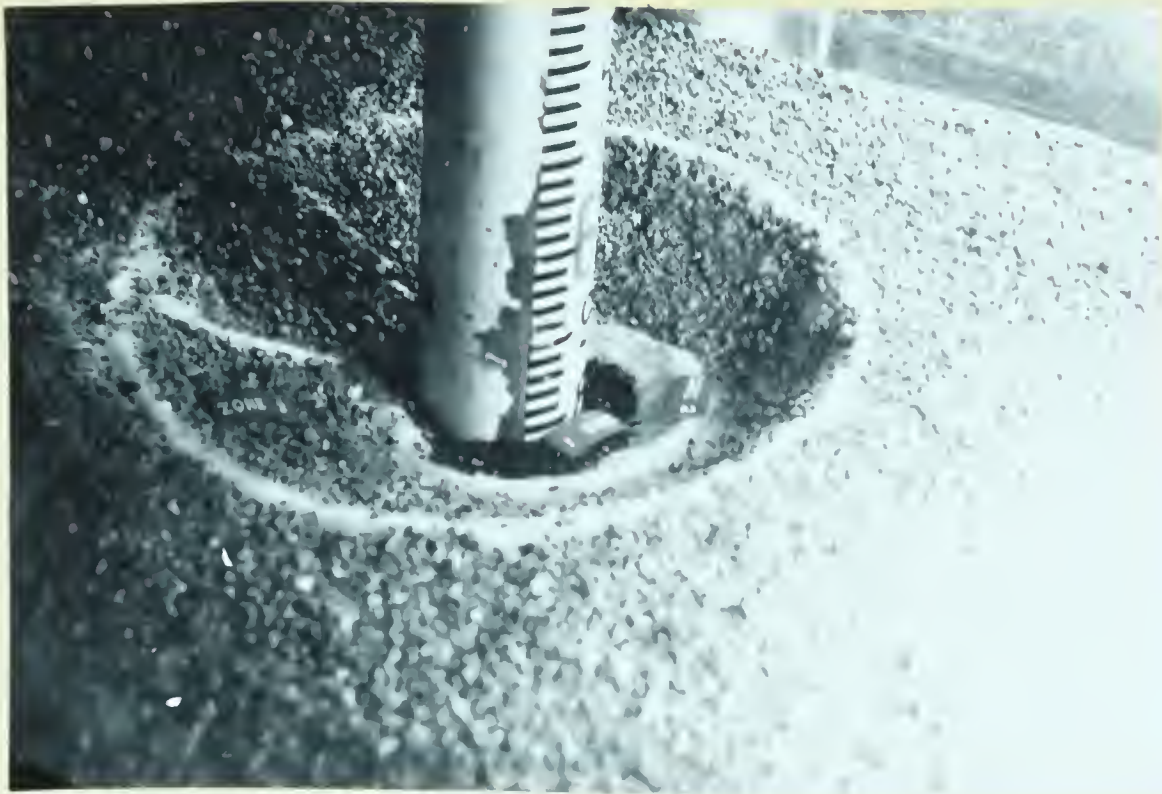


PLATE 14. TYPICAL SCOUR HOLE IN HEAVY WEIGHT  
BED MATERIAL.



PLATE 15. TYPICAL SCOUR HOLE IN LIGHT WEIGHT  
BED MATERIAL.





APPENDIX II

NOTATIONS



## NOTATIONS

- $B$  = width of channel
- $C$  = charge in part per hundred thousand
- $C_d$  = Drag coefficient
- $d$  = Depth of flow.
- $d_m$  = Median size of bed particle
- $d_s$  = Maximum scour depth measured below general bed level to the deepest point in scour hole.
- $F_b$  = Blench 's Bed Factor
- $g$  = acceleration due to gravity
- $Q$  = total discharge
- $q$  = discharge per unit width of flume.
- $s$  = Water surface slope
- $S$  = Specific gravity of bed material
- $t$  = time
- $T$  = temperature
- $V$  = Mean velocity of flow.
- $V_s$  = Terminal velocity
- $W$  = diameter of pier
- $\alpha$  = Angle of flow with the axis of symmetry of pier.
- $\rho_f$  = density of water
- $\rho_s$  = density of solid
- $\mu$  = dynamic viscosity of water
- $\nu$  = kinematic viscosity of water







**B29830**